Discovery of Natural Products Suppressing Cancer Cell Proliferation and Autophagy

がん細胞の増殖およびオートファジーを抑制する天然物の網羅的探索

Shinya Okubo

2020

Graduate School of Pharmaceutical Sciences

Nagasaki International University

Abbreviations

3-MA; 3-methyladenine

AMPK; AMP-activated protein kinase

ARC; arctiin

ARG; arctigenin

BBR; berberine

Bcl-2; B-cell lymphoma 2

BuOH; butanol

CL; costunolide

CQ; chloroquine

DAPI; 4',6-diamidino-2-phenylindole

DCL; dehydrocostuslactone

DMEM; Dulbecco's Modified Eagle's Medium

DMSO; dimethyl sulfoxide

EtOAc; ethyl acetate

ETP; etoposide

FBS; fetal bovine serum

HCQ; hydroxychloroquine

HPLC; high performance liquid chromatography

LC3; microtubule-associated protein light chain 3

MeOH; methanol

MS; mass spectrometer

mTOR; mammalian target of rapamycin

MTT; 3-(4,5-dimethylthiazol-2-yl)-2,5-diphenyltetrazolium bromide

NMR; nuclear magnetic resonance

p62; sequestosome 1/p62

PBS; phosphate-buffered saline

PI3K; phosphatidylinositol 3-kinase

TLC; thin-layer chromatography

UBA; ubiquitin-associated

Table of contents

Abbreviations i

Table of contents ii

List of tables vi

List of figures vii

Chapter 1: General introduction

1.1. Autophagy and its molecular mechanisms 1

1.2. Relationship between autophagy and cancer..... 4

1.3. Autophagy modulators 6

1.4. Natural products modulating autophagy 9

1.5. Purpose of this thesis 11

1.6. References 12

Chapter 2: Screening of extracts prepared from crude drugs for autophagy-mediated cell survival of the human hepatocellular carcinoma cell line HepG2

2.1. Introduction 15

2.2. Materials and methods 20

2.2.1. Preparation of crude extracts 20
2.2.2. Reagents 20
2.2.3. Cell culture and treatment 21
2.2.4. Western blot analysis 21
2.2.5. Determination of cell proliferation 21
2.2.6. Statistical analysis 22

2.3. Results 23

2.3.1. Establishment of an assay for autophagy-mediated cell survival 23
2.3.2. Effects of 130 crude extracts on autophagosome formation 29
2.3.3. Effects of 24 crude extracts on cell proliferation 33

2.3.4. Effects of five crude extracts on autophagy flux 35
2.3.5. Effects of three crude extracts on autophagy flux 37

2.4. Discussion 38

2.5. Conclusion 40

2.6. References 41

Chapter 3: Suppression of autophagy by arctigenin contained in the fruits of *Arctium lappa* (Goboshi) and the fruits of *Forsythia suspense* (Rengyo) and the molecular mechanisms

3.1. Introduction 44

3.2. Materials and methods 47

3.2.1. Reagents 47
3.2.2. Cell culture and treatment 47
3.2.3. Determination of cell proliferation 47
3.2.4. Western blot analysis 47
3.2.5. Fluorescence microscopy 48
3.2.6. Statistical analysis 48

3.3. Results 49

3.3.1. Effects of ARG and ARC on cell proliferation 49
3.3.2. Effect of ARG on autophagy-related proteins 50
3.3.3. Effect of ARG on starvation-induced autophagy 54
3.3.4. Effect of ARG on apoptosis-related proteins 56

3.4. Discussion 57

3.5. Conclusion 60

3.6. References 61

Chapter 4: Isolation of active compounds derived from the rhizome of *Dioscorea tokoro* (Hikai) that inhibit autophagy

4.1. Introduction 63

4.2. Materials and methods 65

4.2.1. General procedures 65
4.2.2. Extraction and isolation 65
4.2.3. Acid hydrolyses 66
4.2.4. Materials for biological assays 67
4.2.5. Cell culture and treatment 67
4.2.6. Determination of cell proliferation 67
4.2.7. Western blot analysis 67
4.2.8. Statistical analysis 67

4.3. Results 68

4.3.1. Comparison of antiproliferative effects of each fraction 68
4.3.2. Effect of *n*-BuOH fraction on autophagosome formation and autophagy flux 70
4.3.3. Isolation, acid hydrolyses, and structural identification of **1**–**5** 71
4.3.4. Effects of **1**–**5** on cell proliferation, and its structure–activity relationships 72
4.3.5. Effects of **1**–**5** on autophagosome formation and autophagy flux 73
4.3.6. Effects of **1**–**3** on apoptosis-related proteins 75

4.4. Discussion 76

4.5. Conclusion 77

4.6. References 78

Chapter 5: Inhibition of autophagy by major active compounds contained in the root of *Saussurea lappa* (Mokko)

5.1. Introduction 80

5.2. Materials and methods 83

5.2.1. General procedures 83
5.2.2. Extraction 83
5.2.3. Preparation of sample solution 83
5.2.4. Preparation of standard solution 83
5.2.5. HPLC instruments and conditions for CL and DCL 84
5.2.6. Calibration 84

5.2.7. Materials for biological assays.. 84
5.2.8. Cell culture and treatment.. 85
5.2.9. Determination of cell proliferation 85
5.2.10. Western blot analysis.. 85
5.2.11. Statistical analysis.. 85

5.3. Results.. 86
5.3.1. Comparison of antiproliferative effects of each fraction 86
5.3.2. Effect of hexane fraction on autophagosome formation and autophagy flux 87
5.3.3. TLC and HPLC analyses of CL, DCL, MeOH extract, and fractions 88
5.3.4. Effects of CL and DCL on cell proliferation 89
5.3.5. Effects of CL and DCL on autophagosome formation and autophagy flux. 90
5.3.6. Effects of CL and DCL on apoptosis-related proteins.......................... 92

5.4. Discussion 94

5.5. Conclusion 95

5.6. References 96

Chapter 6: Conclusions.. 98

References 106

Acknowledgement 108

List of tables

TABLE

Table 1.1. Current HCQ clinical trials ……. 8

Table 2.1. List of crude drugs …… 16

Table 2.2. Effects of each autophagy modulator on LC3-II and p62 expression levels... 28

Table 2.3. Effects of selected 24 crude extracts on cell proliferation ……..…… 34

Table 6.1. List of autophagy-inhibiting compounds identified in this thesis…...……... 102

List of figures

Chapter 1

Figure 1.1. Schematic diagram to illustrate the process of autophagy and in the role of LC3-II, p62, and beclin-1 …… 3

Figure 1.2. High metabolic demand of cancer cell and activation of autophagy …… 5

Figure 1.3. Chemical structures of BBR ……..…. 9

Chapter 2

Figure 2.1. Effects of 3-MA and CQ on LC3-II and p62 expression levels ...…… 24

Figure 2.2. Effect of BBR on LC3-II expression levels ……..……. 25

Figure 2.3. Effect of BBR on cell proliferation ……..…….…….…….…… 26

Figure 2.4. Effect of BBR on p62 expression levels ……..…….…… 27

Figure 2.5. Effects of 130 crude extracts on LC3-II expression levels …….…… 29

Figure 2.6. Effects of eight crude extracts on cell proliferation ……..... 35

Figure 2.7. Effects of five crude extracts on p62 expression levels …… 36

Figure 2.8. Effects of three crude extracts on p62 expression levels …… 37

Chapter 3

Figure 3.1. The flower and the fruits of *Arctium lappa* (Goboshi) …… 44

Figure 3.2. The flower and the fruits of *Forsythia suspensa* (Rengyo) ……..……..… 45

Figure 3.3. Chemical structures of ARG and ARC ……... 45

Figure 3.4. Effects of ARG and ARC on cell proliferation …….. 49

Figure 3.5. Effect of ARG on autophagy-related proteins…...…… 50

Figure 3.6. Effect of ARG on p62 expression levels …… 51

Figure 3.7. Effect of ARG on proliferation of MCF-7 cells and autophagy-related proteins …….……..…….…..... 52

Figure 3.8. Effects of 3-MA and CQ on autophagy-related proteins …… 53

Figure 3.9. Effect of ARG on starvation-induced LC3-II expression levels ...……. 54

Figure 3.10. Effect of ARG on increased autophagosome/autolysosome formation by starvation 55

Figure 3.11. Effect of ARG on the activation of caspase-3 and PARP cleavage …… 56
Figure 3.12. Proposed mechanism of inhibition of autophagy by ARG, 3-MA, and CQ……..……... 58

Chapter 4

Figure 4.1. The flower and the rhizome of *Dioscorea tokoro* (Hikai) ……..…. 63
Figure 4.2. Effects of fractions prepared from Hikai extract on cell proliferation ……. 69
Figure 4.3. Effect of *n*-BuOH fraction on LC3-II and p62 expression levels…...…….. 70
Figure 4.4. Chemical structures of **1–5** from *n*-BuOH fraction …….……..…. 72
Figure 4.5. Effects of **1–5** on cell proliferation ……..…. 73
Figure 4.6. Effects of **1–5** on LC3-II and p62 expression levels……...…….. 74
Figure 4.7. Effects of **1–3** on the activation of caspase-3 and PARP cleavage…...…... 75

Chapter 5

Figure 5.1. The flower and the root of *Saussurea lappa* (Mokko)…… 80
Figure 5.2. Chemical structures of CL and DCL …….…….. 81
Figure 5.3. Effects of fractions prepared from Mokko extract on cell proliferation ….. 86
Figure 5.4. Effect of hexane fraction on LC3-II and p62 expression levels ….…..... 87
Figure 5.5. TLC analysis of CL, DCL, MeOH extract, and fractions …… 88
Figure 5.6. HPLC chromatograms of CL, DCL, MeOH extract, and fractions……. 89
Figure 5.7. Effects of CL and DCL on cell proliferation ……..…….……..... 90
Figure 5.8. Effects of CL and DCL on LC3-II and p62 expression levels …...…..…… 91
Figure 5.9. Effects of CL and DCL on the activation of caspase-3 and PARP cleavage ……..……...……..... 92
Figure 5.10. Effects of ETP on LC3-II and p62 expression levels ……...……..…. 93

Chapter 6

Figure 6.1. Schematic illustrating the results of screening using crude extract library.. 100
Figure 6.2. Summary of autophagy-inhibiting compounds identified in this thesis ….. 103

Chapter 1

General introduction

1.1. Autophagy and its molecular mechanisms

Macroautophagy (hereafter, autophagy) is an evolutionarily conserved and self-consumption process that degrades cellular organelles and proteins and maintains cellular biosynthesis during nutrient deprivation or metabolic stress [1–4]. Accumulating evidence has indicated the importance of autophagy in various human diseases [2–4]. The steps in autophagy are initiation, phagophore elongation, autophagosome formation and maturation, autophagosome fusion with the lysosome, and proteolytic degradation of the contents (Fig. 1.1) [1–4]. The products of degradation are recycled back into the cytosol and are reused to enhance cell survival during nutrient deprivation. In response to starvation, autophagy provides a nutrient source, promoting cell survival; however, autophagy is also induced by a broad range of other stressors and can degrade protein substrates, oxidized lipids, and damaged organelles [1–5].

The entire autophagy process is complex and involves many critical proteins. Among these, microtubule-associated protein light chain 3 (LC3) and sequestosome 1/p62 (p62) are responsible for autophagy's membranes remodeling and trafficking events (Fig. 1.1) [6–12]. LC3 is an autophagosome membrane-bound protein that was first found in mammals [6]. Although there are several proteins that bind to the phagophore and autophagosome membranes, LC3 is widely used as a standard marker for these membranes because its binding is particularly stable [6]. After LC3 is synthesized as proLC3, it is immediately cleaved by cysteine protease to form LC3-I. Covalent binding of phosphatidylethanolamine to LC3-I results in LC3-II, which localizes to the phagophore and autophagosome membranes. The amount of LC3-II is

proportional to the number of autophagosomes present within the cell [6,7]. The protein p62 is a multifunctional signaling molecule involved in a variety of cellular pathways [8–12] that contains an ubiquitin-associated (UBA) domain for binding to ubiquitinated proteins. The presence of the UBA domain enables p62 to serve as an adaptor for selective autophagy of ubiquitinated substrates [8]. In addition, p62 itself can translocate not only to the phagophore membrane but also to the autophagosome formation site, even doing so independently of LC3 binding [12]. Therefore, p62 is a critical autophagic substrate and is widely used as an indicator of autophagic degradation [13]. Moreover, beclin-1 is also one of the most important proteins for autophagy. While beclin-1 is generally ubiquitously expressed, it can also stimulate autophagy when overexpressed in mammalian cells [14]. It is known that beclin-1 is directly phosphorylated by AMP-activated protein kinase (AMPK) to induce autophagy [15]. Thus, an increase in the expression levels of p-beclin 1 indicates induction of autophagy.

The number of autophagosomes is known as an indicator of the level of autophagic activity. However, only the assessment of autophagosome numbers is not enough to monitor reliable autophagy steps because that the autophagosome is an intermediate structure in the dynamic process of autophagy. The analysis of the degradation of autophagic substrates inside the lysosome, which is a phenomenon of final step of autophagy, is a more reliable indicator of autophagy. Most studies of the autophagy process have examined the effects of inducers/inhibitors on autophagy-related proteins by immunoblotting analysis, and then observed these proteins by microscopic analysis.

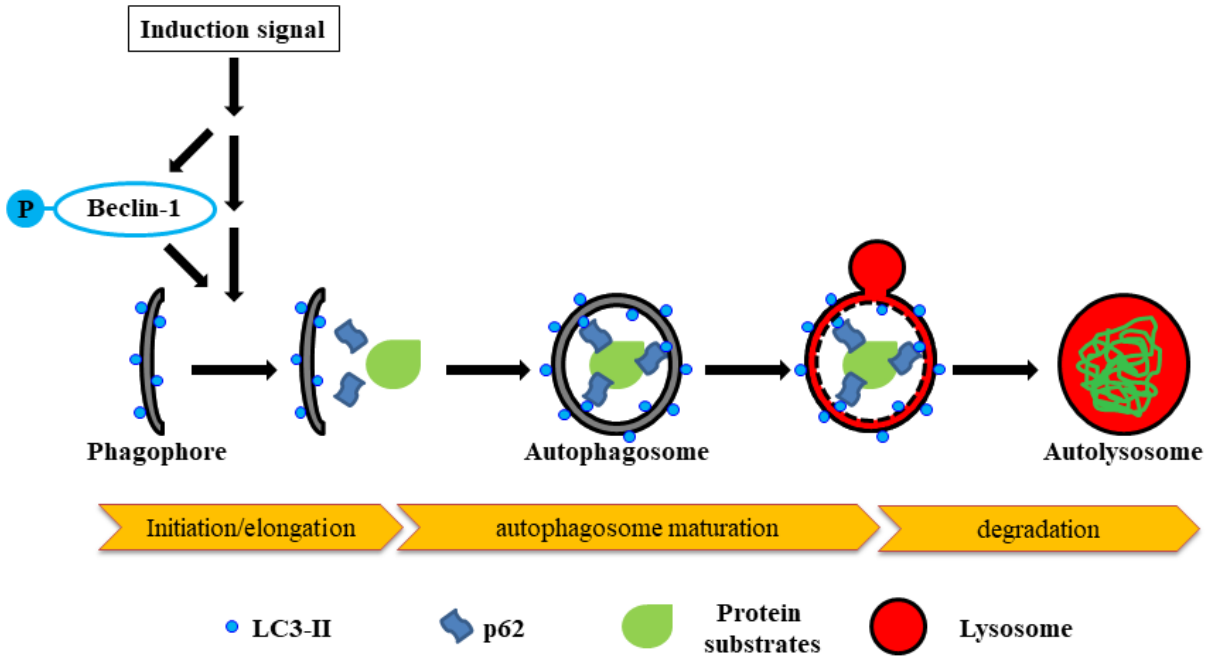

Figure 1.1. Schematic diagram to illustrate the process of autophagy and in the role of LC3-II, p62, and beclin-1. Protein substrates (a portion of cytoplasm, including organelles) are enclosed by a phagophore or isolation membrane to form an autophagosome. The outer membrane of the autophagosome subsequently fuses with the lysosome, and the internal material is degraded in the autolysosome. LC3-II is present both inside and outside of the autophagosome membrane, and the amount of LC3-II is proportional to the number of autophagosomes present in the cell. On the other hand, p62 is localized only inside the autophagosome in the autophagy process, thus the amount of p62 is widely used as an indicator of autophagic degradation. While beclin-1 is generally ubiquitously expressed, which can also stimulate autophagy when overexpressed. Beclin-1 is directly phosphorylated by AMPK to induce autophagy.

1.2. Relationship between autophagy and cancer

In contrast to normal cells in tissues, tumors often locate within an environment deprived of nutrients, growth factors, and oxygen as a result of insufficient or abnormal vascularization. Thus, autophagy is important for supporting tumor growth (Fig. 1.2) [16–19]. In cancers, both the upregulation and downregulation of autophagy have been observed, which indicates its dual oncogenic and tumor-suppressing properties during malignant transformation [18, 19]. Liver cancer is the second leading cause of cancer-related death and the sixth most diagnosed cancer worldwide [20]. Autophagy plays multiple roles in maintaining liver homeostasis. In the absence of autophagy-related genes -5 and -7, which are key genes involved in autophagy initiation, nonfunctional proteins and organelles accumulate in liver cells [21]. It has been reported that autophagy-related gene 7-conditional knockout mice developed hepatomegaly and different metabolic liver disorders [22]; therefore, autophagy is important for suppressing tumorigenesis in the liver. It has been reported that in advanced hepatocellular carcinomas, autophagy plays an oncogenic (pro-survival) role observed as an increased LC3-II expression levels that positively correlates with progression of malignancy and a poor prognosis [23].

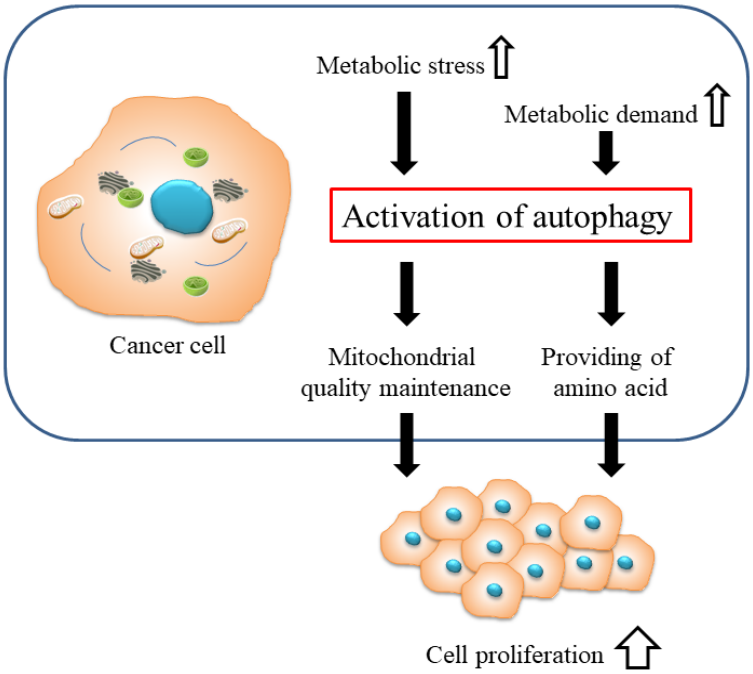

Figure 1.2. High metabolic demand of cancer cell and activation of autophagy. Tumor cells are exposed to metabolic stress due to their high metabolic demand. To respond those, several tumor cells activate their own autophagy to produce the amino acids for the energy production.

The role of autophagy in cancer is complex because it depends on tumor type, stage, and genetic context. In addition, autophagy acts potently to either promote or inhibit tumorigenesis, leading to a complex picture of the relationship between autophagy and cell proliferation [24]. To implement an attractive tool for cancer therapy, further studies to elucidate the role of autophagy in cancer will be required. However, at present, there have been few reports of compounds with modulation of autophagy. Therefore, it would be desirable if more such compounds could be discovered.

1.3. Autophagy modulators

For medical purposes, it is valuable to identify compounds that induction or inhibition of autophagy [1-5, 13, 16-19, 23–28]. Autophagy inducers may have specific value in certain neurodegenerative diseases, some infectious diseases, and cytoprotection [1-5, 27]. The most potent known physiological inducer of autophagy is starvation (amino acid withdrawal), which induces autophagy within 1 h after starvation in most cell lines [13]. The mammalian target of rapamycin (mTOR) is known as a potent suppressor of autophagy [13]. Drugs or signals that modulate autophagy can be divided into two categories, depending on whether they act via mTOR or not [13, 27]. Rapamycin and its analogs CCI-779, which are mTOR inhibitors, and torin 1, which is an ATP-competitive inhibitor of mTOR, are well-known as mTOR-dependent autophagy inducers [13, 27]. On the other hand, several compounds have been reported to induce autophagy without the involvement of mTOR. Lithium and carbamazepine induce autophagy through inhibition of inositol and inositol-1,4,5-trisphosphate (Ins(1,4,5)P3) levels [13, 27, 28]. It is also reported that trehalose induces autophagy by inhibition of solute carrier 2A (SLC2A) and activation of 5' adenosine monophosphate-activated protein kinase [13, 19, 27]. Metformin, a widely used antidiabetic agent, activates AMPK and induces autophagy [19, 27, 28]. It is notable that neither mTOR-independent nor mTOR-dependent inhibitors are specific inducers of autophagy. In addition to autophagy activation, these compounds affect a wide range of cellular responses, particularly protein synthesis and cellular metabolism [13, 25]. For example, lithium attenuates autophagy through glycogen synthase kinase-3β inhibition (which is mTOR-dependent); therefore, if used to activate autophagy, lithium should always be combined with mTOR inhibitors [13].

On the other hand, it has been suggested that autophagy inhibition may be valuable in cancers [1-5, 13, 16-19, 21-28]. In addition, preclinical evidence has demonstrated the effectiveness of inhibiting autophagy to enhance chemotherapy-induced cytotoxicity [19, 25-

27]. Autophagy inhibitors can be divided according to whether inhibition occurs before or after autophagosome formation. In general, inhibition of autophagosome formation is recognized as early-stage inhibition, and inhibition of the degradation step after autophagosome formation is recognized as late-stage inhibition [24, 27, 28]. Because autophagosome formation requires class III phosphatidylinositol 3-kinase (PI3K) activity, inhibitors of PI3K, such as 3-methyladenine (3-MA), wortmannin, and LY294002, inhibit autophagy at an early-stage [13, 19, 28]. On the other hand, chloroquine (CQ), hydroxychloroquine (HCQ), bafilomycin A1, ammonium chloride, and Lys05 are known as suppressors at the late-stage of autophagy [13, 19, 24-28]. The use of CQ and HCQ is one of the most commonly used pharmacological approaches to inhibit autophagy in vitro and vivo [18, 19, 24-28]. HCQ is the preferred analog of CQ because of its enhanced potency and limited side effects when compared with CQ [29]. In addition, HCQ is one of the leading compound for anticancer drug development by modulating an autophagy [26]. CQ and HCQ are lysosomotropic agents with an extensive range of biological effects. CQ and HCQ accumulate in acidic lysosomes and increase the pH. Alteration of pH causes the inhibition of lysosomal hydrolases and the prevention of autophagosomal fusion and degradation, which can result in the inhibition of the autophagy process [18, 19, 25, 26, 29]. A large number of current clinical trials using HCQ indicates the enormous relevance of combinatory treatments with autophagy inhibition to overcome resistance to existing cancer therapies (Table 1.1) [19, 25, 26]. Moreover, although 3-MA is an early-stage inhibitor, the concentration is very high to inhibit autophagy process [13]. Therefore, it would be beneficial if a greater number of potent inhibitors affecting the early-stage of autophagy could be discovered.

Table 1.1. Current HCQ clinical trials.

Combination agent	Mode of action	Cancer phenotypes	Phase	Trial reference at ClinicalTrials.gov
(As a single agent)		ER + breast cancer	I	NCT02414776
Sunitinib	Tyrosine kinase inhibitor	Adult solid neoplasm	I	NCT00813423
Vorinostat	Histone deacetylase inhibitor	Malignant solid tumour	I	NCT01023737
Vorinostat or sirolimus	Histone deacetylase inhibitor/mTOR inhibitor	Advanced cancers	I	NCT01266057
MKK2206	Akt inhibitor	Advanced cancers	I	NCT01480154
Vorinostat	Histone deacetylase inhibitor	Colorectal cancer	I/II	NCT02316340
Gemcitabine	Anti-metabolite	Advanced adenocarcinoma	I/II	NCT01506973
Gemcitabine/carboplatin	Anti-metabolite/alkylating agent	Small cell lung cancer	I/II	NCT02722369
Interleukin-2	Immune modulator	Renal cell carcinoma	I/II	NCT01550367
(As a single agent)		Prostate cancer	II	NCT00726596
Capecitabine	Anti-metabolite	Pancreatic carcinoma	II	NCT01494155
Abraxane and gemcitabine	Anti-microtubule agent/anti-metabolite	Pancreatic carcinoma	II	NCT01978184

1.4. Natural products modulating autophagy

Recent studies have shown that natural products have beneficial effects on cancer therapy through autophagy [30–34]. Most of this research has reported that natural products induce autophagy in cancer cells. Berberine (BBR) (Fig. 1.3), an isoquinoline alkaloid isolated from *Coptis chinensis*, induces autophagic cell death by inhibiting the mTOR complex 1 through AMPK activation in human hepatocellular carcinoma HepG2 cells [30]. BBR was also reported to induce autophagic cell death by enhancing glucose-regulated protein 78 levels in HepG2 cells and human colon carcinoma HCT-116 and DLD1 cells [31].

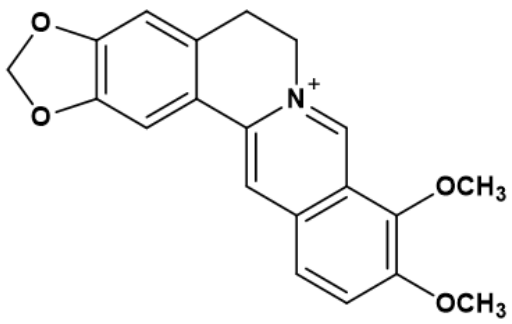

Figure 1.3. Chemical structures of BBR.

Zanthoxylum fruit extracts from the Japanese pepper plant *Zanthoxylum piperitum* enhance autophagic cell death through the phosphorylation of c-Jun N-terminal kinase in DLD1 cells [32]. On the other hand, it has recently been indicated that natural products also have beneficial effects on cancer therapy by inhibition of autophagy. RA-XII, a natural cyclopeptide isolated from *Rubia yunnanensis*, suppresses protective autophagy to enhance apoptosis through AMPK/mTOR/70 kDa ribosomal protein S6 kinase pathways in HepG2 cells [33].

Moreover, phyllanthusmins, which are isolated from various *Phyllanthus* species, inhibit late-stage autophagy by reducing lysosomal acidification, similar to the effects of bafilomycin A1 inhibiting autophagy at late-stage, and followed by apoptotic cell death in high-grade serous ovarian cancer (OVCAR3 and OVCAR8) cells [34]. These demonstrate the importance of identifying the modulators from natural products to intensify cancer therapy strategies that modulating autophagy.

1.5. Purpose of this thesis

The purpose of this thesis is to discover natural products that suppress cancer cell proliferation and autophagy modulation by screening our crude extract library based on traditional medicine and analyzing the molecular mechanisms of the products identified. This thesis is divided into four experimental chapters. First, in Chapter 2, we screened crude drug extracts to identify the extracts that modulated autophagy and cell proliferation in HepG2 cells. Subsequently, we demonstrated that the four extracts identified through screening showed inhibition of autophagy with high levels of antiproliferative activity. In Chapters 3, 4, and 5, we identified the active compounds that modulating autophagy in the four extracts and clarified their molecular mechanisms.

1.6. References

[1] Rabinowitz, J.D.; White, E. Autophagy and metabolism. *Science* **2010**, *330*, 1344–1348.

[2] Augustine, M.K.; Choi, M.D.; Stefan, W.; Ryter, P.H.D.; Beth Levine, M.D. Autophagy in human health and disease. *N. Engl. J. Med*. **2013**, *368*, 651–662.

[3] Lassen, K.G.; Xavier, R.J. Mechanisms and function of autophagy in intestinal disease. *Autophagy* **2018**, *14*, 216–220.

[4] Ueno, T.; Komatsu, M. Autophagy in the liver: Functions in health and disease. *Nat. Rev. Gastroenterol. Hepatol.* **2017**, *14*, 170–184.

[5] Maiuri, M.C.; Kroemer, G. Autophagy in stress and disease. *Cell Death Differ.* **2015**, *22*, 365–366.

[6] Kabeya, Y.; Mizushima, N.; Ueno, T.; Yamamoto, A.; Kirisako, T.; Noda, T.; Kominami, E.; Ohsumi, Y.; Yoshimori, T. LC3, a mammalian homologue of yeast Apg8p, is localized in autophagosome membranes after processing. *EMBO J.* **2000**, *19*, 5720–5728.

[7] Kabeya, Y.; Mizushima, N.; Yamamoto, A.; Oshitani-Okamoto, S.; Ohsumi, Y.; Yoshimori, T. LC3, GABARAP and GATE16 localize to autophagosomal membrane depending on form-II formation. *J. Cell Sci.* **2004**, *117*, 2805–2812.

[8] Geetha, T.; Wooten, M.W. Structure and functional properties of the ubiquitin binding protein p62. *FEBS Lett.* **2002**, *512*, 19–24.

[9] Seibenhener, M.L.; Babu, J.R.; Geetha, T.; Wong, H.C.; Krishna, N.R.; Wooten, M.W. Sequestosome 1/p62 is a polyubiquitin chain binding protein involved in ubiquitin proteasome degradation. *Mol. Cell. Biol.* **2004**, *24*, 8055–8068.

[10] Johansen, T.; Lamark, T. Selective autophagy mediated by autophagic adapter proteins. *Autophagy* **2011**, *7*, 279–296.

[11] Pankiv, S.; Clausen, T.H.; Lamark, T.; Brech, A.; Bruun, J.A.; Outzen, H.; Øvervatn, A.; Bjørkøy, G.; Johansen, T. p62/SQSTM1 binds directly to Atg8/LC3 to facilitate degradation of ubiquitinated protein aggregates by autophagy. *J. Biol. Chem.* **2007**, *282*, 24131–24145.

[12] Itakura, E.; Mizushima, N. p62 targeting to the autophagosome formation site requires self-oligomerization but not LC3 binding. *J. Cell. Biol*. **2011**, *192*, 17–27.

[13] Mizushima, N.; Yoshimori, T.; Levine, B. Methods in mammalian autophagy research. *Cell* **2010**, *140*, 313–326.

[14] Liang, X. H.; Jackson, S.; Seaman, M.; Brown, K.; Kempkes, B.; Hibshoosh, H.; Levine, B. Induction of autophagy and inhibition of tumorigenesis by beclin 1. *Nature* **1999**, *402*, 672–676.

[15] Kim, J.; Kim, Y.C.; Fang, C.; Russell, R.C.; Kim, J.H.; Fan, W.; Liu, R.; Zhong, Q.; Guan, K.L. Differential regulation of distinct Vps34 complexes by AMPK in nutrient stress and autophagy. *Cell* **2013**, *152*, 290–303.

[16] Degenhardt, K.; Mathew, R.; Beaudoin, B.; Bray, K.; Anderson, D.; Chen, G.; Mukherjee, C.; Shi, Y.; Gélinas, C.; Fan, Y.; et al. Autophagy promotes tumor cell survival and restricts necrosis, inflammation, and tumorigenesis. *Cancer Cell* **2006**, *10*, 51–64.

[17] Turcotte, S.; Chan, D.A.; Sutphin, P.D.; Hay, M.P.; Denny, W.A.; Giaccia, A.J. A molecule targeting VHL-deficient renal cell carcinoma that induces autophagy. *Cancer Cell* **2008**, *14*, 90–102.

[18] Yang, Z.J.; Chee, C.E.; Huang, S.; Sinicrope, F.A. The role of autophagy in cancer: Therapeutic implications. *Mol. Cancer Ther.* **2011**, *10*, 1533–1541.

[19] Marinković, M.; Šprung, M.; Buljubašić, M.; Novak, I. Autophagy modulation in cancer: Current knowledge on action and therapy. *Oxid. Med. Cell. Longev.* **2018**, *2018*, 8023821.

[20] Gravitz, L. Liver cancer. *Nature* **2014**, *516*, 7529.

[21] Takamura, A.; Komatsu, M.; Hara, T.; Sakamoto, A.; Kishi, C.; Waguri, S.; Eishi, Y.; Hino, O.; Tanaka, K.; Mizushima, N. Autophagy-deficient mice develop multiple liver tumors. *Genes. Dev.* **2011**, *25*, 795–800.

[22] Komatsu, M.; Waguri, S.; Ueno, T.; Iwata, J.; Murata, S.; Tanida, I.; Ezaki, J.; Mizushima, N.; Ohsumi, Y.; Uchiyama, Y.; et al. Impairment of starvation-induced and constitutive autophagy in Atg7-deficient mice. *J. Cell Biol.* **2005**, *169*, 425–434.

[23] Wu, D.H.; Jia, C.C.; Chen, J.; Lin, Z.X.; Ruan, D.Y.; Li, X.; Lin, Q.; Min-Dong; Ma, X.K.; Wan, X.B.; Cheng, N.; et al. Autophagic LC3B overexpression correlates with malignant progression and predicts a poor prognosis in hepatocellular carcinoma. *Tumour Biol.* **2014**, 12225–12233.

[24] Kimmelman, A.C. The dynamic nature of autophagy in cancer. *Genes Dev.* **2011**, *25*, 1999-2010.

[25] Bishop, E.; Bradshaw, T.D. Autophagy modulation: A prudent approach in cancer treatment? *Cancer Chemother. Pharmacol.* **2018**, *82*, 913–922.

[26] Cynthia, I.C.; Ravi, K.A. Targeting autophagy in cancer: Update on clinical trials and novel inhibitors. *Int. J. Mol. Sci.* **2017**, *18*, 1279.

[27] Panda, P.K.; Fahrner, A.; Vats, S.; Seranova, E.; Sharma, V.; Chipara, M.; Desai, P.; Torresi, J.; Rosenstock, T.; Kumar, D.; Sarkar, S. Chemical screening approaches enabling drug discovery of autophagy modulators for biomedical applications in human diseases. *Front. Cell Dev. Biol.* **2019**, *19*, 38.

[28] Rubinsztein, D.C.; Codogno, P.; Levine, B. Autophagy modulation as a potential therapeutic target for diverse diseases. *Nat. Rev. Drug Discov.* **2012**, *11*, 709–730.

[29] Finbloom, D.S.; Silver, K.; Newsome, D.A.; Gunkel, R. Comparison of hydroxychloroquine and chloroquine use and the development of retinal toxicity. *J. Rheumatol.* **1985**, *12*, 692–694.

[30] Yu, R.; Zhang, Z.Q.; Wang, B.; Jiang, H.X.; Cheng, L.; Shen, L.M. Berberine-induced apoptotic and autophagic death of HepG2 cells requires AMPK activation. *Cancer Cell Int*. **2014**, *14*, 49.

[31] La, X.; Zhang, L.; Li, Z.; Yang, P.; Wang, Y. Berberine-induced autophagic cell death by elevating GRP78 levels in cancer cells. *Oncotarget* **2017**, *8*, 20909–20924.

[32] Nozaki, R.; Kono, T.; Bochimoto, H.; Watanabe, T.; Oketani, K.; Sakamaki, Y.; Okubo, N.; Nakagawa, K.; Takeda, H. Zanthoxylum fruit extract from Japanese pepper promotes autophagic cell death in cancer cells. *Oncotarget* **2016**, *7*, 70437–70446.

[33] Song, L.; Wang, Z.; Wang, Y.; Guo, D.; Yang, J.; Chen, L.; Tan, N. Natural cyclopeptide RA-XII, a new autophagy inhibitor, suppresses protective autophagy for enhancing apoptosis through AMPK/mTOR/P70S6K pathways in HepG2 cells. *Molecules* **2017**, *22*, 1934.

[34] Young, A.N.; Herrera, D.; Huntsman, A.C.; Korkmaz, M.A.; Lantvit, D.D.; Mazumder, S.; Kolli, S.; Coss, C.C.; King, S.; Wang, H.; et al. Phyllanthusmin derivatives induce apoptosis and reduce tumor burden in high-grade serous ovarian cancer by late-stage autophagy inhibition. *Mol. Cancer Ther.* **2018**, *17*, 2123–2135.

Chapter 2

Screening of extracts prepared from crude drugs for autophagy-mediated cell survival of the human hepatocellular carcinoma cell line HepG2

2.1. Introduction

In Chapter 2, we screened 130 extracts prepared from different crude drugs in a comprehensive search for crude drugs able to modulate autophagy. Our laboratory has a crude drug extract (hereafter, crude extract) library containing these 130 different crude drugs (Table 2.1). These crude drugs are based on traditional medicines, including Japanese Kampo medicines. Although several biological activities of the crude drugs used in Kampo medicine have been evaluated, few studies have investigated their effects on autophagy.

Human hepatocellular carcinoma cell lines (HCC) such as HepG2 cells have long been used for autophagy research and are known to be highly sensitive to autophagy [1-7]. It is also known that several types of cancer cell are resistant to chemotherapeutic agents that are potent apoptosis inducers [8]. HCC including HepG2 cells are resistant to apoptosis because of the high expression of B-cell lymphoma-extra-large, which is an antiapoptotic member of the B-cell lymphoma-2 (Bcl-2) family [9]. Therefore, HepG2 cells are suitable for this study to identify crude extracts modulating autophagy under conditions of apoptosis resistance.

We first established an assay for analyzing autophagy and antiproliferation using 3-MA, CQ, and BBR as compounds that modulate autophagy in HepG2 cells. Next, we screened 130 different crude extracts. Finally, we investigated the effects of the selected crude extracts on cell proliferation and autophagy modulation.

Table 2.1. List of crude drugs.

Drug No.	Japanese Name	English Name	Scientific Name	Medicinal Part	Manufacturer
1	Akyo	Donkey Glue	*Equus asinus*	glue	Daido
2	Ireisen	Clematis Root	*Clematis chinensis, C. mandshurica, C. hexapetala*	root with rhizome	Tochimoto
3	Inchinko	Artemisia Capillaris Flower	*Artemisia capillaris*	capitulum	Uchida
4	Uikyo	Fennel	*Foeniculum vulgare*	fruit	Uchida
5	Uzu [a)]	Aconite Root	*Aconitum carmichaeli, A. japonicum*	tuberous root (mother root)	Tochimoto
6	Uyaku	Lindera Root	*Lindera strychnifolia*	root	Tochimoto
7	Engosaku	Corydalis Tuber	*Corydalis turtschaninovii*	tuber	Tochimoto
8	Ogi	Astragalus Root	*Astragalus membranaceus, A. mongholicus*	root	Tochimoto
9	Ogon	Scutellaria Root	*Scutellaria baicalensis*	root	Tochimoto
10	Obaku	Phellodendron Bark	*Phellodendron amurense, P. chinense*	bark	Tochimoto
11	Oren	Coptis Rhizome	*Coptis japonica, C. chinensis, C. deltoidea, C. teeta*	rhizome	Tochimoto
12	Onji	Polygala Root	*Polygala tenuifolia*	root or root bark	Tochimoto
13	Gaiyo	Artemisia Leaf	*Artemisia princeps, A. montana*	leaf and twig	Uchida
14	Kashi	Myrobalan Fruit	*Terminalia chebula*	fruit	Tochimoto
15	Kashu	Polygonum Root	*Polygonum multiflorum*	root	Uchida
16	Gajutsu	Zedoary	*Curcuma zedoaria*	rhizome	Tochimoto
17	Kakko	Pogostemon Herb	*Pogostemon cablin*	aerial part	Uchida
18	Kakkon	Pueraria Root	*Pueraria lobate*	root	Tochimoto
19	Kasseki	Aluminum Silicate Hydrate with Silicon Dioxide	-	-	Uchida
20	Karokon	Trichosanthes Root	*Trichosanthes kirilowii, T. kirilowii* var. *japonica, T. bracteata*	root	Tochimoto
21	Karonin	Trichosanthes Seed	*Trichosanthes kirilowii, T. kirilowii* var. *japonica, T. bracteata*	seed	Tochimoto
22	Kankyo [b)]	Processed Ginger	*Zingiber officinale*	rhizome	Tochimoto
23	Kanzo	Glycyrrhiza	*Glycyrrhiza uralensis, G. glabra*	root and stolon	Tochimoto
24	Kikyo	Platycodon Root	*Platycodon grandiflorum*	root	Tochimoto
25	Kikuka	Chrysanthemum Flower	*Chrysanthemum morifolium, C. indicum*	capitulum	Tochimoto
26	Kijitsu	Immature Orange	*Citrus aurantium* var. *daidai, C. aurantium, C. natsudaidai*	fruit	Tochimoto
27	Kyokatsu	Notopterygium	*Notopterygium incisum, N. forbesii*	rhizome and root	Tochimoto
28	Kyonin	Apricot Kernel	*Prunus armeniaca, P. armeniaca* var. *ansu, P. sibirica*	seed	Tochimoto
29	Kinginka	Lonicera Flower	*Lonicera japonica*	flower bud	Tochimoto
30	Kukoshi	Lycium Fruit	*Lycium chinense, L. barbarum*	fruit	Tochimoto
31	Kujin	Sophora Root	*Sophora flavescens*	root	Uchida

32	Keigai	Schizonepeta Spike	*Schizonepeta tenuifolia*	spike	Uchida
33	Keihi	Cinnamon Bark	*Cinnamomum cassia*	bark	Tochimoto
34	Kengoshi	Pharbitis Seed	*Pharbitis nil*	seed	Daido
35	Genjin	Scrophularia Root	*Scrophularia ningpoensis, S. buergeriana*	root	Tochimoto
36	Koka	Safflower	*Carthamus tinctorius*	tubulous flower	Tochimoto
37	Kobushi	Cyperus Rhizome	*Cyperus rotundus*	rhizome	Tochimoto
38	Koboku	Magnolia Bark	*Magnolia obovata, M. officinalis, M. officinalis* var. *biloba*	bark	Tochimoto
39	Goshitsu	Achyranthes Root	*Achyranthes fauriei, A. bidentata*	root	Tochimoto
40	Goshuyu	Euodia Fruit	*Euodia ruticarpa, E. officinalis, E. bodinieri*	fruit	Uchida
41	Goboshi	Burdock Fruit	*Arctium lappa*	fruit	Tochimoto
42	Gomishi	Schisandra Fruit	*Schisandra chinensis*	fruit	Daido
43	Saiko	Bupleurum Root	*Bupleurum falcatum*	root	Tochimoto
44	Saishin	Asiasarum Root	*Asiasarum sieboldii, A. heterotropoides* var. *mandshuricum*	root with rhizome	Tochimoto
45	Sankirai	Smilax Rhizome	*Smilax glabra*	tuber	Uchida
46	Sanzashi	Crataegus Fruit	*Crataegus cuneata, C. pinnatifida* var. *major*	pseudocarp	Uchida
47	Sanshishi	Gardenia Fruit	*Gardenia jasminoides*	fruit	Tochimoto
48	Sanshuyu	Cornus Fruit	*Cornus officinalis*	pulp of pseudocarp	Tochimoto
49	Sansho	Japanese Zanthoxylum Peel	*Zanthoxylum piperitum*	pericarp	Uchida
50	Sansonin	Jujube Seed	*Zizyphus jujuba* var. *spinosa*	seed	Tochimoto
51	San'yaku	Dioscorea Rhizome	*Dioscorea japonica, D. batatas*	rhizome	Tochimoto
52	Jio [c)]	Rehmannia Root	*Rehmannia glutinosa* var. *purpurea, R. glutinosa*	root	Tochimoto
53	Jukujio [c)]	Rehmannia Root	*Rehmannia glutinosa* var. *purpurea, R. glutinosa*	root	Tochimoto
54	Shion	Aster Root	*Aster tataricus*	root and rhizome	Uchida
55	Jikoppi	Lycium Bark	*Lycium chinense, L. barbarum*	root bark	Uchida
56	Shikon	Lithospermum Root	*Lithospermum erythrorhizon*	root	Tochimoto
57	Shisoshi	Perilla Fruit	*Perilla frutescens* var. *crispa*	fruit	Uchida
58	Shitsurishi	Tribulus Fruit	*Tribulus terrestris*	fruit	Uchida
59	Shitei	Persimmon Calyx	*Diospyros kaki*	calyx	Uchida
60	Shakuyaku	Peony Root	*Paeonia lactiflora*	root	Tochimoto
61	Jashoshi	Cnidium Monnieri Fruit	*Cnidium monnieri*	fruit	Uchida
62	Shajin	Adenophora Root	*Adenophora tetraphylla, A. stricta, A. triphylla, A. hunanensis*	root	Tochimoto
63	Shazenshi	Plantago Seed	*Plantago asiatica*	seed	Tochimoto
64	Shazenso	Plantago Herb	*Plantago asiatica*	entire plant	Tochimoto
65	Shukusha	Amomum Seed	*Amomum xanthioides*	seed mass	Tochimoto
66	Shokyo [b)]	Ginger	*Zingiber officinale*	rhizome	Tochimoto
67	Shobaku	Wheat	*Triticum aestivum*	fruit	Uchida
68	Shoma	Cimicifuga Rhizome	*Cimicifuga simplex, C. dahurica, C. foetida, C. heracleifolia*	rhizome	Tochimoto

69	Shin'i	Magnolia Flower	*Magnolia salicifolia, M. kobus, M. biondii, M. sprengeri*	flower bud	Tochimoto
70	Sekko	Gypsum	-	-	Tochimoto
71	Senkyu	Cnidium Rhizome	*Cnidium officinale*	rhizome	Tochimoto
72	Sentai	Cicada Slough	*Cryptotympana atrata, Platylomia pieli, Oncotympana maculaticollis, Tanna chekiangensis, Graptopsaltria tienta, Lyristes pekinensis, L. atrofasciatus, Meimuna mongolica, Leptosemia sakaii, Platypleura kaempferi* Distant or allied insects	cast-off shell	Tochimoto
73	Sojutsu	Atractylodes Lancea Rhizome	*Atractylodes lancea, A. chinensis*	rhizome	Tochimoto
74	Sohakuhi	Mulberry Bark	*Morus alba*	root bark	Uchida
75	Soboku	Sappan Wood	*Caesalpinia sappan*	duramen	Tochimoto
76	Soyo	Perilla Herb	*Perilla frutescens* var. *crispa*	leaf and tip of branch	Tochimoto
77	Daio	Rhubarb	*Rheum palmatum, R. tanguticum, R. officinale, R. coreanum*	rhizome	Uchida
78	Daihukuhi	Areca Pericarp	*Areca catechu, A. dicksonii*	pericarp	Uchida
79	Taiso	Jujube	*Zizyphus jujuba* var. *inermis*	fruit	Tochimoto
80	Takusha	Alisma Tuber	*Alisma orientale*	tuber	Tochimoto
81	Chikujo	Bamboo Culm	*Bambusa textilis, B. pervariabilis, B. beecheyana, B. tuldoides, Phyllostachys nigra* var. *henonis, P. bambusoides*	inner layer of culm	Tochimoto
82	Chimo	Anemarrhena Rhizome	*Anemarrhena asphodeloides*	rhizome	Tochimoto
83	Choji	Clove	*Syzygium aromaticum*	flower bud	Uchida
84	Chotoko	Uncaria Hook	*Uncaria rhynchophylla, U. sinensis, U. macrophylla*	hook	Tochimoto
85	Chorei	Polyporus Sclerotium	*Polyporus umbellatus*	sclerotium	Tochimoto
86	Chimpi	Citrus Unshiu Peel	*Citrus unshiu, C. reticulata*	pericarp	Tochimoto
87	Tennansho	Arisaema Tuber	*Arisaema heterophyllum, A. erubescens, A. amurense*	tuber	Tochimoto
88	Temma	Gastrodia Tuber	*Gastrodia elata*	tuber	Matsuura
89	Temmondo	Asparagus Root	*Asparagus cochinchinensis*	root	Tochimoto
90	Togashi	Benincasa Seed	*Benincasa cerifera, B. cerifera* forma *emarginata*	seed	Tochimoto
91	Toki	Japanese Angelica Root	*Angelica acutiloba, A. acutiloba* var. *sugiyamae*	root	Tochimoto
92	Todokukatsu	Angelica Pubescens Root	*Angelica pubescens, A. biserrata*	root	Tochimoto
93	Tonin	Peach Kernel	*Prunus persica, P. persica* var. *davidiana*	seed	Tochimoto
94	Dokukatsu	Aralia Rhizome	*Aralia cordata*	rhizome	Tochimoto
95	Tochu	Eucommia Bark	*Eucommia ulmoides*	bark	Tochimoto
96	Ninjin	Ginseng	*Panax ginseng*	root	Tochimoto
97	Baimo	Fritillaria Bulb	*Fritillaria verticillata* var. *thunbergii*	bulb	Tochimoto
98	Bakuga	Malt	*Hordeum vulgare*	caryopsis	Uchida
99	Bakumondo	Ophiopogon Root	*Ophiopogon japonicus*	enlarged part of root	Tochimoto

100	Hakka	Mentha Herb	*Mentha arvensis* var. *piperascens*	aerial part	Tochimoto
101	Hange	Pinellia Tuber	*Pinellia ternate*	tuber	Tochimoto
102	Hishinomi	Water Chestnut	*Trapa japonica, T. incisa,T. japonica* var. *rubeola*	fruit	Tochimoto
103	Byakugo	Lilium Bulb	*Lilium lancifolium, L. brownii* var. *colchesteri, L. brownie, L. pumilum*	scaly leaf	Tochimoto
104	Byakushi	Angelica Dahurica Root	*Angelica dahurica*	root	Tochimoto
105	Byakujutsu	Atractylodes Rhizome	*Atractylodes japonica, A. macrocephala*	rhizome	Tochimoto
106	Biwayo	Loquat Leaf	*Eriobotrya japonica*	leaf	Tochimoto
107	Binroji	Areca	*Areca catechu*	seed	Tochimoto
108	Bukuryo	Poria Sclerotium	*Wolfiporia cocos*	sclerotium	Tochimoto
109	Boi	Sinomenium Stem and Rhizome	*Sinomenium acutum*	stem and rhizome	Tochimoto
110	Bokon	Imperata Rhizome	*Imperata cylindrica*	rhizome	Tochimoto
111	Bofu	Saposhnikovia Root and Rhizome	*Saposhnikovia divaricata*	root and rhizome	Tochimoto
112	Hobushi [a)]	Processed Aconite Root	*Aconitum carmichaeli, A. japonicum*	tuberous root (daughter root)	Tochimoto
113	Botampi	Moutan Bark	*Paeonia suffruticosa*	root bark	Tochimoto
114	Mao	Ephedra Herb	*Ephedra sinica, E. intermedia, E. equisetina*	aerial stem	Tochimoto
115	Mashinin	Hemp Fruit	*Cannabis sativa*	fruit	Uchida
116	Mankeishi	Shrub Chaste Tree Fruit	*Vitex rotundifolia, V. trifolia*	fruit	Uchida
117	Mokutsu	Akebia Stem	*Akebia quinata, A. trifoliata*	stem	Uchida
118	Mokko	Saussurea Root	*Saussurea lappa*	root	Tochimoto
119	Yakuchi	Bitter Cardamon	*Alpinia oxyphylla*	fruit	Uchida
120	Yakumoso	Leonurus Herb	*Leonurus japonicus, L. sibiricus*	aerial part	Tochimoto
121	Yokuinin	Coix Seed	*Coix lachryma-jobi* var. *mayuen*	seed	Tochimoto
122	Ryugan'niku	Longan Aril	*Euphoria longana*	aril	Tochimoto
123	Ryutan	Japanese Gentian	*Gentiana scabra, G. manshurica, G. triflora*	root and rhizome	Uchida
124	Ryokyo	Alpinia Officinarum Rhizome	*Alpinia officinarum*	rhizome	Kinokuniya
125	Rengyo	Forsythia Fruit	*Forsythia suspensa*	fruit	Tochimoto
126	Renniku	Nelumbo Seed	*Nelumbo nucifera*	seed	Tochimoto
127	Tanjin	Salvia Miltiorrhiza Root	*Salvia miltiorrhiza*	root	Takasago
128	Hanshiren	Barbated Skullcup Herb	*Scutellaria barbata*	entire plant	Kojima
129	Byakkajazetsuso	Oldenlandia diffusa	*Hedyotis diffusa* var. *longipe*	entire plant	Kojima
130	Hikai	Dioscorea	*Dioscorea tokoro*	rhizome	Tochimoto

a,b,c) specific processing is different

2.2. Materials and methods

2.2.1. Preparation of crude extracts

All crude drugs were purchased from one of the following manufacturers, respectively; Daido Pharmaceutical Co., Ltd. (Daido: Toyama, Japan); Kinokuniya Han Pharmacy (Kinokuniya: Tokyo, Japan); Kojima Kampo Co., Ltd. (Kojima: Osaka, Japan); MATSUURA YAKUGYO Co., Ltd. (Matsuura: Aichi, Japan); Tochimoto Tenkaido Co., Ltd. (Tochimoto: Osaka, Japan); Takasago Pharmaceutical Co., Ltd. (Takasago: Osaka, Japan); or UCHIDA WAKANYAKU Ltd. (Uchida: Tokyo, Japan). See Table 2.1 for details. All crude drug samples met the grade standards of the Japanese Pharmacopoeia 17th Edition (Pharmaceutical and Medical Device Regulatory Science Society of Japan, 2016) or the Japanese standards for non-Pharmacopoeial crude drugs 2018. The quality managers of each manufacturer identified and certificated the plant species. Five grams was extracted from each crude drug overnight at room temperature using methanol (MeOH). The supernatant was evaporated under nitrogen gas to obtain the crude extract. The crude extracts were dissolved in dimethyl sulfoxide (DMSO) as a stock solution at a concentration of 100 mg/mL and stored at −20 °C.

2.2.2. Reagents

BBR (purity > 90%), Etoposide (ETP, purity > 98%), and 3-MA (purity > 98%) were purchased from FUJIFILM Wako Pure Chemical Corporation (Osaka, Japan). CQ (purity > 98%) was purchased from Nacalai Tesque Industries (Kyoto, Japan). Antibodies against LC3B and p62 were obtained from Cell Signaling Technology (Beverly, MA, USA). The antibody against β-actin and RIPA lysis buffer were purchased from Santa Cruz Biotechnology (Santa Cruz, CA, USA). Fetal bovine serum (FBS) was purchased from GIBCO (Gaithersburg, MD, USA). All other materials were obtained from FUJIFILM Wako Pure Chemical Corporation.

2.2.3. Cell culture and treatment

HepG2 cells were obtained from the RIKEN BioResource Center Cell Bank (Ibaraki, Japan). The cells were grown in Dulbecco's modified Eagle's medium (DMEM) supplemented with 10% FBS and 1% penicillin-streptomycin-L-glutamine and incubated at 37 °C with 5% CO_2 under fully humidified conditions. During the cell treatments, the concentration of DMSO in the cell culture medium did not exceed 0.2% (v/v), and the controls were always treated with the same amount of DMSO as was used in the corresponding experiments.

2.2.4. Western blot analysis

Cells (1×10^6 cells/dish) were plated on 6 cm dishes. After replacing with fresh medium, the cells were treated with each crude extract or BBR for various time periods, after which they were harvested and lysed in RIPA lysis buffer containing protease and phosphatase inhibitors. After centrifugation for 15 min at 12,000 × g and 4 °C, the protein content of the samples was determined using a dye-binding protein assay kit, following the manufacturer's instructions (Bio-Rad, Richmond, CA, USA). Equal amounts of lysate protein were subjected to SDS-PAGE. The proteins were electrotransferred to PVDF membranes and detected as previously described [10]. BBR was then used as a positive control [3,4]. The relative intensity of the indicated band was quantified using ImageJ software (1.50i; Java 1.6.0_24 (64-bit), National Institutes of Health, Bethesda, MD, USA), and the value was normalized to corresponding loading control and expressed as the fold change in the control group.

2.2.5. Determination of cell proliferation

Cell proliferation was determined using a 3-(4,5-dimethylthiazol-2-yl)-2,5-diphenyltetrazolium bromide (MTT) assay. The number of 0.9×10^4 cells/well were cultured on 96-well plates. After replacing the original medium with a fresh medium, the cells were

treated with various concentrations of each crude extract for 24 h. At the end of treatment, 10 μL of 5 mg/mL MTT solution was added to each well, and the cells were incubated for another 4 h. The precipitated MTT-formazan was dissolved in 100 μL of 0.04 N HCl-isopropanol, and the amount of formazan was measured at 595 nm using an iMark microplate reader (Bio-Rad, Tokyo, Japan). Cell proliferation was expressed as a percentage of that for the control culture.

2.2.6. Statistical analysis

All data were derived from at least three independent treatment repetitions. The results are expressed as the mean ± S.D. under each condition. The data were analyzed by ANOVA followed by Tukey's test using GraphPad Prism 6 software (San Diego, CA, USA), and $p < 0.05$ was considered statistically significant.

2.3. Results

2.3.1. Establishment of an assay for autophagy-mediated cell survival

As described in Chapter 1.3, 3-MA and CQ are known as autophagy inhibitors. 3-MA inhibits the early-stage of autophagy by suppressing autophagosome maturation [1]. On the other hand, CQ blocks the late-stage of autophagy by inhibiting proteolytic degradation [1]. To define the stages of autophagy inhibition that can be evaluated in this assay, we first examined the effects of 3-MA and CQ on each autophagy-related protein. The expression level of LC3-II generally correlates with the number of autophagosomes [11, 12]. Thus, we examined the effect of 3-MA and CQ on LC3-II levels in HepG2 cells. The cells were treated with 3-MA at 5 mM or CQ at 25 μM for various time periods, respectively. Protein levels were examined using western blotting. As shown in Fig. 2.1A, 3-MA showed a weak induction of LC3-II level. Conversely, CQ showed a clear increase of LC3-II level.

To confirm that 3-MA and CQ are related to autophagy, it was necessary to determine the autophagic flux assessed by monitoring p62 levels. p62 directly interacts with LC3 on the isolated membrane, and subsequently p62 is incorporated into the autophagosome and then degraded [13, 14]. Previously, it was reported that the accumulation of p62 occurs when the late-stage of autophagy is inhibited [1, 6]. Therefore, we conducted a time-course experiment to determine the effect of 3-MA and CQ on p62 levels. As shown in Fig. 2.1B, 3-MA showed no apparent accumulation of p62, and conversely, CQ showed a clear accumulation of p62.

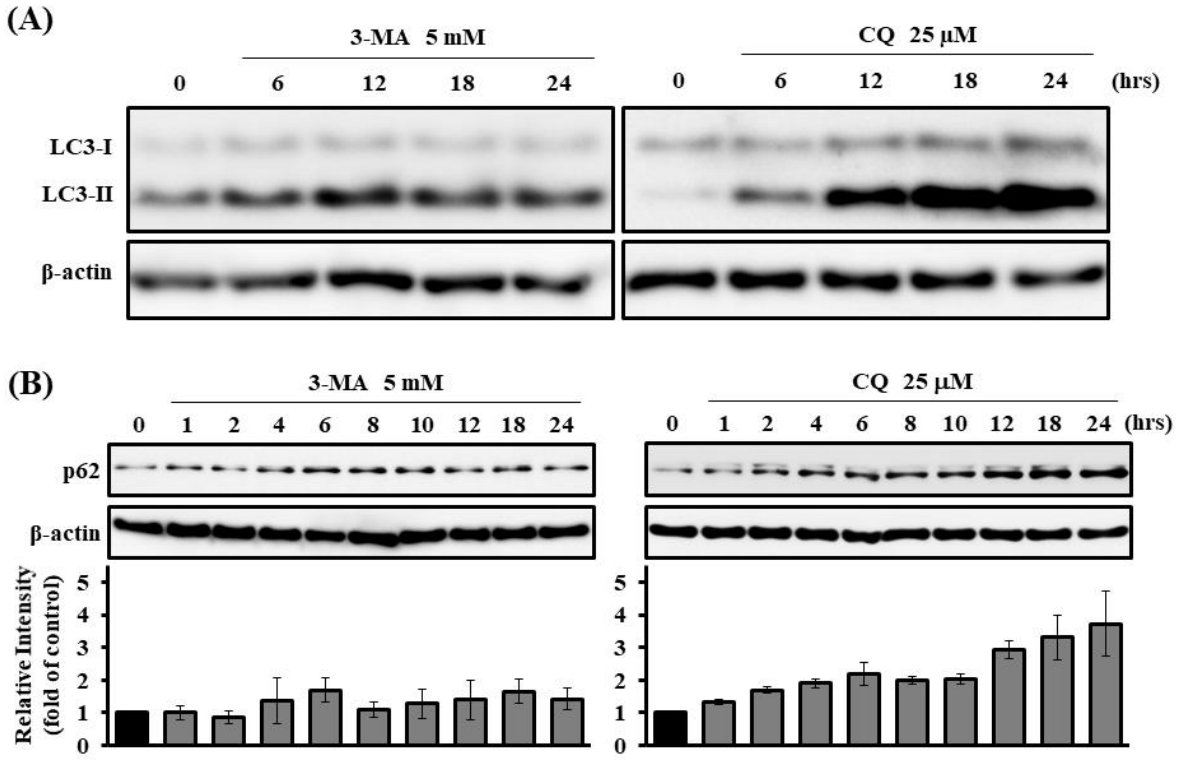

Figure 2.1. Effects of 3-MA and CQ on LC3-II and p62 expression levels. HepG2 cells were treated with 3-MA (5 mM) or CQ (25 μM) for the times indicated. The expression levels of LC3B (A), p62 (B), and β-actin were determined by western blotting. Relative intensity of p62 is shown as a bar graph. The data shown are representative of three independent treatments using the same parameters with similar results.

In previous studies, we reported that BBR (see page 9, Chapter 1, Fig. 1.3), an isoquinoline alkaloid contained in *Coptis japonica* and *Phellodendron amurense*, suppresses the proliferation of HL-60 cells [15]. It has been reported that BBR causes autophagic cell death by excessively inducing autophagy in HepG2 cells [3, 4]. Based on the above, we established an assay for analyses of autophagy and antiproliferation using BBR as an autophagy-inducing compound. First, we examined the effect of BBR on LC3-II level in HepG2 cells. The cells were treated with BBR at 10 and 50 μM for 24 h. As shown in Fig. 2.2A, BBR treatment remarkably increased LC3-II level at 50 μM. Next, to examine the optimum time for treatment,

the cells were treated with BBR at 50 μM for various time periods. As shown in Fig. 2.2B, BBR increased LC3-II level when the treatment time was more than 18 h; thus, we decided to treat the cells with each crude extract for 24 h to evaluate the expression level of LC3-II.

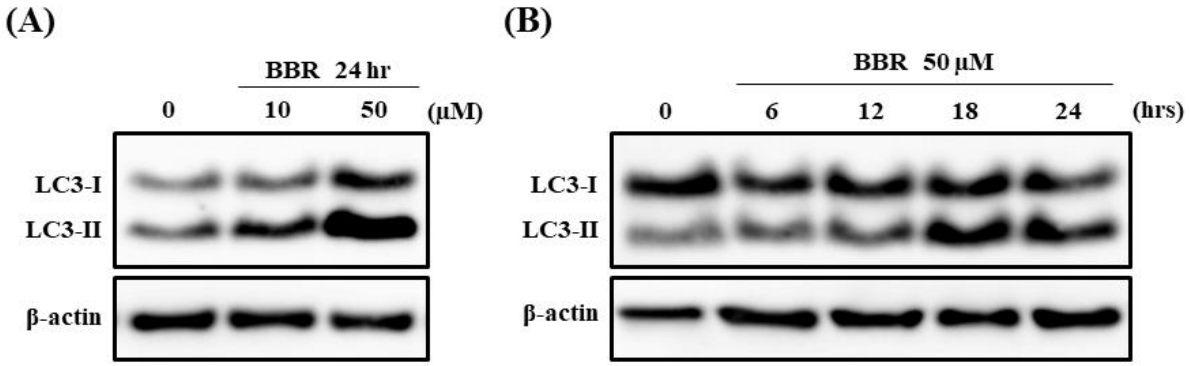

Figure 2.2. Effect of BBR on LC3-II expression levels. HepG2 cells were treated with 10 or 50 μM BBR for 24 h (A), and cells were treated with BBR (50 μM) for the times indicated (B). The expression levels of LC3B and β-actin were determined by western blotting. The data shown are representative of three independent treatments using the same parameters with similar results.

It has been suggested that autophagy is intimately related to the proliferation of cancer cells [3-6, 16-20]; therefore, we next investigated the effects of BBR on the proliferation of HepG2 cells. The cells were treated with BBR at various concentrations for 24 or 48 h, and cell proliferations were determined using MTT assay. As shown in Fig. 2.3, significant decrease in the proliferation of HepG2 cells was observed in the presence of BBR.

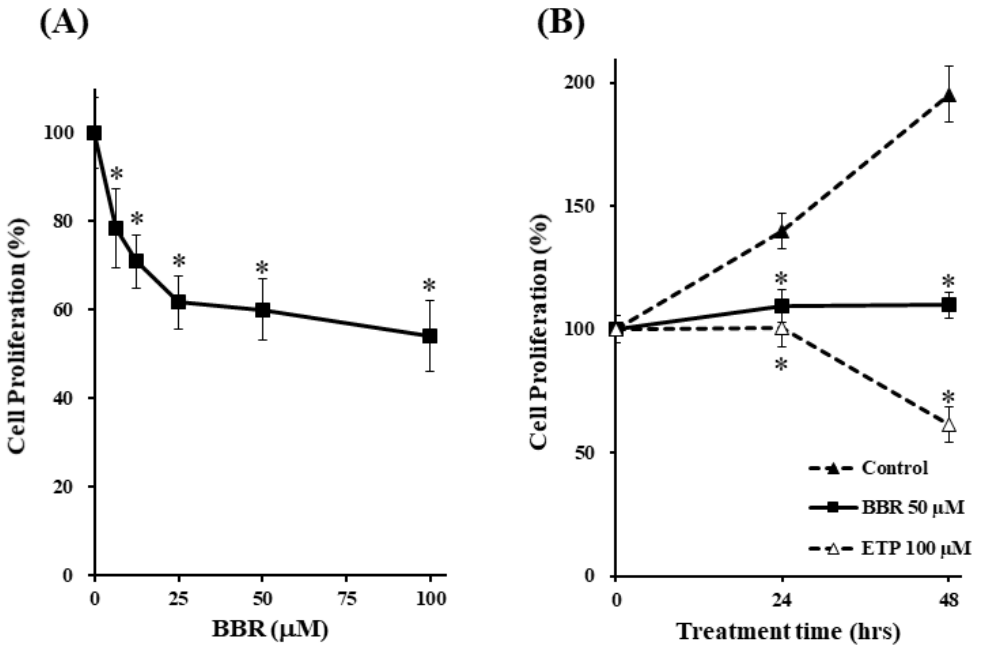

Figure 2.3. Effect of BBR on cell proliferation. HepG2 cells were treated with BBR at various concentrations for 48 h (A), and cells were treated with BBR (50 μM) for the times indicated (B) and cell proliferations were determined using MTT assay. ETP was used as a model for inducing apoptotic cell death against HepG2 cells [21]. The data are presented as the mean ± S.D. of three individual experiments. $*p < 0.05$ compared with the control group.

As with 3-MA and CQ, we conducted a time-course experiment to determine the effect of BBR on p62 level. Previously, it was reported that p62 is rapidly degraded by the autophagosome when autophagy is activated by starvation, and then recovers to basal levels after several hours in HepG2 cells [22]. As shown in Fig. 2.4, BBR temporarily decreased p62 level upon a short period of incubation (approximately 4 h) and then the level recovered to basal level after 12 h. Therefore, the p62 levels with BBR treatment were consistent with the autophagy-inducing characteristics; these results agree with previous studies indicating that BBR induces autophagy.

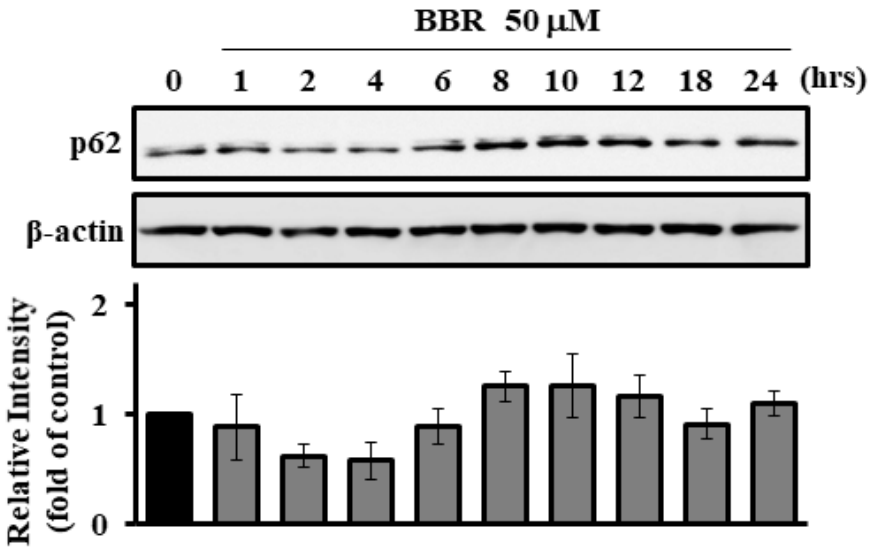

Figure 2.4. Effect of BBR on p62 expression levels. HepG2 cells were treated with BBR (50 μM) for the times indicated. The expression levels of p62 and β-actin were determined by western blotting. Relative intensity of p62 is shown as a bar graph. The data shown are representative of three independent treatments using the same parameters with similar results.

As described above, we decided to apply this assay established using 3-MA, CQ, and BBR to screen each crude extract for the investigation of autophagic activity. As shown in Table 2.2, this assay can divide crude extracts into autophagy inducers or late-stage inhibitors by the observation of LC3-II level. Subsequently, the results of p62 accumulation by extracts can determine autophagy inducers or late-stage inhibitors.

Table 2.2. Effects of each autophagy modulator on LC3-II and p62 expression levels.

Modulation of autophagy		Modulator	LC3-II	p62
Inhibition	Early-stage	3-MA	→	→
	Late-stage	CQ	↑↑	↑↑
Induction		Starvation [22]	↑↑	↓ or →
		BBR	↑↑	↓ or →

2.3.2. Effects of 130 crude extracts on autophagosome formation

We next investigated the effects of MeOH extracts prepared from the crude drugs on the levels of LC3-II in HepG2 cells. The cells were treated with 130 crude extracts at 20 μg/mL for 24 h. LC3-II levels were examined using western blotting, and the band intensities were quantified and expressed as the fold changes relative to those in the control. BBR was used as a positive control (Fig. 2.2). As shown in Fig. 2.5A and B, among the 130 crude extracts, 24 crude extracts, which are shown in black stars and columns, increased LC3-II levels, which suggests that they might exhibit modulation of autophagy.

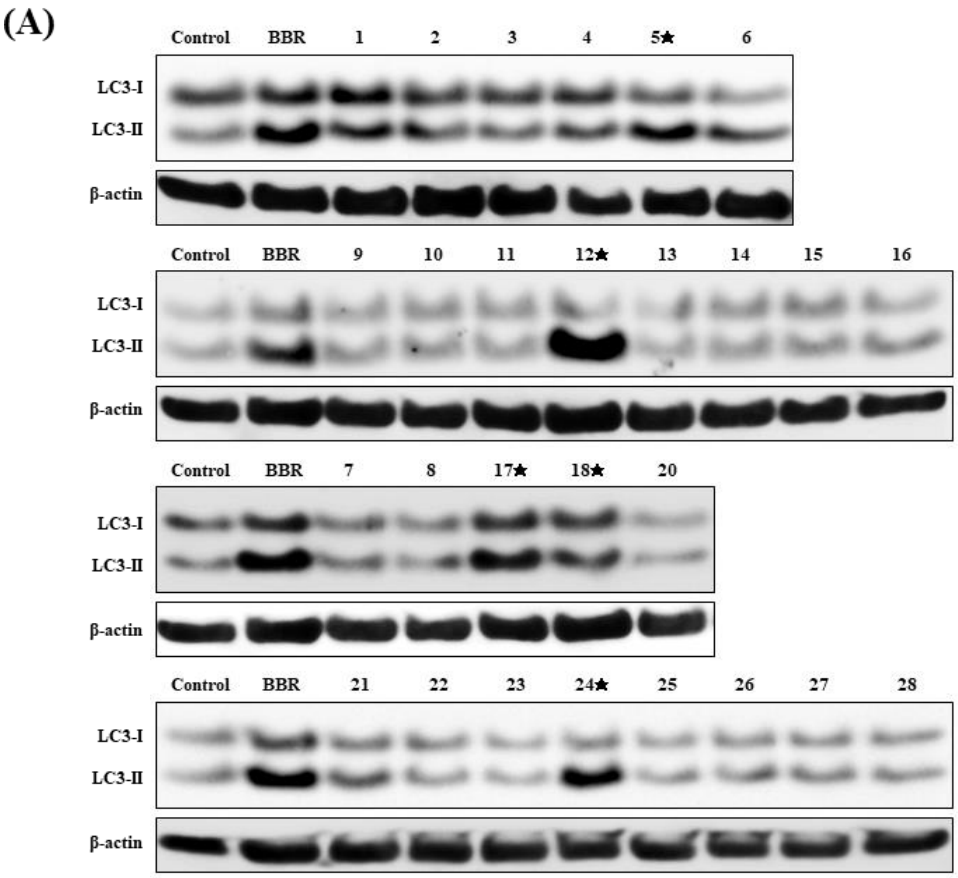

Figure 2.5. *Cont.*

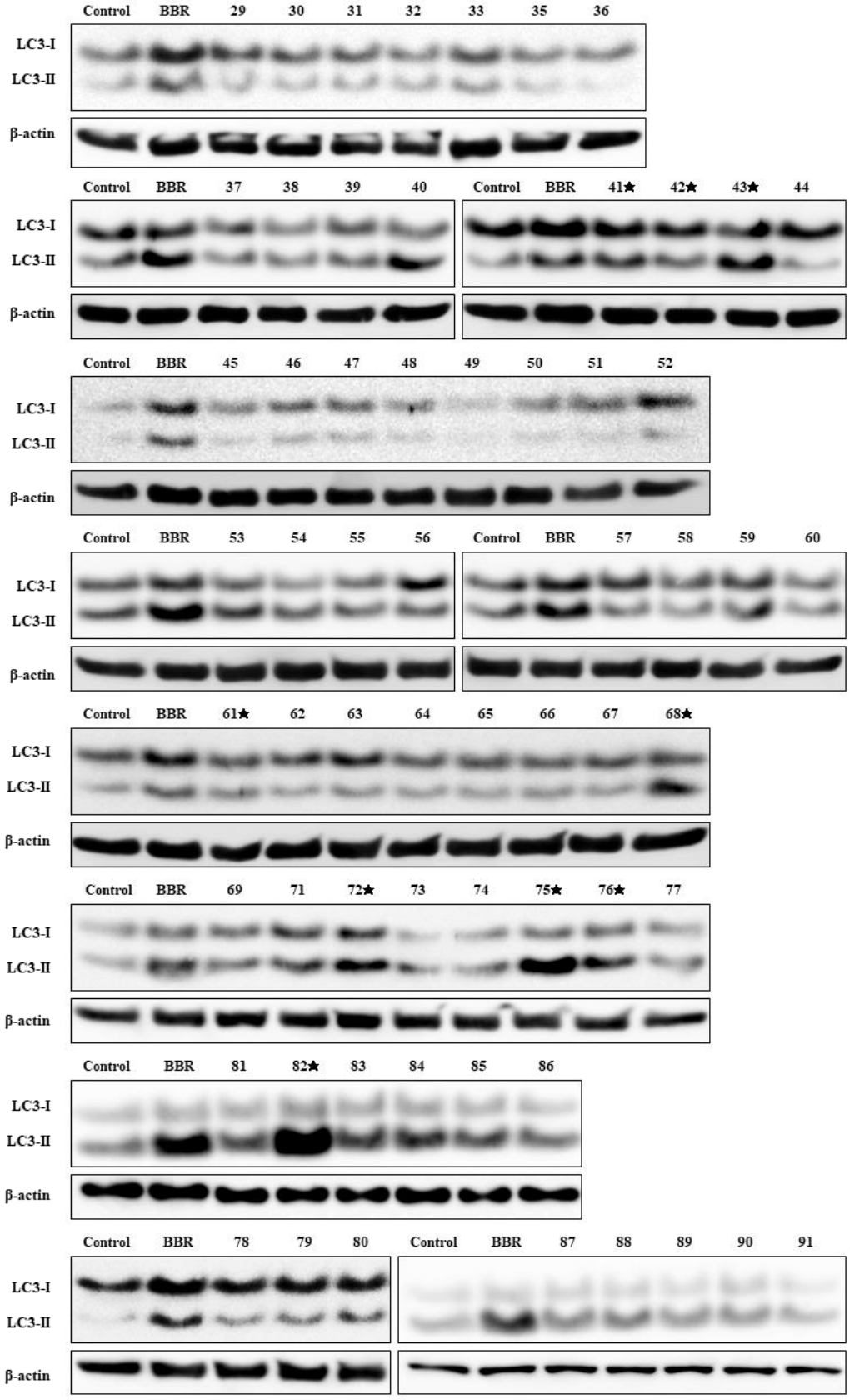

Figure 2.5. *Cont.*

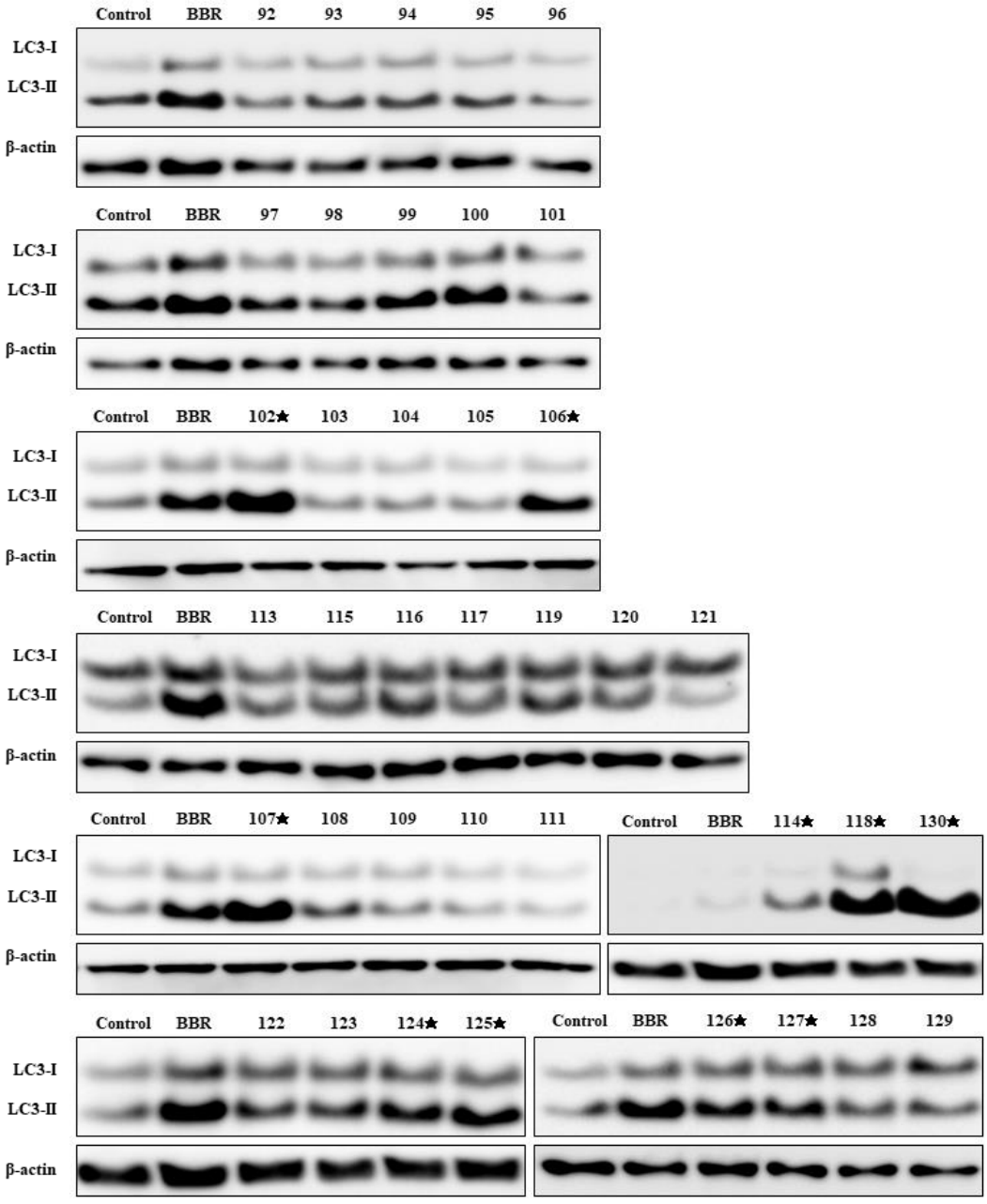

Figure 2.5. *Cont.*

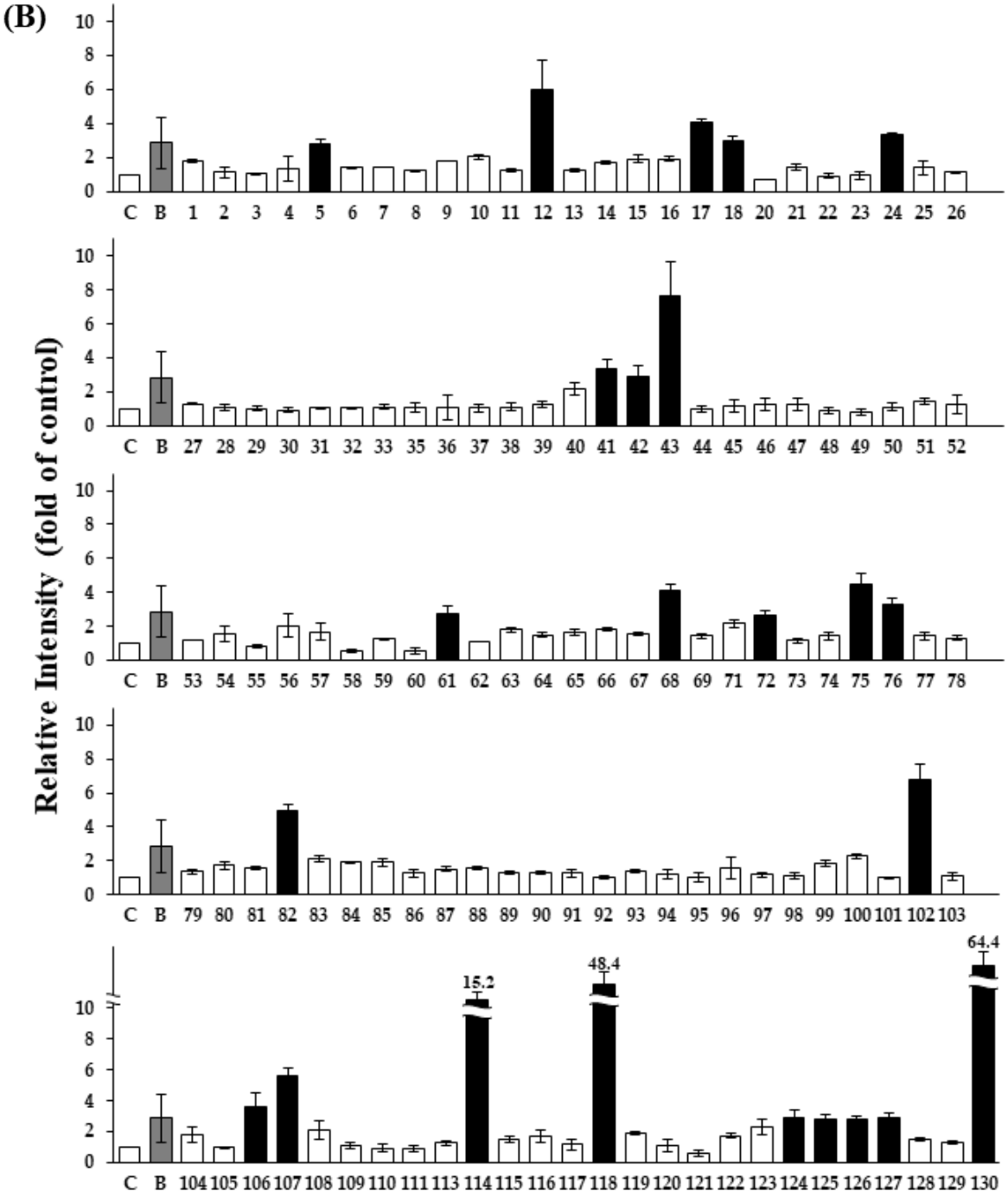

Figure 2.5. Effects of 130 crude extracts on LC3-II expression levels. All raw data (A) and relative intensity of LC3-II expression levels by 130 crude extracts (B). Notable increases are shown by a black star (★) (A) and black column (B). HepG2 cells were treated with 20 μg/mL of each crude extract for 24 h, and the expression levels of LC3B and β-actin were determined by western blotting. The data shown are representative of three independent treatments using the same parameters with similar results. Note: BBR, positive control (BBR 50 μM); 1–130, crude drug number (see Table 2.1).

2.3.3. Effects of 24 crude extracts on cell proliferation

We further investigated the effects of the selected 24 crude extracts on the proliferation of HepG2 cells. The cells were treated with 5, 10, and 20 μg/mL of each of the 24 crude extracts for 24 h, and cell proliferation was measured using MTT assay. Table 2.3 indicates the percentage of cell proliferation after treatment with 5, 10, and 20 μg/mL of each extract. Among the 24 crude extracts, cell proliferation was significantly suppressed by >10% compared with that in the control using the following five crude extracts: 41 (Goboshi; burdock fruit), 75 (Soboku; sappan wood), 118 (Mokko; saussurea root), 125 (Rengyo; forsythia fruit), and 130 (Hikai; dioscorea). On the other hand, three extracts, namely, 102 (Hishinomi; water chestnut), 106 (Biwayo; loquat leaf), and 107 (Binroji; areca), increased cell proliferation by >10% compared with that of the control. The remaining 16 crude extracts had no effect on cell proliferation. Fig. 2.6 shows the cell proliferation of only eight crude extracts (five extracts that suppressed cell proliferation and three extracts that increased it). These results suggest that these eight crude drugs might influence cell proliferation and autophagy.

Table 2.3. Effects of selected 24 crude extracts on cell proliferation.

Drug No.	Japanese Name	English Name	Concentration (μg/mL)		
			5	10	20
5	Uzu	Aconite Root	100.4	100.3	103.3
12	Onji	Polygala Root	100.4	97.3	96.4
17	Kakko	Pogostemon Herb	96.6	100.2	100.5
18	Kakkon	Pueraria Root	101.6	107.4	109.5
24	Kikyo	Platycodon Root	103.6	106.9	106.8
41 [b)]	Goboshi	Burdock Fruit	89.5	82.9	76.7
42	Gomishi	Schisandra Fruit	105.5	107.3	106.2
43	Saiko	Bupleurum Root	100.8	100.3	96.1
61	Jashoshi	Cnidium Monnieri Fruit	96.1	96.1	92.6
68	Shoma	Cimicifuga Rhizome	100.2	104.3	106.3
72	Sentai	Cicada Slough	105.6	103.2	101.4
75 [b)]	Soboku	Sappan Wood	100.8	94.0	86.9
76	Soyo	Perilla Herb	102.7	103.8	105.9
82	Chimo	Anemarrhena Rhizome	99.4	100.8	96.9
102 [a)]	Hishinomi	Water Chestnut	105.1	108.1	116.3
106 [a)]	Biwayo	Loquat Leaf	106.9	110.7	113.9
107 [a)]	Binroji	Areca	105.1	114.6	108.7
114	Mao	Ephedra Herb	101.5	95.0	97.7
118 [b)]	Mokko	Saussurea Root	94.2	82.3	67.3
124	Ryokyo	Alpinia Officinarum Rhizome	101.4	103.2	109.5
125 [b)]	Rengyo	Forsythia Fruit	90.4	89.5	88.7
126	Renniku	Nelumbo Seed	103.5	105.6	103.2
127	Tanjin	Salvia Miltiorrhiza Root	98.2	99.8	95.3
130 [b)]	Hikai	Dioscorea	71.8	50.1	20.0

[a)]Extracts that increased cell proliferation by >10% compared with the control. [b)]Extracts that suppressed cell proliferation by >10% compared with the control.

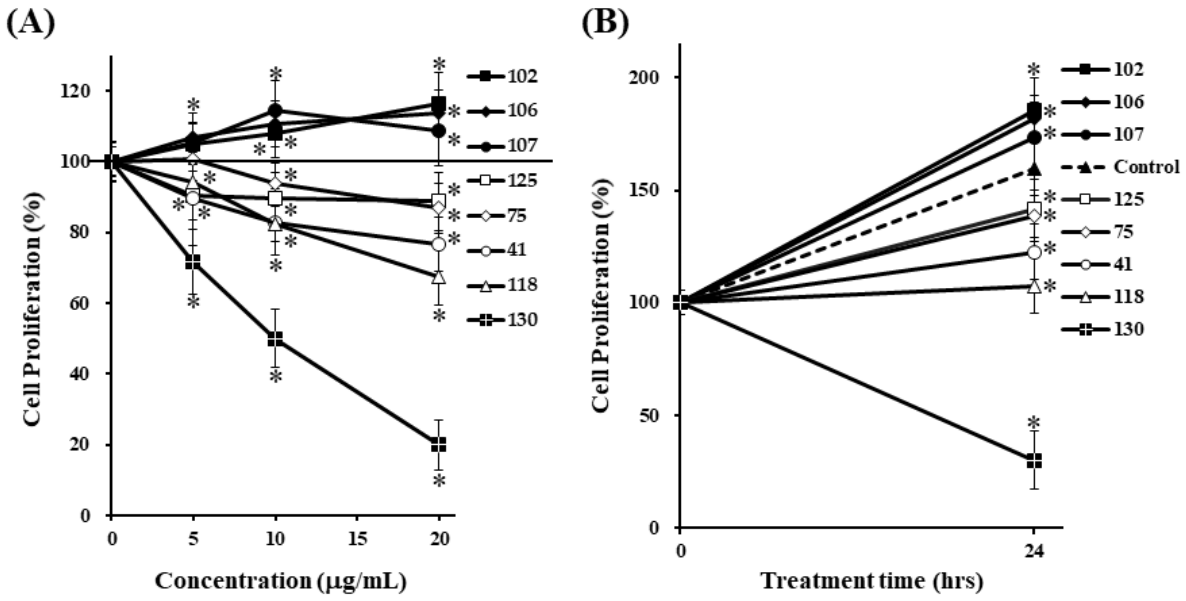

Figure 2.6. Effects of eight crude extracts on cell proliferation. HepG2 cells were treated with each crude extract at various concentrations for 24 h (A), and cells were treated with each crude extract (20 μg/mL) for the times indicated (B) and cell proliferations were determined using MTT assay. The data are presented as the mean ± S.D. of three individual experiments. $*p < 0.05$ compared with the control group.

2.3.4. Effects of five crude extracts on autophagy flux

Fig. 2.7 shows p62 levels upon treatment with five crude extracts suppressing cell proliferation. All of these crude extracts increased p62 levels. In particular, Hikai (130) strongly induced p62 level by more than fourfold after treatments for 12 and 24 h. Mokko (118) also induced p62 level by more than fourfold after treatment for 12 h. These results suggest that Goboshi (41), Soboku (75), Mokko (118), Rengyo (125), and Hikai (130) deregulate the autophagic pathway by blocking autophagic flux, which results in p62 accumulation.

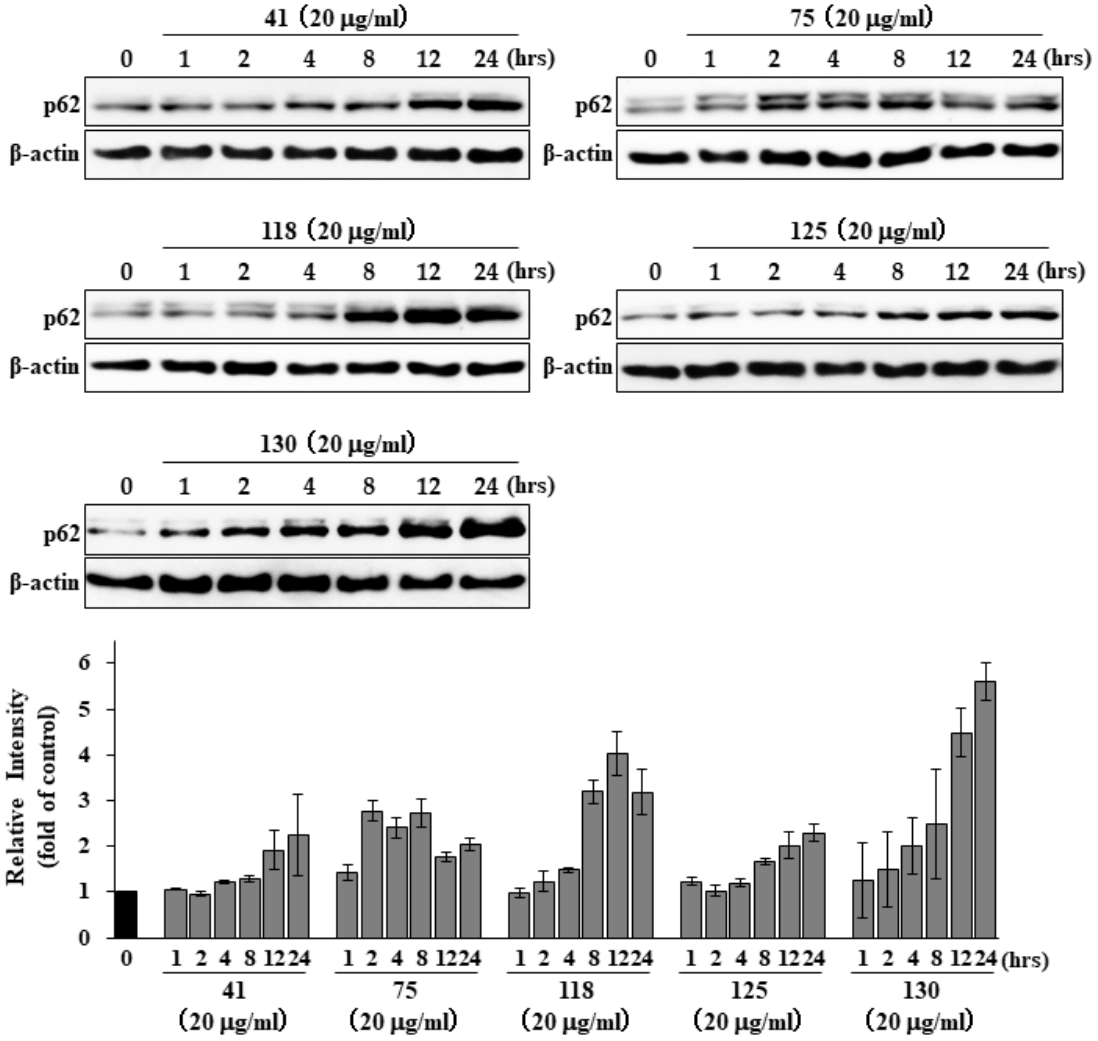

Figure 2.7. Effects of five crude extracts on p62 expression levels. HepG2 cells were treated with 20 μg/mL of each crude extract for different durations. The expression levels of p62 and β-actin were determined by western blotting. The data shown are representative of three independent treatments using the same parameters with similar results.

2.3.5. Effects of three crude extracts on autophagy flux

Fig. 2.8 indicates p62 levels regulated by the three crude extracts that increased cell proliferation. Hishinomi (102) and Biwayo (106) had no effect on p62 levels during treatment. Binroji (107) decreased p62 level within a short time (approximately 4 h) after treatment and then p62 level recovered to basal level after 12 h. The results of these studies suggest that Hishinomi (102), Biwayo (106), and Binroji (107) did not block autophagic flux. Furthermore, Binroji (107) clearly induced autophagy.

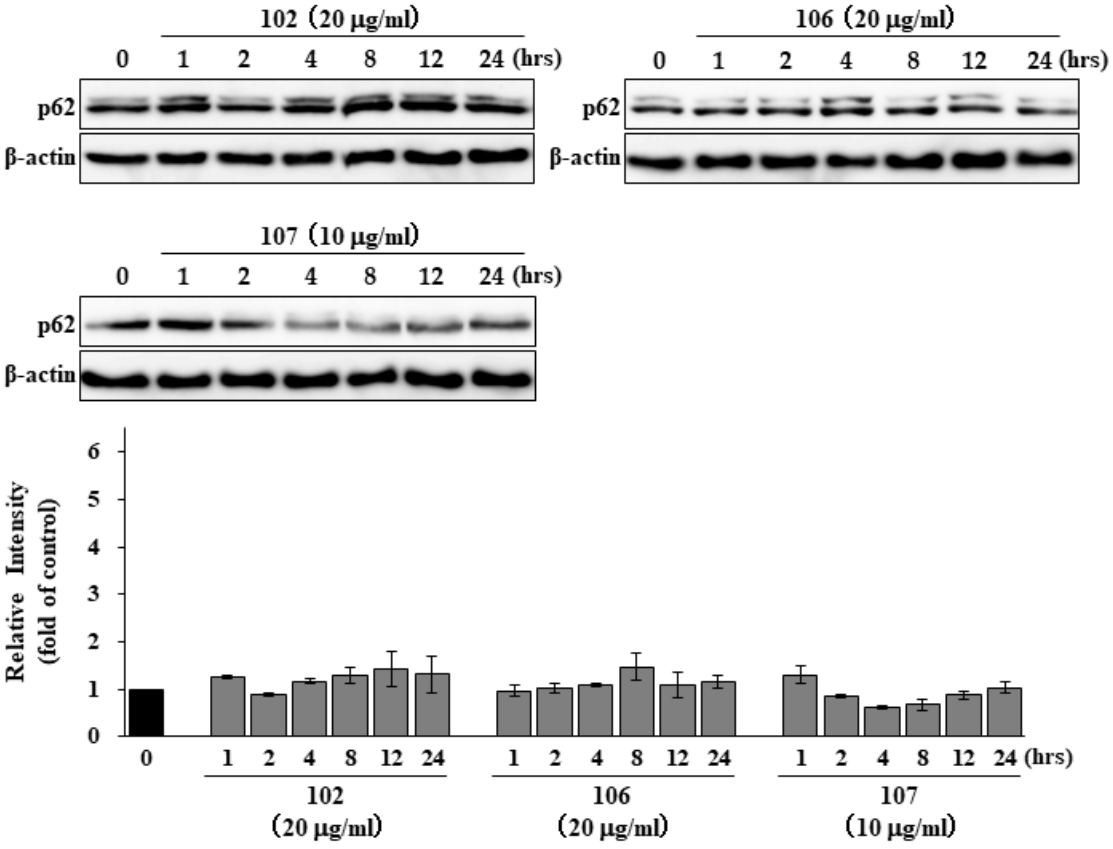

Figure 2.8. Effects of three crude extracts on p62 expression levels. HepG2 cells were treated with each crude extract at the indicated concentrations and for different durations. The expression levels of p62 and β-actin were determined by western blotting. The data shown are representative of three independent treatments using the same parameters with similar results.

2.4. Discussion

As described in this chapter, we screened 130 extracts prepared from different crude drugs to identify those crude drugs that modulate HepG2 proliferation and autophagy. First, we screened 130 crude extracts to select those that increased LC3-II levels. Among them, 24 crude extracts did so, which suggests that these extracts might modulate autophagy. On the other hand, several crude extracts reduced LC3-II levels. These crude extracts may contain inhibitors of early-stage autophagy, but we did not focus on these crude extracts in this thesis. This is because these crude extracts are uncertain to contain autophagy inducers and inhibitors of late-stage that increased LC3-II levels. Therefore, we focused on crude extracts increasing LC3-II levels for effective search of autophagy modulators.

Among the 24 crude extracts increased LC3-II levels, three extracts induced cell growth, but five extracts suppressed cell proliferation. Interestingly, the remaining 16 crude extracts had no effect on cell proliferation despite increasing LC3-II levels. These results suggest that the regulation of HepG2 proliferation is not indispensable for LC3-II induction. We determined that autophagic flux could be assessed by monitoring p62 levels because the results of screening for LC3-II levels cannot be directly applied to the selection of extracts that inhibit autophagy. Among the three crude extracts increased cell proliferation, Hishinomi (102) and Biwayo (106) had no effect on p62 levels. On the other hand, Binroji (107) decreased p62 level within a short duration after treatment, and then the level finally recovered to their basal level. It appears that Binroji (107) induced cell growth with inducing autophagy, and we expect that this crude drug might contain compounds that are specific inducers of autophagy. Although Hishinomi (102) and Biwayo (106) did not show obvious induction of autophagy, they showed that LC3-II levels can be increased without blocking autophagic flux. These results probably reflect that Hishinomi (102) and Biwayo (106) induced cell growth with inducing autophagy, but further investigations are needed to confirm these findings. In fact, Binroji (107) has been reported to

induce autophagy in several cell lines, such as leukemic Jurkat T cells [23] and oral carcinoma cells (OECM-1), Cal-27, and Scc-9 [24], by activating the AMPK/mTOR signaling pathway after the accumulation of reactive oxygen species [24]. However, the relationship between autophagy and Hishinomi (102) or Biwayo (106) has not been previously reported.

On the other hand, five crude extracts suppressed cell proliferation and increased p62 levels, which suggests that these extracts disturb the autophagic pathway by inhibiting autophagic flux, leading to p62 accumulation. Among these five extracts, Goboshi (41) and Rengyo (125) contain arctigenin belonging to lignans as the same major compound. It has been reported that arctigenin protects against drug-induced hepatitis by suppressing the immune system and modulating autophagy by inhibiting the IFN-γ/IL-6/Stat1 and IL-6/Bnip3 pathways in mice [25]. However, our results in this study indicate that Soboku (75) and Mokko (118) inhibited autophagy with p62 accumulation. Brazilin contained in Soboku (75) was reported to induce autophagic cell death by disturbing calcium homeostasis in osteosarcoma MG-63 cells, thereby suppressing cell proliferation [26]. Costunolide contained in Mokko (118) was reported to suppress the proliferation of multidrug-resistant human ovarian cancer OAW42-A cells by activating apoptotic and autophagic pathways via the decreased expression of Bcl-2 [27]. This implies that the differences in the reactivity and signaling pathways depend on the cell type. Our results and those of previous reports indicate that these extracts contain compounds that modulate autophagy. We conclude that the crude drugs selected for this study could serve as sources of lead compounds in the development of reagents for autophagy research and agents for cancer therapy. However, further studies are needed to isolate and identify the active compounds in the drugs.

2.5. Conclusion

Among the 130 crude extracts, 24 increased LC3-II levels. Among these, Goboshi (burdock fruit), Soboku (sappan wood), Mokko (saussurea root), Rengyo (forsythia fruit), and Hikai (dioscorea) notably suppressed the proliferation of HepG2 cells and increased p62 levels, which suggested that these five extracts disturb autophagy, resulting in p62 accumulation. On the other hand, Hishinomi (water chestnut), Biwayo (loquat leaf), and Binroji (areca) induced cell growth and decreased or did not affect p62 levels, which implied that these three extracts might induce autophagy modulators for cell growth. The results suggest that the compounds, which are contained in the crude drugs selected for this study, could control cell proliferation with modulating autophagy in HepG2 cells. The isolation and identification of the active compounds in these drugs might lead to the development of reagents for autophagy research and agents for cancer therapy.

2.6. References

[1] Mizushima, N.; Yoshimori, T.; Levine, B. Methods in mammalian autophagy research. *Cell* **2010**, *140*, 313–326.

[2] Takamura, A.; Komatsu, M.; Hara, T.; Sakamoto, A.; Kishi, C.; Waguri, S.; Eishi, Y.; Hino, O.; Tanaka, K.; Mizushima, N. Autophagy-deficient mice develop multiple liver tumors. *Genes. Dev*. **2011**, *25*, 795–800.

[3] Yu, R.; Zhang, Z.Q.; Wang, B.; Jiang, H.X.; Cheng, L.; Shen, L.M. Berberine-induced apoptotic and autophagic death of HepG2 cells requires AMPK activation. *Cancer Cell Int*. **2014**, *14*, 49.

[4] La, X.; Zhang, L.; Li, Z.; Yang, P.; Wang, Y. Berberine-induced autophagic cell death by elevating GRP78 levels in cancer cells. *Oncotarget* **2017**, *8*, 20909–20924.

[5] Nozaki, R.; Kono, T.; Bochimoto, H.; Watanabe, T.; Oketani, K.; Sakamaki, Y.; Okubo, N.; Nakagawa, K.; Takeda, H. Zanthoxylum fruit extract from Japanese pepper promotes autophagic cell death in cancer cells. *Oncotarget* **2016**, *7*, 70437–70446.

[6] Song, L.; Wang, Z.; Wang, Y.; Guo, D.; Yang, J.; Chen, L.; Tan, N. Natural cyclopeptide RA-XII, a new autophagy inhibitor, suppresses protective autophagy for enhancing apoptosis through AMPK/mTOR/P70S6K pathways in HepG2 cells. *Molecules* **2017**, *22*, 1934.

[7] Wu, D.H.; Jia, C.C.; Chen, J.; Lin, Z.X.; Ruan, D.Y.; Li, X.; Lin, Q.; Min-Dong; Ma, X.K.; Wan, X.B.; Cheng, N.; et al. Autophagic LC3B overexpression correlates with malignant progression and predicts a poor prognosis in hepatocellular carcinoma. *Tumour Biol*. **2014**, 12225–12233.

[8] Green, D.R. Cancer and apoptosis: Who is built to last? *Cancer Cell* **2017**, *31*, 2–4.

[9] Takehara, T.; Liu, X.; Fujimoto, J.; Friedman, S.L.; Takahashi, H. Expression and role of Bcl-xL in human hepatocellular carcinomas. *Hepatology* **2001**, *34*, 55-61.

[10] Uto, T.; Morinaga, O.; Tanaka, H.; Shoyama, Y. Analysis of the synergistic effect of glycyrrhizin and other constituents in licorice extract on lipopolysaccharide-induced nitric oxide production using knock-out extract. *Biochem. Biophys. Res. Commun*. **2012**, *417*, 473–478.

[11] Kabeya, Y.; Mizushima, N.; Ueno, T.; Yamamoto, A.; Kirisako, T.; Noda, T.; Kominami, E.; Ohsumi, Y.; Yoshimori, T. LC3, a mammalian homologue of yeast Apg8p, is localized in autophagosome membranes after processing. *EMBO J.* **2000**, *19*, 5720–5728.

[12] Kabeya, Y.; Mizushima, N.; Yamamoto, A.; Oshitani-Okamoto, S.; Ohsumi, Y.; Yoshimori, T. LC3, GABARAP and GATE16 localize to autophagosomal membrane depending on form-II formation. *J. Cell Sci.* **2004**, *117*, 2805–2812.

[13] Pankiv, S.; Clausen, T.H.; Lamark, T.; Brech, A.; Bruun, J.A.; Outzen, H.; Øvervatn, A.;

Bjørkøy, G.; Johansen, T. p62/SQSTM1 binds directly to Atg8/LC3 to facilitate degradation of ubiquitinated protein aggregates by autophagy. *J. Biol. Chem.* **2007**, *282*, 24131–24145.

[14] Itakura, E.; Mizushima, N. p62 targeting to the autophagosome formation site requires self-oligomerization but not LC3 binding. *J. Cell. Biol*. **2011**, *192*, 17–27.

[15] Okubo, S.; Uto, T.; Goto, A.; Tanaka, H.; Nishioku, T.; Yamada, K.; Shoyama, Y. Berberine induces apoptotic cell death via activation of caspase-3 and -8 in HL-60 human leukemia cells: Nuclear localization and structure-activity relationships. *Am. J. Chin. Med*. **2017**, *45*, 1497–1511.

[16] Degenhardt, K.; Mathew, R.; Beaudoin, B.; Bray, K.; Anderson, D.; Chen, G.; Mukherjee, C.; Shi, Y.; Gélinas, C.; Fan, Y.; et al. Autophagy promotes tumor cell survival and restricts necrosis, inflammation, and tumorigenesis. *Cancer Cell* **2006**, *10*, 51–64.

[17] Turcotte, S.; Chan, D.A.; Sutphin, P.D.; Hay, M.P.; Denny, W.A.; Giaccia, A.J. A molecule targeting VHL-deficient renal cell carcinoma that induces autophagy. *Cancer Cell* **2008**, *14*, 90–102.

[18] Yang, Z.J.; Chee, C.E.; Huang, S.; Sinicrope, F.A. The role of autophagy in cancer: Therapeutic implications. *Mol. Cancer Ther*. **2011**, *10*, 1533–1541.

[19] Marinković, M.; Šprung, M.; Buljubašić, M.; Novak, I. Autophagy modulation in cancer: Current knowledge on action and therapy. *Oxid. Med. Cell. Longev.* **2018**, *2018*, 8023821.

[20] Young, A.N.; Herrera, D.; Huntsman, A.C.; Korkmaz, M.A.; Lantvit, D.D.; Mazumder, S.; Kolli, S.; Coss, C.C.; King, S.; Wang, H.; et al. Phyllanthusmin derivatives induce apoptosis and reduce tumor burden in high-grade serous ovarian cancer by late-stage autophagy inhibition. *Mol. Cancer Ther*. **2018**, *17*, 2123–2135.

[21] Sermeus, A.; Cosse, J.P.; Crespin, M.; Mainfroid, V.; et al. Hypoxia induces protection against etoposide-induced apoptosis: Molecular profiling of changes in gene expression and transcription factor activity. *Mol Cancer*. **2008**, *7*, 27.

[22] Mayurbhai, H.S.; Itakura, E.; Mizushima, N. Expression of the autophagy substrate SQSTM1/p62 is restored during prolonged starvation depending on transcriptional upregulation and autophagy-derived amino acids. *Autophagy* **2014**, *10*, 431–441.

[23] Yen, C.Y.; Chiang, W.F.; Liu, S.Y.; Lin, C.C.; Liao, K.A.; Lin, C.Y.; Hsieh, W.F.; Cheng, Y.C.; Hsu, KC.; Lin, P.Y.; Chen, T.C.; et al. Impacts of autophagy-inducing ingredient of areca nut on tumor cells. *PLoS ONE* **2015**, *10*, e0128011.

[24] Xu, Z.; Huang, C.M.; Shao, Z.; Zhao, X.P.; Wang, M.; Yan, T.L.; Zhou, X.C.; Jiang, E.H.; Liu, K.; Shang, Z.J. Autophagy induced by areca nut extract contributes to decreasing cisplatin toxicity in oral squamous cell carcinoma cells: Roles of reactive oxygen species/AMPK signaling. *Int. J. Mol. Sci.* **2017**, *18*, 524.

[25] Feng, Q.; Yao, J.; Zhou, G.; Xia, W.; Lyu, J.; Li, X.; Zhao, T.; Zhang, G.; Zhao, N.; Yang,

J. Quantitative proteomic analysis reveals that arctigenin alleviates Concanavalin A-induced hepatitis through suppressing immune system and regulating autophagy. *Front. Immunol.* **2018**, *9*, 1881.

[26] Kang, Y.; He, P.; Wang, H.; Ye, Y.; Li, X.; Xie, P.; Wu, B. Brazilin induces FOXO3A-dependent autophagic cell death by disturbing calcium homeostasis in osteosarcoma cells. *Cancer Chemother. Pharmacol.* **2018**, *82*, 479–491.

[27] Fang, Y.; Li, J.; Wu, Y.; Gui, J.; Shen, Y. Costunolide inhibits the growth of OAW42-A multidrug-resistant human ovarian cancer cells by activating apoptotic and autophagic pathways, production of reactive oxygen species (ROS), cleaved caspase-3 and cleaved caspase-9. *Med. Sci. Monit.* **2019**, *25*, 3231–3237.

Chapter 3

Suppression of autophagy by arctigenin contained in the fruits of *Arctium lappa* (Goboshi) and the fruits of *Forsythia suspense* (Rengyo) and the molecular mechanisms

3.1. Introduction

As described in Chapter 2, the screening data demonstrated that extracts of the fruits of *Arctium lappa* (hereafter, Goboshi) and the fruits of *Forsythia suspensa* (hereafter, Rengyo) have beneficial antiproliferative activity with inhibition of autophagy (Fig. 3.1 and 3.2) [1].

Figure 3.1. The flower [2] **and the fruits of *Arctium lappa* (Goboshi).**

Figure 3.2. The flower [2] **and the fruits of *Forsythia suspense* (Rengyo).**

Goboshi has the following pharmacological activities: anti-inflammatory, antibacterial, antiviral, antioxidant, neuro-and hepatoprotective, antitumor, and antiaging [3, 4]. Rengyo has anti-inflammatory, antibacterial, antiviral, antioxidant, neuro- and hepato-protective, antitumor, and anti-atopic dermatitis effects [5, 6]. It is well known that the major compounds of both Goboshi and Rengyo are arctigenin (ARG) and arctiin (ARC) (Fig. 3.3) [7].

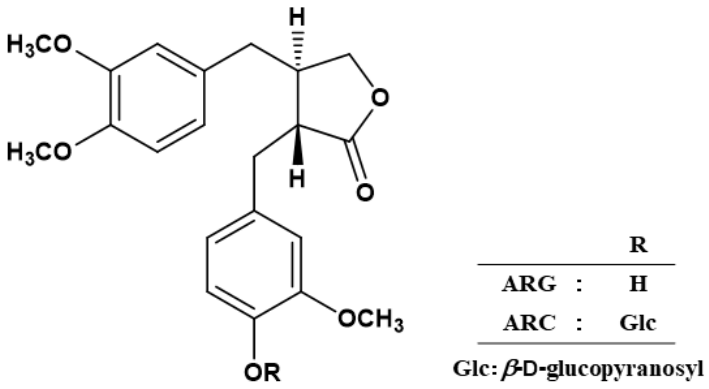

Figure 3.3. Chemical structures of ARG and ARC.

ARG and ARC are bioactive lignans with multiple pharmacological functions such as antitumor [8], antioxidant [9], anti-inflammatory [10], antiviral [11], and neuroprotective effects [12]. Recently, ARG was reported to induce autophagic cell death by inhibiting activation of the mTOR pathway in ER-positive human breast cancer cells [13]. However, it seems likely that ARG could modulate autophagy (induce or inhibit), but its mechanism of action in cancer cells is not fully understood.

As described in this chapter, we first examined the effects of ARG and ARC on the proliferation of HepG2 cells. Next, we investigated the efficacy and molecular mechanism of action of ARG on the modulation of autophagy-related proteins in HepG2 and human breast cancer MCF-7 cells. Furthermore, we confirmed the suppressive effect of ARG on starvation-induced autophagy.

3.2. Materials and methods

3.2.1. Reagents

ARG (purity > 95%) and ARC (purity > 97%) were purchased from Tokyo Chemical Industries (Tokyo, Japan). Antibodies against beclin 1, phospho-beclin 1 (Ser93) (p-beclin 1), caspase-3, and PARP were obtained from Cell Signaling Technology (Beverly, MA, USA). The anti-rabbit Alexa Fluor 488-conjugated antibody was purchased from Thermo Fisher Scientific (Rockford, IL, USA). The ProLong® Gold antifade reagent with 4',6-diamidino-2-phenylindole (DAPI) was obtained from Invitrogen (Carlsbad, CA, USA). Triton X-100 was purchased from Sigma-Aldrich (St. Louis, MO, USA). All other reagents were the same as described in Chapter 2.2.2.

3.2.2. *Cell culture and treatment*

HepG2 and MCF-7 cells were obtained from the RIKEN BioResource Center Cell Bank (Ibaraki, Japan). Both cells were grown in DMEM (regular medium). The cell culture and treatment were performed as explained in Chapter 2.2.3. To induce starvation, cells were washed with phosphate-buffered saline (PBS) and incubated in amino acid-free DMEM without FBS (starvation medium).

3.2.3. Determination of cell proliferation

See Chapter 2.2.5. After replacing the original medium with fresh regular medium, the cells were treated with various concentrations of ARG or ARC for 24 or 48 h. Determination of cell proliferation was performed same MTT assay protocol as described in Chapter 2.2.5.

3.2.4. Western blot analysis

See Chapter 2.2.4.

3.2.5. Fluorescence microscopy

Cells (5×10^4 cells) were plated in two-chamber glass slides in 2 mL of regular medium. After replacing with starvation medium, the cells were incubated with ARG for 4 h. Then, the cells were fixed with 4% paraformaldehyde for 15 min and permeabilized with 0.3% (v/v) Triton X-100 in PBS for 10 min. After washing with PBS, the cells were blocked with PBS containing 0.3% (v/v) Triton X-100 and 1% (w/v) bovine serum albumin for 60 min and incubated with anti-LC3B antibody (1:200) for 1 h. After washing, the cells were incubated with secondary anti-rabbit Alexa Fluor 488-conjugated antibody (1:1000) for 30 min in the dark. Then, the slide was rinsed with PBS and mounted with ProLong® Gold antifade reagent with DAPI. The slides were observed using a confocal laser scanning microscope (FV10i; Olympus, Tokyo, Japan).

3.2.6. Statistical analysis

See Chapter 2.2.6.

3.3. Results

3.3.1. Effects of ARG and ARC on cell proliferation

First, we examined the effects of ARG and ARC on the proliferation of HepG2 cells. The cells were treated with ARG or ARC at several concentrations for 24 or 48 h, after which cell proliferation was determined using MTT assay. As shown in Fig. 3.4, ARG or ARC significantly suppressed cell proliferation. The antiproliferative effect of ARG was higher than that of ARC.

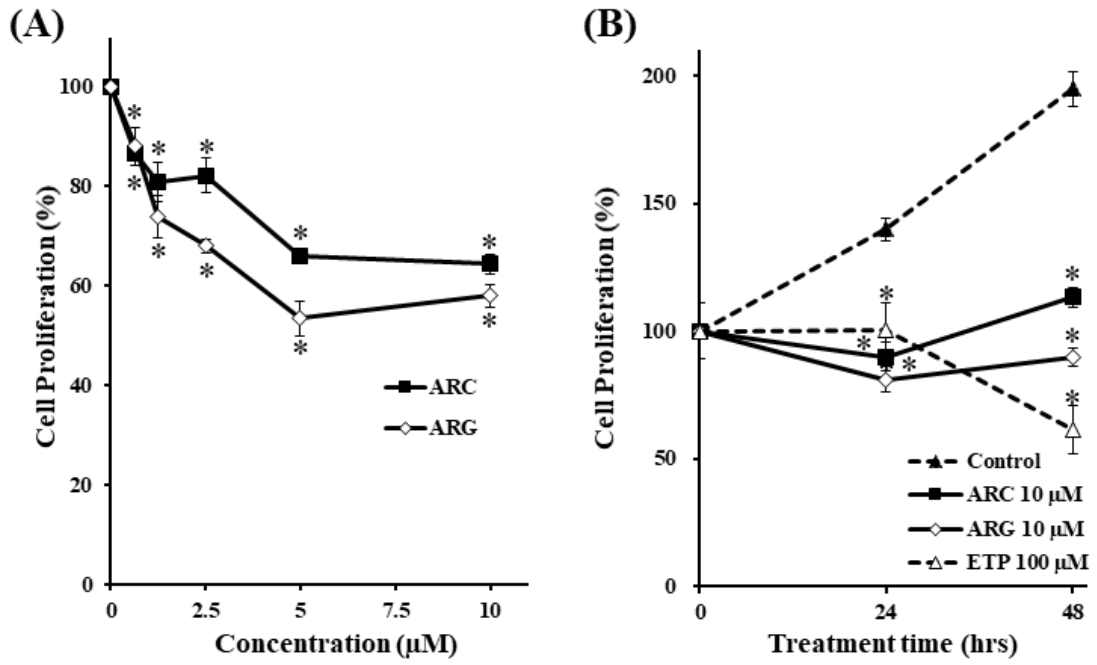

Figure 3.4. Effects of ARG and ARC on cell proliferation. HepG2 cells were treated with ARG or ARC at various concentrations for 48 h (A), and cells were treated with ARG (10 μM) or ARC (10 μM) for the times indicated (B) and cell proliferations were determined using MTT assay. ETP was used as a model for inducing apoptotic cell death against HepG2 cells. The data are presented as the mean ± S.D. of three individual experiments. $*p < 0.05$ compared with the control group.

3.3.2. Effect of ARG on autophagy-related proteins

Next, we determined the effect of ARG on the expression levels of autophagy-related proteins by western blotting. Beclin 1, which is also one of the most important proteins for autophagy, is directly phosphorylated by AMPK to induce autophagy [14]. Thus, an increase in the level of p-beclin 1 indicates induction of autophagy. As shown in Fig. 3.5, ARG slightly increased LC3-II level and enhanced the phosphorylation of beclin 1.

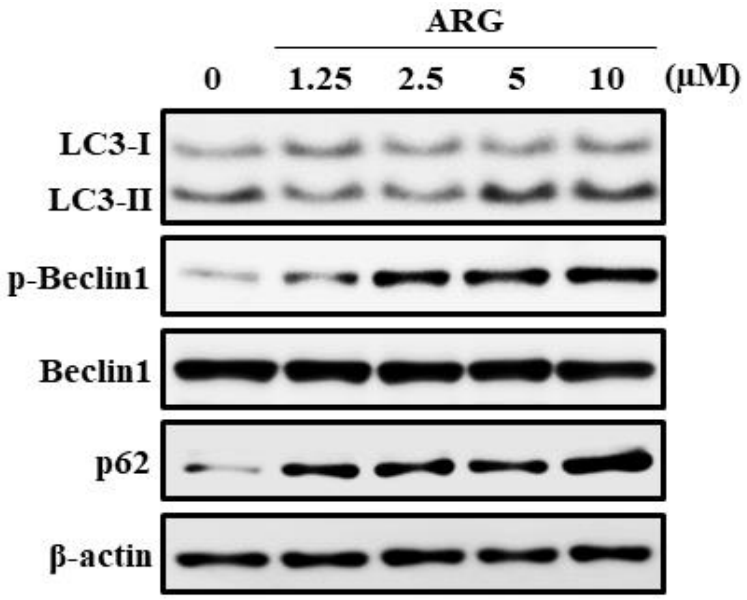

Figure 3.5. Effect of ARG on autophagy-related proteins. HepG2 cells were treated with ARG at the indicated concentrations for 24 h. The expression levels of LC3B, beclin 1, p-beclin 1, p62, and β-actin were determined by western blotting. The data shown are representative of three independent treatments using the same parameters with similar results.

To assess whether ARG induces or inhibits autophagy, we performed time-course experiments to determine the effect of ARG on p62 levels. As shown in Fig. 3.6, ARG clearly increased p62 level as time passes. To confirm the results obtained, we used a different cancer cell line, human breast cancer MCF-7 cells. As shown in Fig. 3.7, ARG suppressed cell proliferation and slightly increased LC3-II level and significantly increased p-beclin 1 and p62 levels in MCF-7 cells. These results suggest that ARG might block the autophagic pathway, which leads to p62 accumulation.

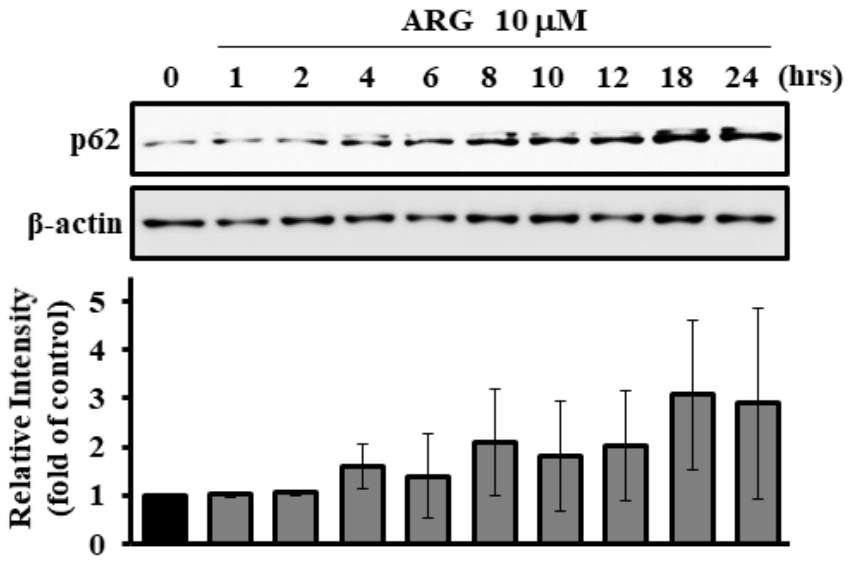

Figure 3.6. Effect of ARG on p62 expression levels. HepG2 cells were treated with ARG (10 μM) for the times indicated. The expression levels of p62 and β-actin were determined by western blotting. Relative intensity of p62 is shown as a bar graph. The data shown are representative of three independent treatments using the same parameters with similar results.

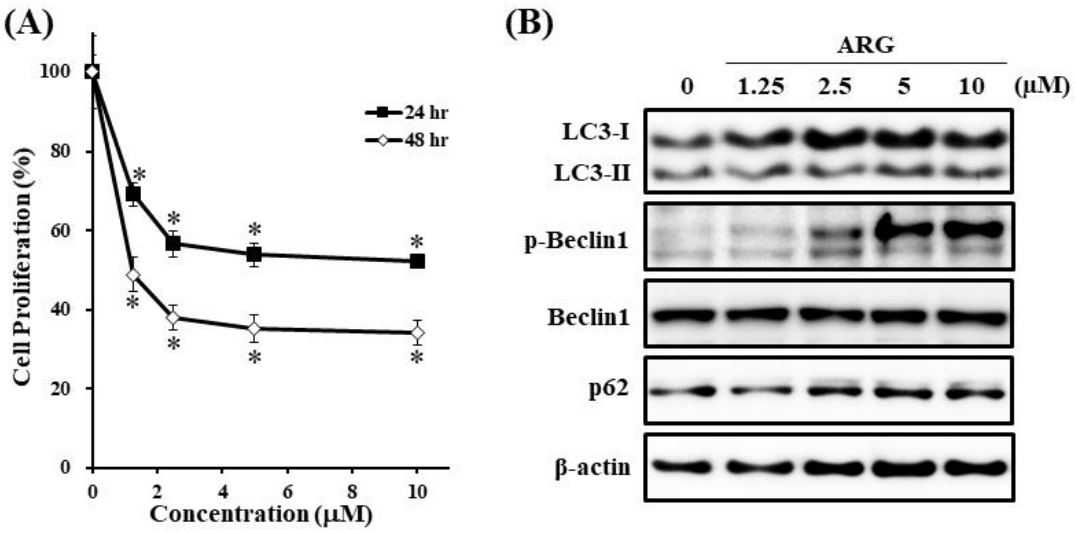

Figure 3.7. Effect of ARG on proliferation of MCF-7 cells and autophagy-related proteins. MCF-7 cells were treated with ARG at various concentrations for 24 or 48 h, and cell proliferations were determined using MTT assay (A). The data are presented as the mean ± S.D. of three individual experiments. $*p < 0.05$ compared with the control group. MCF-7 cells were treated with ARG at various concentrations for 24 h (B). The expression levels of LC3B, beclin 1, p-beclin 1, p62, and β-actin were determined by western blotting. The data shown are representative of three independent treatments using the same parameters with similar results.

As shown in Fig. 3.8, 3-MA slightly increased both LC3-II and p-beclin 1 levels, but not p62 accumulation. Moreover, CQ clearly increased both LC3-II and p62 levels, but not beclin 1 phosphorylation. Taken together, our data imply that the stage of inhibition of autophagy by ARG differed from those by 3-MA or CQ.

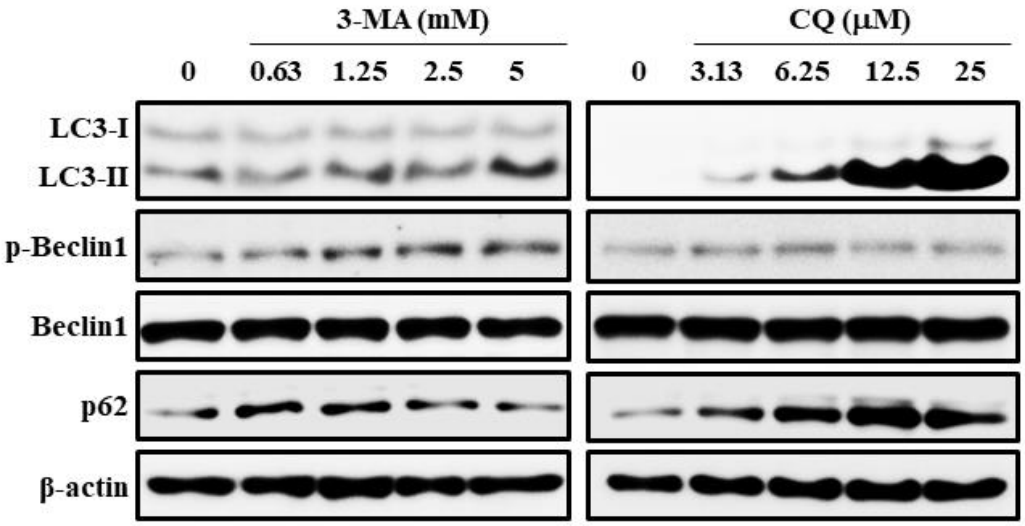

Figure 3.8. Effects of 3-MA and CQ on autophagy-related proteins. HepG2 cells were treated with 3-MA and CQ at the indicated concentrations for 24 h. The expression levels of LC3B, beclin 1, p-beclin 1, p62, and β-actin were determined by western blotting. The data shown are representative of three independent treatments using the same parameters with similar results.

3.3.3. Effect of ARG on starvation-induced autophagy

To confirm the autophagy inhibition by ARG, we further determined whether ARG could influence starvation-induced autophagy. First, we examined the levels of LC3-II in the absence or presence of ARG using HepG2 cells after 4 h of continuous starvation. As shown in Fig. 3.9, although starvation increased LC3-II level, ARG clearly reduced this induction.

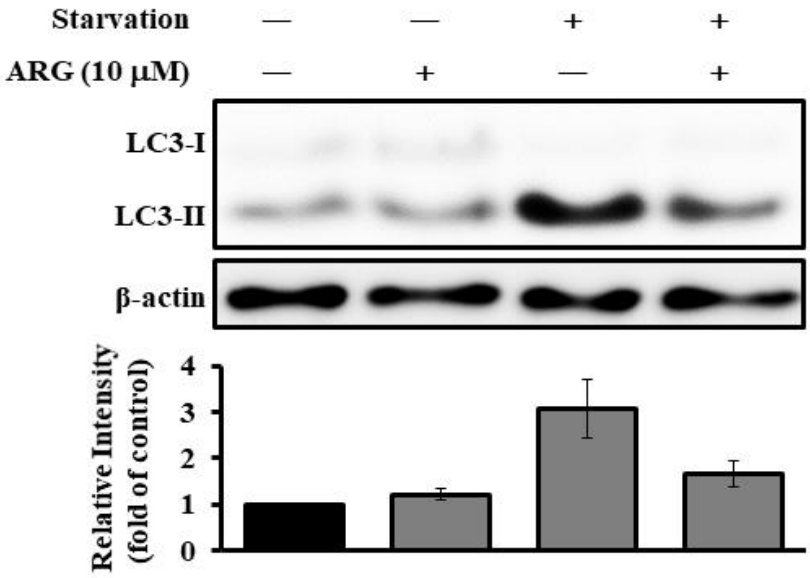

Figure 3.9. Effect of ARG on starvation-induced LC3-II expression levels. HepG2 cells were treated with or without ARG (10 μM) under conditions of regular medium or starvation medium for 4 h. The expression levels of LC3B and β-actin were determined by western blotting. Relative intensity of LC3-II is shown as a bar graph. The data shown are representative of three independent treatments using the same parameters with similar results.

Next, we observed autophagosome/autolysosome formation using a confocal laser scanning microscope. We detected autophagosomes/autolysosomes using anti-LC3B primary antibody and anti-rabbit Alexa Fluor 488-conjugated secondary antibody (green). As shown in Fig. 3.10, starvation treatment formed autophagosomes/autolysosomes, but ARG clearly suppressed this formation. These results demonstrated that ARG could inhibit starvation-induced autophagy.

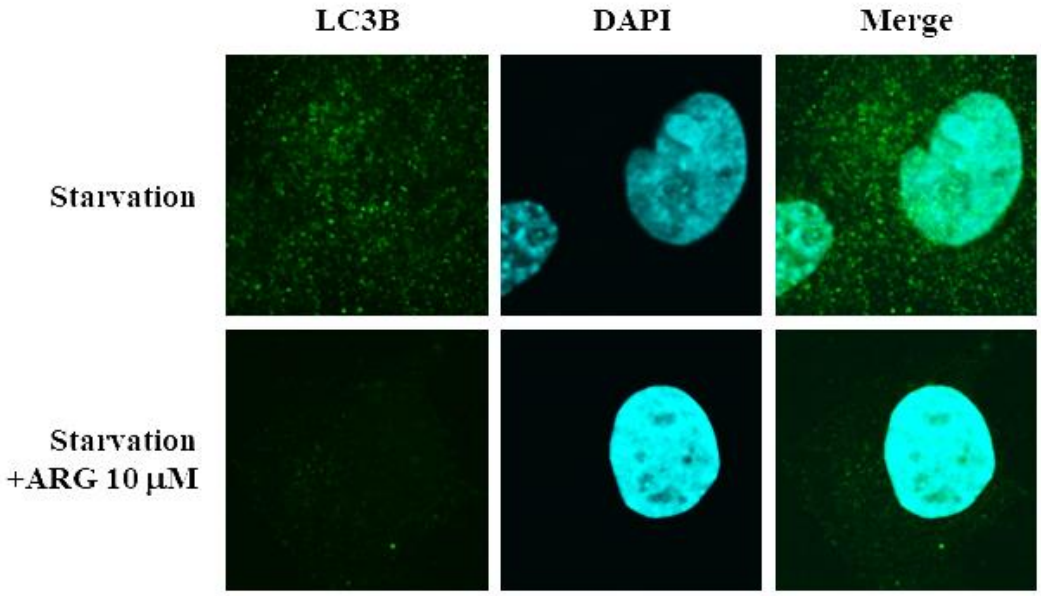

Figure 3.10. Effect of ARG on increased autophagosome/autolysosome formation by starvation. Detection of LC3B-positive organelles (autophagosomes/autolysosomes). HepG2 ells were treated with or without ARG (10 μM) under conditions of regular medium or starvation medium for 4 h. After incubation, cells were fixed, permeabilized, and treated with anti-LC3B antibody followed by treatment with Alexa Fluor 488-conjugated secondary antibody. The images were made at ×250 magnification.

3.3.4. Effect of ARG on apoptosis-related proteins

Caspase-3 activation and PARP cleavage are hallmarks of apoptosis [15-17]. To determine the involvement of ARG in apoptosis, we examined the effect of ARG on caspase-3 and PARP. ETP was used as a positive control [15, 18]. Although ETP induced caspase-3 activation and PARP cleavage, ARG did not affect either of these proteins, even at 100 μM, which is ten times the concentration that modulates LC3-II and p-beclin 1 (Fig. 3.11). These results imply that the antiproliferative effect of ARG may occur independently of the caspase-3 mediated apoptosis.

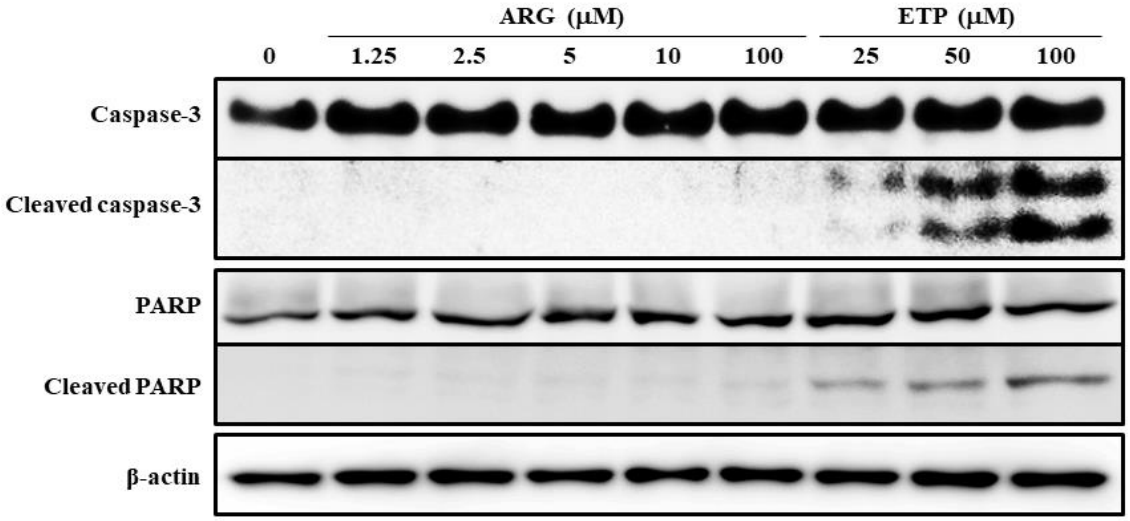

Figure 3.11. Effect of ARG on the activation of caspase-3 and PARP cleavage. HepG2 cells were treated with ARG or ETP at the indicated concentrations for 24 h. The expression levels of caspase-3, PARP, and β-actin were determined by western blotting. ETP was used as a positive control. The data shown are representative of three independent treatments using the same parameters with similar results.

3.4. Discussion

As described in this chapter, we found that ARG and ARC significantly suppressed the proliferation of HepG2 cells, and the antiproliferative effect of ARG was higher than that of ARC. Molecular analysis showed that ARG slightly increased LC3-II level and strongly induced beclin 1 phosphorylation and p62 level. In addition, we also observed similar patterns for beclin 1 phosphorylation and p62 level in human breast cancer MCF-7 cells. These results suggest that ARG might block the autophagic pathway, which leads to p62 accumulation. Starvation is the most potent known physiological inducer of autophagy, and it has been commonly used to study the molecular mechanism of autophagy [19]. Hence, we further verified the inhibitory effect of ARG on starvation-induced autophagy. Our data indicated that the expression of LC3-II was induced by starvation medium, but ARG clearly reduced this induction. Moreover, the data using confocal laser scanning microscopy demonstrated that autophagosomes/autolysosomes formed by starvation were decreased by ARG. These data suggest the autophagy inhibition by ARG.

Several autophagy inhibitors have been developed to analyze the mechanism of autophagy and enhance the therapeutic effects of anticancer drugs. 3-MA and CQ are well-known autophagy inhibitors. 3-MA is one of the most commonly used inhibitors to suppress autophagy at an early-stage. It is reported that 3-MA acts as a PI3K inhibitor that suppresses class III PI3K activity required for autophagosome maturation [19]. Thus, 3-MA inhibits autophagy without affecting LC3-II and p62 levels [19]. Indeed, our data showed that 3-MA induced beclin 1 phosphorylation, but not LC3-II and p62 levels. In contrast, CQ is known as an inhibitor to block autophagy at a late-stage [19]. CQ inhibits acidification inside the lysosome and disturbs autophagosome–lysosome fusion [19]. We demonstrated that CQ clearly increased the levels of both LC3-II and p62. Interestingly, ARG slightly increased LC3-II level and strongly induced beclin 1 phosphorylation and p62 level. 3-MA slightly increased LC3-II level. Both ARG and

3-MA lack significant induction of LC3-II, indicating a low number of autophagosomes. This suggested that ARG suppresses the stage prior to autophagosome maturation, similar to 3-MA. Furthermore, although p62 accumulation was not observed in 3-MA, ARG significantly induced p62 accumulation like CQ. These findings imply that the stage of inhibition in autophagy by ARG differed from those by 3-MA and CQ (Fig. 3.12).

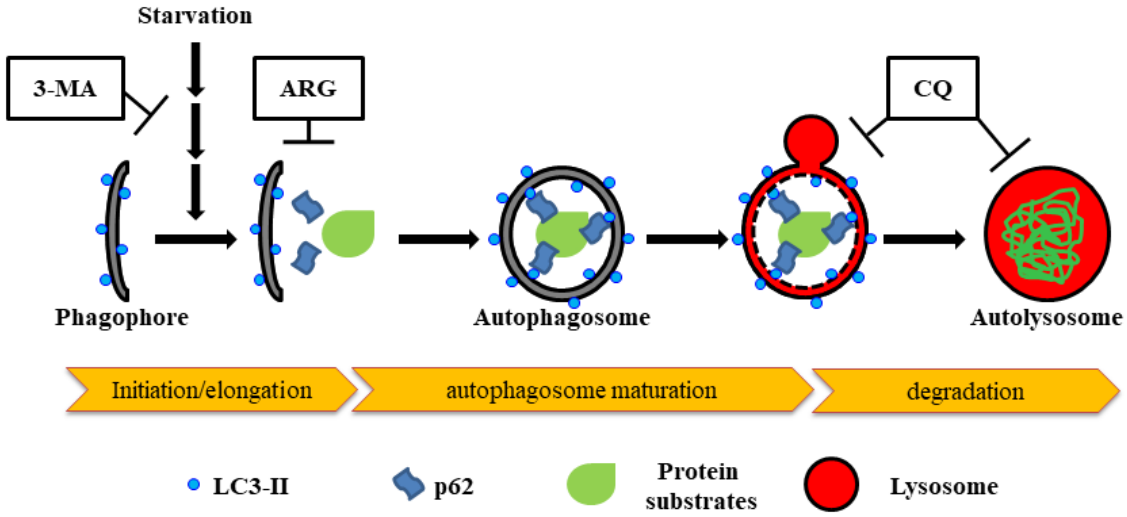

Figure 3.12. Proposed mechanism of inhibition of autophagy by ARG, 3-MA, and CQ. The autophagy inhibition mechanism of ARG shown is guess based on this study. Further investigation is needed to clarify the mechanism of ARG.

Apoptosis is one of the main factors reducing cell proliferation. Numerous studies have reported many kinds of natural products that trigger apoptosis in various cancer cell lines [16. 17]. In recent years, it has been reported that several natural products induce autophagy in parallel with inducing apoptosis. For example, toxicarioside O derived from *Antiaris toxicaria* was found to induce both apoptosis and autophagy in the colorectal cancer cell lines HCT116 and SW480 [20]. BBR also induces both apoptosis and autophagy in human glioma cell lines [21] and HepG2 cells [22]. In addition, sodium cantharidinate derived from Chinese blister

beetle induces both apoptosis and autophagy in HepG2 cells [23]. Moreover, durmillone, a flavonoid in *Millettia pachyloba*, also activates both in human cervix adenocarcinoma HeLa cells and the breast cancer cell line MCF-7 [24]. However, there are few reports regarding natural products that specifically modulate only autophagy without affecting apoptosis. Here, our data demonstrated that treatment with ARG even at 100 μM, which is ten times the concentration that modulates autophagy, did not activate caspase-3 and cleave of PARP. These results imply that the antiproliferative activity of ARG may occur independently of caspase-3 mediated apoptosis.

3.5. Conclusion

In this chapter, we explored the effect of ARG, a bioactive lignan from both Goboshi and Rengyo, on cell proliferation and autophagy-related proteins in HepG2 cells. ARG suppressed the proliferation of HepG2 cells. Analysis of autophagy-related proteins using HepG2 and MCF-7 cells demonstrated that ARG might block the autophagy that leads to p62 accumulation. The stages of inhibition in autophagy by ARG differed from those by the autophagy inhibitors 3-MA or CQ. ARG could also inhibit starvation-induced autophagy. Further analysis of apoptosis-related proteins indicated that ARG did not affect caspase-3 activation and PARP cleavage, suggesting that the antiproliferative activity of ARG can occur independently of caspase-3 mediated apoptosis. In summary, we conclude that ARG suppresses cell proliferation and autophagy in HepG2 cells.

3.6. References

[1] Okubo, S.; Komori, H.; Kuwahara, A.; Ohta, T.; Shoyama, Y.; Uto, T. Screening of crude drugs used in Japanese Kampo formulas for autophagy-mediated cell survival of the human hepatocellular carcinoma cell line. *Medicines* **2019**, *3*, 6.

[2] Takeya, K.; Kiuchi, H.; Komatsu, K. "Section, Goboshi and Rengyo", *Supplement to the Pharmacognosy third edition*, Nankodo Co., Ltd., Tokyo, **2018**, p. 321 and 260. (In Japanese).

[3] Chan, Y.S.; Cheng, L.N.; Wu, J.H; et al. A review of the pharmacological effects of *Arctium lappa* (burdock), *Inflammopharmacology* **2011**, *19*, 245–254.

[4] Knott, A.; Reuschlein, K.; Mielke, H.; et al. Natural *Arctium lappa* fruit extract improves the clinical signs of aging skin, *J. Cosmet. Dermatol*. **2008**, *7*, 281–289.

[5] Dong, Z.; Lu, X.; Tong, X.; et al. *Forsythiae fructus*: A review on its phytochemistry, quality control, pharmacology and pharmacokinetics, *Molecules* **2017**, *22*, 1466.

[6] Sung, Y.Y.; Yoon, T.; Jang, S.; et al. *Forsythia suspensa* suppresses house dust mite extract-induced atopic dermatitis in NC/Nga mice, *PLoS One* **2016**, *11*, e0167687.

[7] Hata, N.; Kobayashi, A.; Muranaka, T.; Okazawa, A. Multifunctionality and use of plants containing high concentrations of arctiin/arctigenin. *Agriculture and horticulture* **2011**, *86*, 10–20. (In Japanese).

[8] He, Y.; Fan, Q.; Cai, T.; Huang, W.; Xie, X.; Wen, Y.; Shi, Z. Molecular mechanisms of the action of arctigenin in cancer. *Biomed Pharmacother*. **2018**, *108*, 403–407.

[9] Wu, R.M.; Sun, Y.Y.; Zhou, T.T.; Zhu, Z.Y.; Zhuang, J.J.; Tang, X.; Chen, J.; Hu, L.H.; Shen, X., Arctigenin enhances swimming endurance of sedentary rats partially by regulation of antioxidant pathways. *Acta Pharmacol. Sin.* **2014**, *35*, 1274–1284.

[10] Hwangbo, M.; Jung, J.Y.; Ki, S.H.; Park, S.M.; Jegal, K.H.; Cho, I.J.; Lee, J.H.; Kang, S.H.; Park, S.D.; Ku, S.K.; Kim, S.C.; Zhao, R.J.; Jee, S.Y.; Kim, Y.W. U-Bang-Haequi Tang: A herbal prescription that prevents acute inflammation through inhibition of NF-κB-mediated inducible nitric oxide synthase. *Evid. Based Complement. Alternat. Med*. **2014**, *2014*, 542825.

[11] Chen, W.C.; Hu, Y.; Liu, L.; Shen, Y.F.; Wang, G.X.; Zhu, B. Synthesis and in vitro activities evaluation of arctigenin derivatives against spring viraemia of carp virus. *Fish. Shellfish Immunol*. **2018**, *82*, 17–26.

[12] Zhu, Z.; Yan, J.; Jiang, W.; Yao, X.G.; Chen, J.; Chen, L.; Li, C.; Hu, L.; Jiang, H.; Shen, X.J. Arctigenin effectively ameliorates memory impairment in Alzheimer's disease model mice targeting both β-amyloid production and clearance. *Neurosci*. **2013**, *33*, 13138–13149.

[13] Maxwell, T.; Lee, K.S.; Kim, S.; Nam, K.S. Arctigenin inhibits the activation of the mTOR

pathway, resulting in autophagic cell death and decreased ER expression in ER-positive human breast cancer cells. *Int. J. Oncol.* **2018**, *52*, 1339–1349.

[14] Kim, J.; Kim, Y.C.; Fang, C.; Russell, R.C.; Kim, J.H.; Fan, W.; Liu, R.; Zhong, Q.; Guan, K.L. Differential regulation of distinct Vps34 complexes by AMPK in nutrient stress and autophagy. *Cell* **2013**, *152*, 290–303.

[15] Sermeus, A.; Cosse, J.P.; Crespin, M.; Mainfroid, V.; de Longueville, F.; Ninane, N.; Raes, M.; Remacle, J.; Michiels, C. Hypoxia induces protection against etoposide-induced apoptosis: Molecular profiling of changes in gene expression and transcription factor activity. *Mol. Cancer* **2008**, *7*, 27.

[16] Uto, T.; Tung, N.H.; Ohta, T.; Juengsanguanpornsuk, W.; Hung, L.Q.; Hai, N.T.; Long, D.D.; Thuong, P.T.; Okubo, S.; Hirata, S.; et al. Antiproliferative activity and apoptosis induction by trijuganone C isolated from the root of *Salvia miltiorrhiza* Bunge (Danshen). *Phytother. Res.* **2018**, *32*, 657–666.

[17] Okubo, S.; Uto, T.; Goto, A.; Tanaka, H.; Nishioku, T.; Yamada, K.; Shoyama, Y. Berberine induces apoptotic cell death via activation of caspase-3 and -8 in HL-60 human leukemia cells: Nuclear localization and structure-activity relationships. *Am. J. Chin. Med.* **2017**, *45*, 1497–1511.

[18] Xie, B.S.; Zhao, H.C.; Yao, S.K.; Zhuo, D.X.; Jin, B.; Lv, D.C.; Wu, C.L.; Ma, D.L.; Gao, C.; Shu, X.M.; Ai, Z.L. Autophagy inhibition enhances etoposide-induced cell death in human hepatoma G2 cells. *Int. J. Mol. Med.* **2011**, *27*, 599–606.

[19] Mizushima, N.; Yoshimori, T.; Levine, B. Methods in mammalian autophagy research. *Cell* **2010**, *140*, 313–326.

[20] Huang, Y.H.; Sun, Y.; Huang, F.Y.; Li, Y.N.; Wang, C.C.; Mei, W.L.; Dai, H.F.; Tan, G.H.; Huang, C. Toxicarioside O induces protective autophagy in a sirtuin-1-dependent manner in colorectal cancer cells. *Oncotarget* **2017**, *8*, 52783–52791.

[21] Wang, J.; Qi, Q.; Feng, Z.; Zhang, X.; Huang, B.; Chen, A.; Prestegarden, L.; Li, X.; Wang, J. Berberine induces autophagy in glioblastoma by targeting the AMPK/mTOR/ULK1-pathway. *Oncotarget* **2016**, *7*, 66944–66958.

[22] Yu, R.; Zhang, Z.Q.; Wang, B.; Jiang, H.X.; Cheng, L.; Shen, L.M. Berberine-induced apoptotic and autophagic death of HepG2 cells requires AMPK activation. *Cancer Cell Int.* **2014**, *14*, 49.

[23] Tao, R.; Sun, W.Y.; Yu, D.H.; Qiu, W.; Yan, W.Q.; Ding, Y.H.; Wang, G.Y.; Li, H.J. Sodium cantharidinate induces HepG2 cell apoptosis through LC3 autophagy pathway. *Oncol. Rep.* **2017**, *38*, 1233–1239.

[24] Yan, W.; Yang, J.; Tang, H.; Xue, L.; Chen, K.; Wang, L.; Zhao, M.; Tang, M.; et al. Flavonoids from the stems of *Millettia pachyloba* Drake mediate cytotoxic activity through apoptosis and autophagy in cancer cells. *J. Adv. Res.* **2019**, *20*, 117–127.

Chapter 4

Isolation of active compounds derived from the rhizome of *Dioscorea tokoro* (Hikai) that inhibit autophagy

4.1. Introduction

As described in Chapter 2, the screening data demonstrated that the extract of the rhizome of *Dioscorea tokoro* (hereafter, Hikai) (Fig. 4.1) exerted the strongest suppression on cell proliferation.

Figure 4.1. The flower [1] **and the rhizome of *Dioscorea tokoro* (Hikai).**

Hikai, which is thought to have an effect on *improving the circulation of water in the body* (利水作用), has an anti-inflammatory effect, and is mainly used for treating dysuria, joint pain, and skin eczema, although it is rarely used. Hikai is a wild yam and its rhizomes are not generally used in the diet. However, in especially the north of Japan such as Iwate and Aomori prefectures, they are believed to be effective in recovering from fatigue and have been used to support health [2]. From chemical analyses, it has been reported that Hikai contains steroidal

saponins such as dioscin and protodioscin [3, 4]. A report from pharmacological studies provided evidence that the MeOH extract of Hikai have a potential of treating rheumatoid arthritis [4]. However, data on the pharmacological activities of Hikai and its active compounds are very limited.

As described in this chapter, we focused on the isolation of active compounds in Hikai exerting antiproliferative and inhibition of autophagy. First, we compared the activities of the fractions prepared from the MeOH extract of Hikai. The bioassay-guided fractionations of active fractions led to the isolation of several active compounds. Finally, we investigated the effects of isolated compounds on cell proliferation to explore the structure–activity relationship and confirmed the inhibition of autophagy.

4.2. Materials and methods

4.2.1. General procedures

Specific rotations were measured with a DIP-360 digital polarimeter (JASCO, Easton, PA, USA). Nuclear magnetic resonance (NMR) spectra were recorded on a JEOL ECX 400 FT-NMR spectrometer (JEOL, Tokyo, Japan) at room temperature. Electrospray ionization time-of-flight mass spectrometer (ESI-TOF-MS) experiments employed a Waters Xevo G2-XS Q-TOF mass spectrometer (Waters, Milford, MA, USA). Column chromatography was performed on Silica Gel 60 (Nacalai Tesque., Kyoto, Japan, 230-400 mesh) and YMC ODS-A gel (YMC Co. Ltd., Kyoto, Japan, 50 μm,). Thin-layer chromatography (TLC) was performed on TLC Silica gel 60F254 (Merck, Damstadt, Germany) and TLC Silica gel 60 RP-18 F254S (Merck, Damstadt, Germany) plates. Spots were visualized by spraying with 10% aq. sulfuric acid, followed by heating. HPLC (high performance liquid chromatography) was performed on UV-8020 UV-VIS detector (Tosoh Corp., Tokyo, Japan), DP-8020 pump (Tosoh Corp., Tokyo, Japan) and DP-8020 degasser (Tosoh Corp., Tokyo, Japan). XBridge BEH C18 Column (Waters, Milford, MA, USA, 130Å, 3.5 μm, 10 mm × 250 mm) were used for preparative purposes.

4.2.2. Extraction and isolation

Hikai (2.5 kg) was extracted three times with MeOH under reflux for 12 h. Evaporation of the solvent under reduced pressure provided a MeOH extract (338.77 g). A part of the MeOH extract (333.77 g) was partitioned into hexane–water (H_2O) (1:1, v/v) mixture to furnish a hexane-soluble fraction (0.45 g) and an aqueous phase. The aqueous phase was further partitioned into ethyl acetate (EtOAc)–H_2O (1:1, v/v) mixture to furnish an EtOAc-soluble fraction (19.23 g) and an aqueous phase. The aqueous phase was further extracted with *n*-butanol (BuOH) to give an *n*-BuOH-soluble fraction (138.24 g) and an H_2O-soluble fraction (124.17 g). A part of the *n*-BuOH-soluble fraction (21.15 g) was subjected to normal phase

silica gel column chromatography [580 g, chloroform–MeOH–H_2O (20:3:1 → 15:3:1 → 10:3:1 → 7:3:1 → 6:4:1, v/v/v, lower layer) → MeOH] to give 12 fractions [Fr. B1 (143.2 mg), Fr. B2 (185.2 mg), Fr. B3 (437.6 mg), Fr. B4 (191.5 mg), Fr. B5 (266.9 mg), Fr. B6 (537.3 mg), Fr. B7 (971.1 mg), Fr. B8 (5.14 g), Fr. B9 (2.07 g), Fr. B10 (2.67 g), Fr. B11 (6.24 g), Fr. B12 (1.39 g)]. Fraction B8 (5.14 g) was subjected to reversed‑phase silica gel column chromatography [305 g, MeOH: H_2O (7:3 → 8:2 → 9:1, v/v) → MeOH] to give 14 fractions [Fr. B8–1 (111.5 mg), Fr. B8–2 (32.6 mg), Fr. B8–3 (12.3 mg), Fr. B8–4 (17.4 mg) , Fr. B8–5 (18.7 mg), Fr. B8–6 (11.5 mg), Fr. B8–7 (152.1 mg), Fr. B8–8 (3.72 g) , Fr. B8–9 (632.2 mg), Fr. B8–10 (15.7 mg), Fr. B8–11 (5.6 mg), Fr. B8–12 (5.2 g), Fr. B8–13 (14.9 mg), Fr. B8–14 (48.5 mg)]. Fraction B11 (6.24 g) was subjected to reversed‑phase silica gel column chromatography [330 g, MeOH: H_2O (5:5 → 6:4 → 7:3 → 8:2 →, v/v) → MeOH] to give 14 fractions [Fr. B11–1 (1.50 g), Fr. B11–2 (50.3 mg), Fr. B11–3 (46.9 mg), Fr. B11–4 (54.8 mg) , Fr. B11–5 (221.4 mg), Fr. B11–6 (757.6 mg), Fr. B11–7 (1.10 g), Fr. B11–8 (1.51 g), Fr. B11–9 (485.8 mg), Fr. B11–10 (201.7 mg), Fr. B11–11 (203.6 mg), Fr. B11–12 (139.3 mg), Fr. B11–13 (30.5 mg), Fr. B11–14 (44.8 mg)]. A part of the Fr. B8–8 (200.0 mg) was purified by HPLC [acetonitrile: H_2O: acetic acid (88:12:0.3), XBridge BEH C18] to give **1** (63.9 mg, purity > 92%) and **2** (34.2 mg, purity > 90%). A part of the Fr. B11–8 (1.51 g) was purified by HPLC [acetonitrile: H_2O: acetic acid (88:12:0.3), XBridge BEH C18] to give **3** (29.4 mg, purity > 95%). The known compounds were identified by comparison of their physical data ($[\alpha]_D$, ^{1}H-NMR, ^{13}C-NMR, and MS) with reported values.

4.2.3. Acid hydrolyses

Compounds **1** and **2** (10.1 and 10.4 mg) were dissolved in 5 mL of 3 mol/L sulfuric acid and each solution was heated at 90 ℃ for 6 h. After neutralizing with sodium hydroxide, each hydrolysate was extracted 5 mL of ethyl acetate. Evaporation of the solvent under reduced

pressure yielded **4** (5.6 mg from **1**, purity > 95%) and **5** (6.0 mg from **2**, purity > 81%). Each compound was identified by comparison of their physical data ($[\alpha]_D$, ^{1}H-NMR, ^{13}C-NMR, and MS) with reported values.

4.2.4. Materials for biological assays

All materials using for biological assays were the same as described in Chapter 3.2.1.

4.2.5. Cell culture and treatment

See Chapter 2.2.3.

4.2.6. Determination of cell proliferation

The cell culture was performed as explained in Chapter 2.2.5. After replacing with fresh medium, the cells were treated with various concentrations of each fraction or each compound for 24 h. Determination of cell proliferation was performed same MTT assay protocol as described in Chapter 2.2.5.

4.2.7. Western blot analysis

Cells (1×10^6 cells/dish) were plated on 6 cm dishes. After replacing with fresh medium, the cells were treated with *n*-BuOH fraction or each compound for various time periods. All subsequent steps were performed same western blot analysis protocol as described in Chapter 2.2.4.

4.2.8. Statistical analysis

See Chapter 2.2.6.

4.3. Results

4.3.1. Comparison of antiproliferative effects of each fraction

To identify the bioactive compounds responsible for the antiproliferative effect, the crude extract was suspended in water and successively partitioned using hexane, EtOAc, and *n*-BuOH. The cells were treated with 5, 10, and 20 μg/mL of each fraction for 24 h, and cell proliferation was measured using MTT assay. As shown in Fig. 4.2A, both *n*-BuOH and H_2O fractions significantly suppressed cell proliferation compared with hexane and EtOAc fractions. To further determine which fraction exerts stronger effects, the cells were treated at much lower concentrations than 5 μg/mL of the *n*-BuOH and H_2O fractions for 24 h (Fig. 4.2C). The results showed that the suppression of the *n*-BuOH fraction was stronger than that of the H_2O fraction.

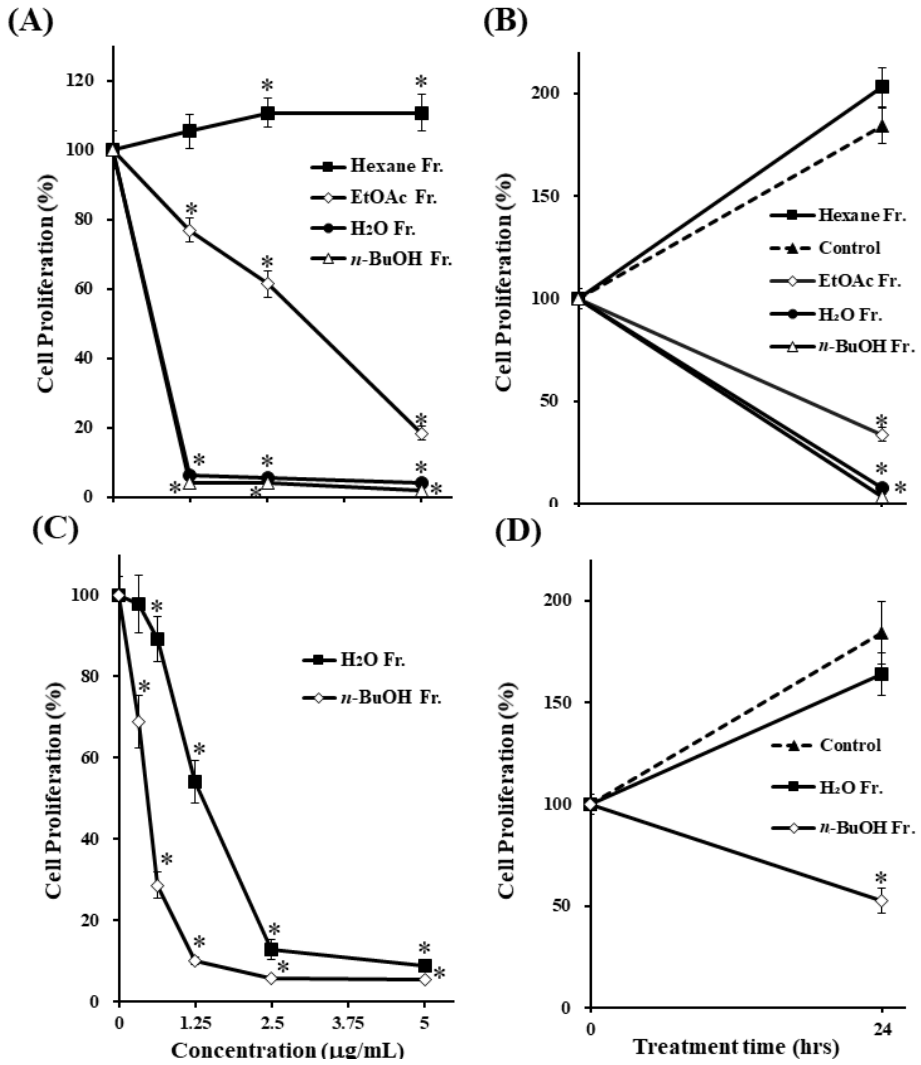

Figure 4.2. Effects of fractions prepared from Hikai extract on cell proliferation. HepG2 cells were treated with each fraction prepared from the crude extract of Hikai at various concentrations (A: 5–20 μg/mL, C: 0.313–5 μg/mL) for 24 h, and cells were treated with each fraction (B: 20 μg/mL, D: 0.625 μg/mL) for the times indicated and cell proliferations were determined using MTT assay. The data are represented as the mean ± S.D. of three individual experiments. $*p < 0.05$ compared with the control group.

4.3.2. Effect of n-BuOH fraction on autophagosome formation and autophagy flux

To confirm the effect of *n*-BuOH fraction on autophagy, we observed the expression levels of both LC3-II and p62. The cells were treated with the *n*-BuOH fraction at 0.313 μg/mL for various time periods, and the levels of each protein were examined using western blotting. As shown in Fig. 4.3, treatment of the *n*-BuOH fraction clearly increased the levels of both LC3-II and p62. These results suggest that the *n*-BuOH fraction might inhibits autophagy by blocking autophagic flux, which results in p62 and LC3-II accumulation.

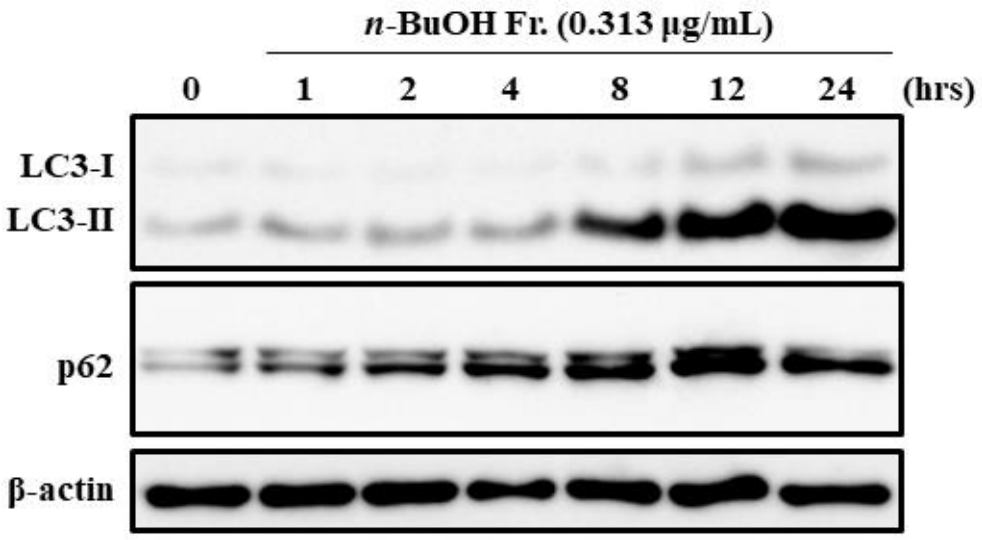

Figure 4.3. Effect of *n*-BuOH fraction on LC3-II and p62 expression levels. HepG2 cells were treated with *n*-BuOH fraction prepared from the crude extract of Hikai at 0.313 μg/mL for the times indicated. The expression levels of LC3B, p62, and β-actin were determined by western blotting. The data shown are representative of three independent treatments using the same parameters with similar results.

*4.3.3. Isolation, acid hydrolyses, and structural identification of **1**–**5***

Since the *n*-BuOH fraction reduced cell proliferation most strongly and inhibited autophagy, we performed the isolation of bioactive compounds from the *n*-BuOH fraction.

Further bioassay-guided separation using solvent partition, fractionation, and combined chromatography techniques was performed, and then we achieved the isolation of three compounds from the *n*-BuOH fraction. We isolated two spirostan-type steroidal saponins, dioscin (**1**) [5, 6], and yamogenin 3-*O*-α-L-rhamnopyranosyl(1→4)-*O*-α-L-rhamnopyranosyl (1→2)-β-D-glucopyranoside (**2**) [5, 7, 8], and a frostane-type steroidal saponins, protodioscin (**3**) [5, 9]. The structures were identified by physicochemical date including NMR and MS data, together with comparison those in the literature. In addition, **1** and **2** were acid-hydrolyzed to obtain each aglycone, diosgenin (**4**) [5, 10] and yamogenin (**5**) [5, 11]. The chemical structures of **1**–**5** are shown in Fig. 4.4. Among them, **1** and **3** are steroidal saponins that were well known as the main compounds from Hikai extract [3, 4, 12].

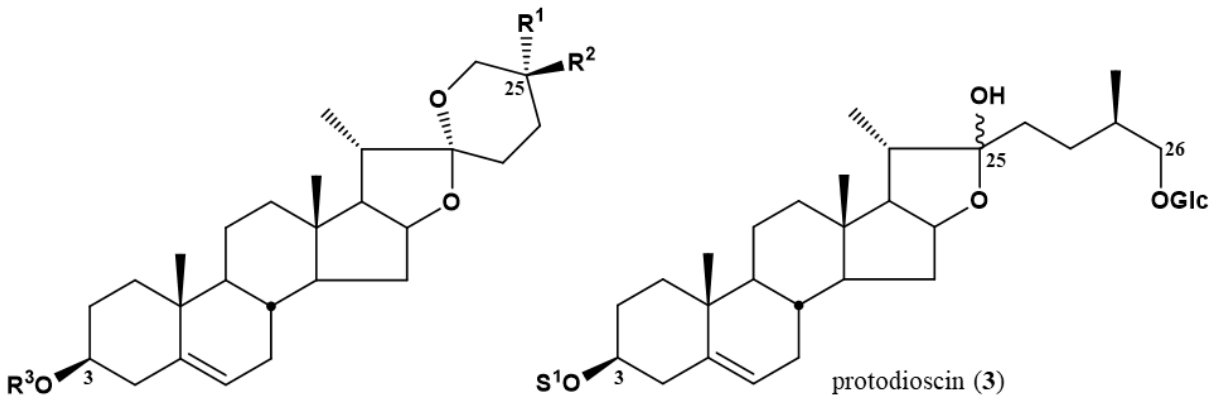

	R^1	R^2	R^3
dioscin (**1**):	CH_3	H	S^1
※(**2**):	H	CH_3	S^1
diosgenin (**4**):	CH_3	H	H
yamogenin (**5**):	H	CH_3	H

S^1 = Glc (2→1) Rha, Glc (4→1) Rha

Glc: *β*-D-glucopyranosyl
Rha: *α*-L-rhamnopyranosyl

※ yamogenin 3-*O*-*α*-L-rhamnopyranosyl(1→4)-*O*-*α*-L-rhamnopyranosyl(1→2)-*β*-D-glucopyranoside

Figure 4.4. Chemical structures of 1–5 from *n*-BuOH fraction.

*4.3.4. Effects of **1**–**5** on cell proliferation, and its structure–activity relationships*

To investigate the effects of **1**–**5** on the proliferation of HepG2 cells, we treated the cells using 6.25, 12.5, 25, 50, and 100 μM of **1**–**5** for 24 h, followed by the MTT assay. When we compared the antiproliferative effect of each compound, all compounds reduced cell proliferation and the potency was in the following order: **1** > **2** > **3** > **4** > **5** (Fig. 4.5).

The effects of **1** and **4** with a 25(*R*)-conformation were stronger than those of **2** and **5** with a 25(*S*)-conformation. These results indicated that the efficacy due to the 25(*R*)-conformation is maintained with or without the sugar moiety. Next, the effects of **1**, **2**, and **3** containing a sugar moiety were found to be stronger than those of **4** and **5** lacking one. In addition, **1** and **2**, which possess a spirostan-type aglycone moiety, showed stronger effects than **3**, which possesses a furostan-type aglycone moiety. From these results of structure–activity relationships, it was found that the 25(*R*)-conformation, structures containing a sugar moiety, and spirostan-type aglycone moiety might be important for antiproliferative effect.

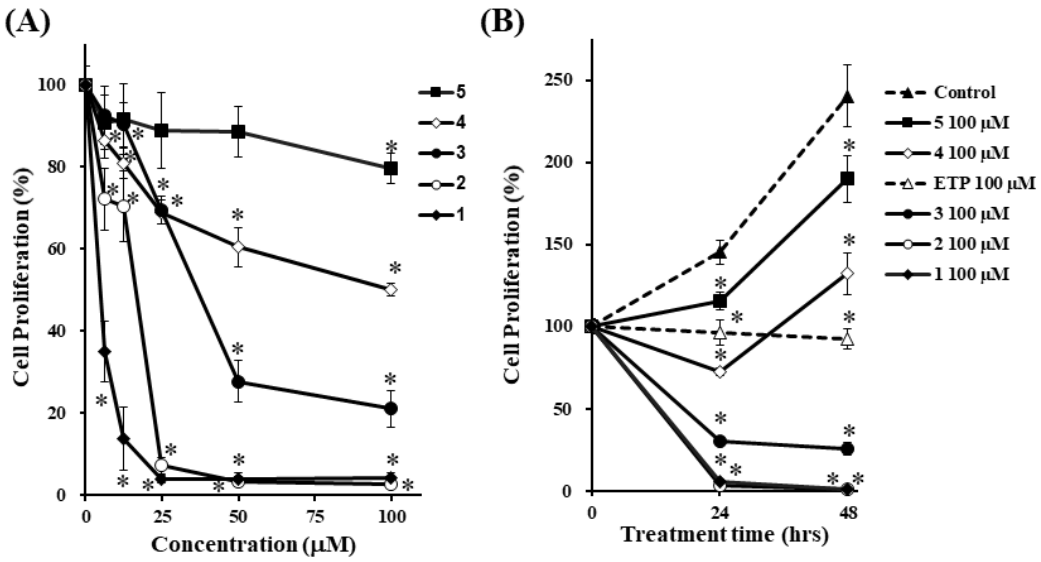

Figure 4.5. Effects of 1–5 on cell proliferation. HepG2 cells were treated with **1**–**5** at various concentrations for 24 h (A), and cells were treated with **1**–**5** (100 μM) for the times indicated (B), and cell proliferations were determined using MTT assay. ETP was used as a model for inducing apoptotic cell death against HepG2 cells. The data are presented as the mean ± S.D. of three individual experiments. $*p < 0.05$ compared with the control group.

*4.3.5. Effects of **1**–**5** on autophagosome formation and autophagy flux*

To determine whether **1**–**5** inhibit autophagy, we investigated their effects on the levels of both LC3-II and p62 in HepG2 cells. The cells were treated with **1** and **2** at 10 μM, **3** and **5** at 50 μM, and **4** at 20 μM for various time periods. As shown in Fig. 4.6, the treatment with **1**, **2**, and **3** clearly increased the levels of both LC3-II and p62. These results suggest that **1**, **2**, and **3** deregulate the autophagic pathway by blocking autophagic flux, which results in p62 and LC3-II accumulation. On the other hand, the treatments with **4** and **5** did not show a clear increase in the levels of both LC3-II and p62. These results suggest that **4** and **5** do not affect autophagy.

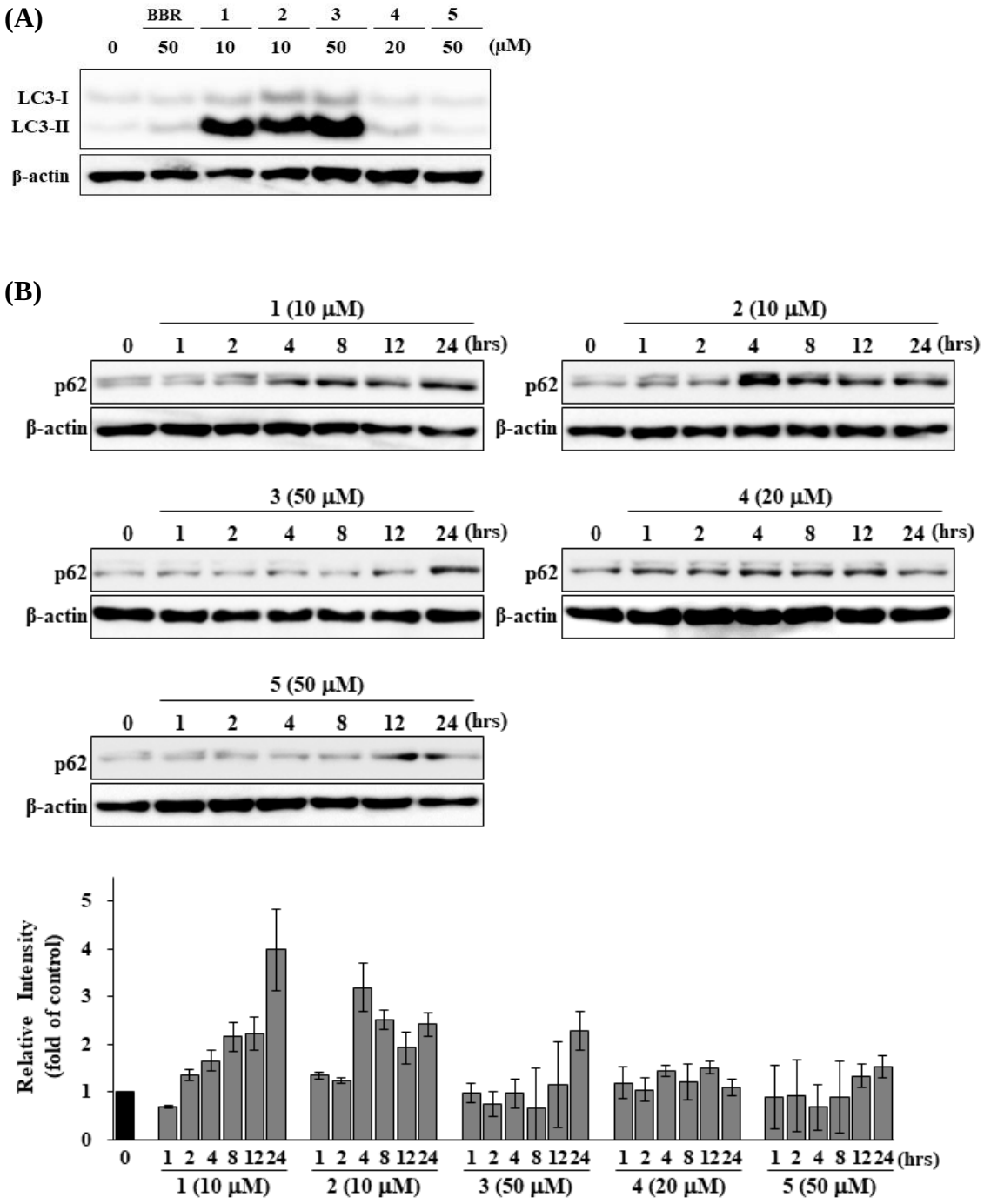

Figure 4.6. Effects of 1–5 on LC3-II and p62 expression levels. HepG2 cells were treated with the indicated concentrations of **1**–**5** for 24 h (A), or different durations (B). The expression levels of LC3B (A), p62 (B), and β-actin were determined by western blotting. BBR (50 μM) is a positive control. The data shown are representative of three independent treatments using the same parameters with similar results.

*4.3.6. Effects of **1**–**3** on apoptosis-related proteins*

To determine whether the effects of **1**, **2**, and **3** regarding high antiproliferative effect are associated with apoptosis induction, we examined the effects of **1**, **2**, and **3** on caspase-3 and PARP. ETP was used as a positive control [13, 14]. As shown in Fig. 4.7, the treatments with **1** and **2** at 10 μM, and **3** at 50 μM for 12 and 24 h did not induce the activation of caspase-3 and cleaved PARP, at all concentrations. These results suggest that the treatments with **1**, **2**, and **3** did not induce caspase-3 mediated apoptosis in HepG2 cells.

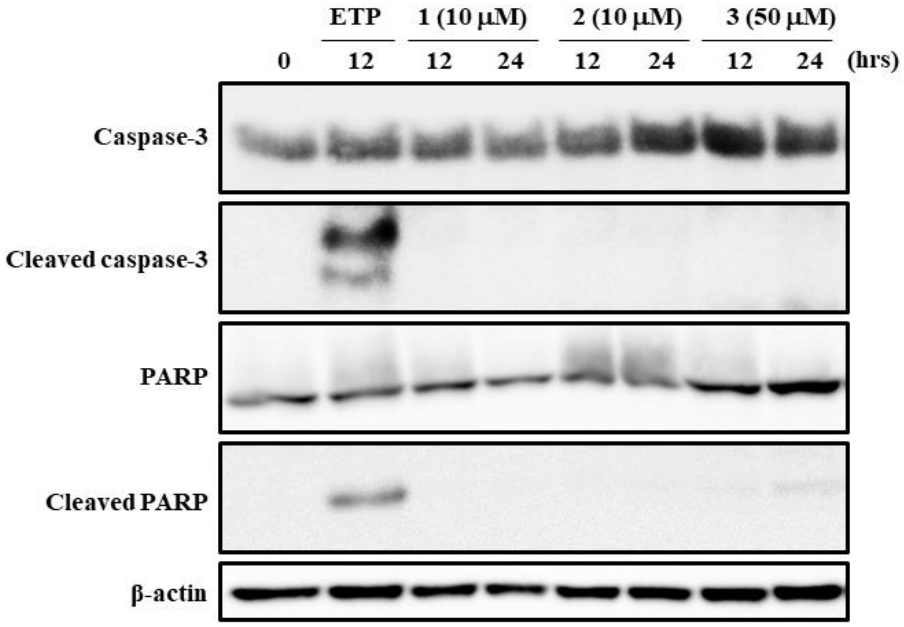

Figure 4.7. Effects of 1–3 on the activation of caspase-3 and PARP cleavage. HepG2 cells were treated with the indicated concentrations of **1**–**3** for 12 or 24 h, respectively. The expression levels of caspase-3, PARP, and β-actin were determined by western blotting. ETP (100 μM, 12 h) was used as a positive control. The data shown are representative of three independent treatments using the same parameters with similar results.

4.4. Discussion

As described in this chapter, we aimed to isolate active compounds from Hikai or Hikai extract having antiproliferative activity and inhibition of autophagy. Among four fractions prepared by MeOH extract of Hikai, the medium-polar (*n*-BuOH) fraction exhibited stronger antiproliferative effect than the other three fractions (Fig. 4.2). In addition, the *n*-BuOH fraction increased the levels of both LC3-II and p62, leading to the inhibition of autophagy (Fig. 4.3). The bioassay-guided fractionations of active fractions led to the isolation of five compounds (**1**–**5**). Among these, **1** and **3** are well known as the main compounds of Hikai extract [3, 4]. Compounds **1**–**3** are steroidal saponins and **4** and **5** are produced by the acid hydrolysis of **1** and **2** (Fig. 4.4). According to the results of cell proliferation analysis in HepG2 cells, **1–5** exerted antiproliferative activity (Fig. 4.5). Moreover, structure–activity relationship analysis suggested that the 25(*R*)-conformation, structures containing a sugar moiety, and spirostan-type aglycone moiety might be important for antiproliferative activity. To confirm that **1**–**5** inhibit autophagy in HepG2 cells, the autophagic flux was assessed by monitoring p62 levels upon treatments with **1**–**5** for different times. Treatments with **1**–**3** deregulated the autophagic pathway by blocking autophagic flux, which resulted in p62 accumulation (Fig. 4.6). Similarly, the levels of LC3-II was increased upon treatment with **1**–**3**, but not upon that with **4** and **5**. These results suggested the importance of structures containing a sugar moiety in modulating autophagy with LC3-II and p62 accumulation.

Although **1**–**3** exerted inhibitory activity on autophagy, these compounds did not show the activation of caspase-3 and the cleavage of PARP, which are characteristics of apoptosis induction (Fig. 4.7). These results suggest that the antiproliferative activity of **1**–**3** might be modulated by the inhibition of autophagy, but not the induction of caspase-3 mediated apoptosis.

4.5. Conclusion

In this chapter, we found that the medium-polar (*n*-BuOH) to high-polar (H_2O) fractions of Hikai exerted strong antiproliferative activity and inhibition of autophagy on HepG2 cells. Phytochemical investigations of the *n*-BuOH fraction achieved the isolation of steroidal saponins, dioscin (**1**), yamogenin 3-*O*-α-L-rhamnopyranosyl(1→4)-*O*-α-L-rhamno- pyranosyl (1→2)- β-D-glucopyranoside (**2**), and protodioscin (**3**). In addition, acid hydrolysis of **1** and **2** produced each aglycone, diosgenin (**4**) and yamogenin (**5**), respectively. Structure-activity relationship analysis implied that a 25(*R*)-conformation, structures containing a sugar moiety, and spirostan-type aglycone moiety are important for antiproliferative activity. Analysis of autophagy-related proteins using HepG2 cells demonstrated that **1**–**3** might inhibit autophagy, leading to p62 accumulation.

On the other hand, **1**–**3** did not affect caspase-3 activation and PARP cleavage, suggesting that the antiproliferative activity of **1**–**3** can occur independently of caspase-3 mediated apoptosis. Taking these findings together, we conclude that **1**–**3**, active compounds in Hikai extract, suppresses cell proliferation and inhibited autophagy.

4.6. References

[1] Medicinal Plant Garden, Plant database, School of Pharmacy Kumamoto University. http://www.pharm.kumamoto-u.ac.jp/yakusodb/detail/003472.php

[2] Oyama, M.; Tokiwano, T.; Kawaii, S.; Yoshida, Y.; Mizuno, K.; Oh, K.; Yoshizawa, Y. Protodioscin, isolated from the rhizome of *Dioscorea tokoro* collected in northern Japan is the major antiproliferative compound to HL-60 leukemic cells. *Curr. Bioact. Compd*. **2017**, *13*, 170–174.

[3] Xu, X.H.; Li, T.; Fong, C.M.; Chen, X.; Chen, X.J.; Wang, Y.T.; Huang, M.Q.; Lu, J.J. Saponins from Chinese medicines as anticancer agents. *Molecules* **2016**, *5*, 21.

[4] Kim, M.J.; Kim, H.N.; Kang, K.S.; Baek, N.I.; Kim, D.K.; Kim, Y.S.; Jeon, B.H.; Kim, S.H. Methanol extract of *Dioscoreae Rhizoma* inhibits pro-inflammatory cytokines and mediators in the synoviocytes of rheumatoid arthritis. *Int. Immunopharmacol*. **2004**, *4*, 1489–1497.

[5] Yoshikawa, M.; Xu, F.; Morikawa, T.; Pongpiriyadacha, Y.; Nakamura, S.; Asao, Y.; Kumahara, A.; Matsuda, H. Medicinal flowers. XII.(1) New spirostane-type steroid saponins with antidiabetogenic activity from *Borassus flabellifer*. *Chem. Pharm. Bull*. **2007**, *55*, 308–316.

[6] Nakano, K.; Murakami, K.; Takaishi, Y.; Tomimatsu, T.; Nohara, T. Studies on the constituents of *Heloniopsis orientalis* (THUNNB.) C. TANAKA. *Chem. Pharm. Bull*. **1989**, *37*, 116–118.

[7] Asami, A.; Hirai, Y.; Shoji, J. Studies on the constituents of palmae plants. VI. Steroid saponins and flavonoids of leaves of *Phoenix canariensis* hort. ex CHABAUD, *P. humilis* ROYLE var. *hanceana* BECC., *P. dactylifera* L., and *Licuala spinosa* WURMB. *Chem. Pharm. Bull*. **1991**, *39*, 2053–2056.

[8] Viviane, S. P.; Alexandre, T. C. Taketab.; Grace, G.; Eloir, P. S. Saponins and sapogenins from *Brachiaria decumbens* stapf. *J. Braz. Chem. Soc*. **2002**, *13*, 135–139.

[9] Hu, K.; Dong, A.; Yao, X.; Kobayashi, H.; Iwasaki, S. Antineoplastic agents. II. Four furostanol glycosides from rhizomes of *Dioscorea collettii* var. hypoglauca. *Planta Med*. **1997**, *63*, 161–165.

[10] Konishi, T.; Kiyosawa, S.; Shoji, J. Studies on the coloration mechanism of furostanol derivatives with Ehrlich reagent. II. On the reaction of furostanol glycoside with Ehrlich reagent. *Chem. Pharm. Bull*. **1985**, *33*, 591–597.

[11] P.K, Agrawal.; D.C, Jain.; R.K, Gupta.; R.S, Thakur. Carbon-13 NMR spectroscopy of steroidal sapogenins and steroidal saponins. *Phytochemistry* **1985**, *24*, 2479–2496.

[12] Ebizuka, Y.; Morita, H.; Abe, I. "Chapter 4, terpenoid and steroid", *Chemistry of Organic Natural Products third edition*, Nankodo Co., Ltd., Tokyo, **2016**, p.161–165. (In Japanese).

[13] Sermeus, A.; Cosse, J.P.; Crespin, M.; Mainfroid, V.; de Longueville, F.; Ninane, N.; Raes, M.; Remacle, J.; Michiels, C. Hypoxia induces protection against etoposide-induced apoptosis: Molecular profiling of changes in gene expression and transcription factor activity. *Mol. Cancer* **2008**, *7*, 27.

[14] Xie, B.S.; Zhao, H.C.; Yao, S.K.; Zhuo, D.X.; Jin, B.; Lv, D.C.; Wu, C.L.; Ma, D.L.; Gao, C.; Shu, X.M.; Ai, Z.L. Autophagy inhibition enhances etoposide-induced cell death in human hepatoma G2 cells. *Int. J. Mol. Med*. **2011**, *27*, 599–606.

Chapter 5

Inhibition of autophagy by major active compounds contained in the root of *Saussurea lappa* (Mokko)

5.1. Introduction

As described in Chapter 2, the screening data demonstrated that extract of the root of *Saussurea lappa* (hereafter, Mokko) (Fig. 5.1) exerted the second strongest suppression on cell proliferation.

Figure 5.1. The flower [1] **and the root of *Saussurea lappa* (Mokko).**

Mokko has been traditionally used in the alleviation of pain during abdominal distention and tenesmus, indigestion with anorexia, dysentery, nausea, and vomiting because it provides warming effects in the gastrointestinal tract [1–3]. Furthermore, in Japan, Korea, and China, Mokko extract is used for the management of asthma [4], inflammatory diseases [5, 6], and ulcers [7]. Previous studies have demonstrated that the extract of Mokko possesses anticancer activity on several cancer cell lines by inducing apoptosis in the AGS gastric cancer cells,

human prostate carcinoma LNCaP cells, KB human oral cancer cells, and androgen-insensitive human prostate cells [8–11]. As an attractive side, the Japanese name Mokko refers to "wood fragrance," and Mokko has a reputation for its fragrance and use in perfumery, and Mokko extract is also used as aromatic stomachic medicine.

Mokko contains up to 3% essential oil including principal sesquiterpene lactones, such as costunolide (CL) and dehydrocostuslactone (DCL) (Fig. 5.2) [2].

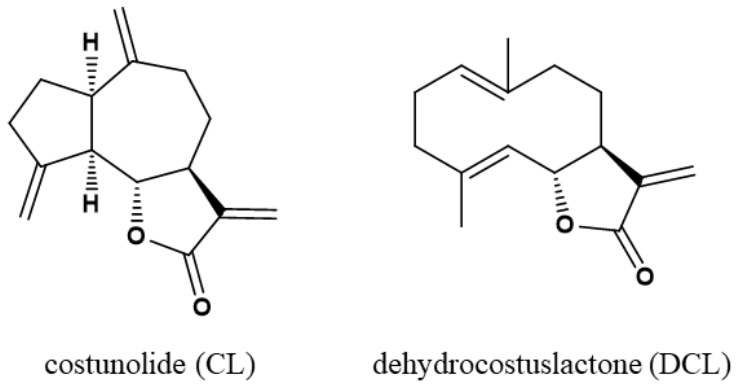

Figure 5.2. Chemical structures of CL and DCL.

Several of sesquiterpene lactones, including CL and DCL, were shown to possess various biological and pharmacological activities such as anti-inflammatory [12], antiulcer [4, 7], antiviral, and hepatoprotective effects [13]. Among them, CL and DCL are well known to possess anticancer effects. CL and DCL have been reported to induce apoptosis in the cell lines of prostate cancer [9, 11], oral cancer [10], lung cancer [14], breast cancer [15], hepatocellular carcinoma [16], colon cancer [17], neuroblastoma [18], and leukemia [19]. Although various beneficial pharmacological activities of CL and DCL have been clarified, the effects of CL and DCL on autophagy are still unclear.

As described in this chapter, we aimed to determine the high antiproliferative activity and

the inhibition of autophagy exerted by the active compounds contained in Mokko on the HepG2 cells. First, we compared the activities of the fractions prepared from the MeOH extract of Mokko. TLC and HPLC analyses of active fractions led to the confirming of CL and DCL containing. Finally, we investigated the effects of CL and DCL on cell proliferation and confirmed the inhibition of autophagy.

5.2. Materials and methods

5.2.1. General procedures

TLC was performed to same methods as described in Chapter 4.2.1.

5.2.2. Extraction

The roots of *Saussurea lappa* (3.0 kg) were extracted three times with MeOH under reflux for 12 h. Evaporation of the solvent under reduced pressure provided a MeOH extract (689.77 g). A part of the MeOH extract (684.35 g) was partitioned same extraction protocol as described in Chapter 4.2.2. The following each soluble fractions were obtained: hexane (92.87 g), EtOAc (57.39 g), *n*-BuOH (72.06 g), and H_2O (450.33 g).

5.2.3. Preparation of sample solution

For each sample, 5.0 mg of each sample (MeOH extract, hexane fraction, EtOAc fraction, BuOH fraction, and H_2O fraction) was suspended in 1 mL of MeOH. The working solution at concentrations of 5.0 mg/mL (MeOH extract, BuOH fraction, and H_2O fraction) and 0.5 mg/mL (hexane fraction, and EtOAc fraction) were used to determine the content of CL and DCL. Each supernatant was then filtered (Millex-LG 0.20 µm, 4 mm, Merck Ltd., MA, USA), and a 10 µL aliquot of each filtrate was analyzed by HPLC.

5.2.4. Preparation of standard solution

A stock standard solution was prepared by placing CL and DCL (each 1.00 mg) adding 1 mL of MeOH. The solution contained CL and DCL at concentrations of each 1.00 mg/mL. The working solutions were used to construct calibration curves. (CL and DCL: 500 µg/mL, 100 µg/mL, 50 µg/mL, 10 µg/mL, 5 µg/mL). Calibration curves were made by injecting a 10 µL aliquot of each working solution into the HPLC system.

5.2.5. HPLC instruments and conditions for CL and DCL

The HPLC system was performed on a JASCO LC-2000 Plus series (JASCO, Tokyo, Japan) equipped with an intelligent UV-VIS detector (UV-2075 Plus), a quaternary gradient pump (PV-2089 Plus), an intelligent column oven (CO-2065 Plus), an intelligent autosampler (AS-2057 Plus), an interface (LC-Net II/ADC), and a data software (Chrom NAV). TSKgel ODS-100V column (4.6 × 250 mm, particle size 5 µm, Tosoh Corp. Tokyo, Japan) was used for the HPLC analysis at 40 ◦C with mobile phases acetonitrile and 0.1% aq. formic acid eluted according to the following gradient program: 0 min (40:60, v/v) → 20 min (100:0, v/v) → 30 min (50:50, v/v, hold). The flow rate was 1 mL/min, the injection volume was 10.0 µL, and the detection wavelength was 225 nm. Peaks for CL and DCL were observed at 15.0 min, and 15.5 min, respectively.

5.2.6. Calibration

Calibration curves were constructed with five standards prepared over the following concentration ranges: 5–500 µg/ml. Calibration curves were constructed by plotting concentration (µg/mL) on the horizontal axis and peak area (µV*sec) on the vertical axis. Linearity was determined using the correlation coefficient (r^2).

5.2.7. Materials for biological assays

CL (purity > 95%) and DCL (purity > 98%) were purchased from Tokyo Chemical Industries (Tokyo, Japan). All other materials for biological assays using were the same as described in Chapter 3.2.1.

5.2.8. Cell culture and treatment

See Chapter 2.2.3.

5.2.9. Determination of cell proliferation

See Chapter 4.2.6.

5.2.10. Western blot analysis

Cells (1×10^6 cells/dish) were plated on 6 cm dishes. After replacing with fresh medium, the cells were treated with hexane fraction or each compound for various time periods. All subsequent steps were performed same western blot analysis protocol as described in Chapter 2.2.4.

5.2.11. Statistical analysis

See Chapter 2.2.6.

5.3. Results

5.3.1. Comparison of antiproliferative effects of each fraction

To identify the active compounds responsible for the antiproliferative effect, the crude extract was suspended in water and successively partitioned with the use of hexane, EtOAc, and *n*-BuOH. The cells were treated with 2.5, 5, 10, and 20 μg/mL of each fraction for 24 h, and cell proliferation was measured using MTT assay. As shown in Fig. 5.3, the hexane fraction most strongly suppressed the cell proliferation than the EtOAc, *n*-BuOH, and H_2O fractions.

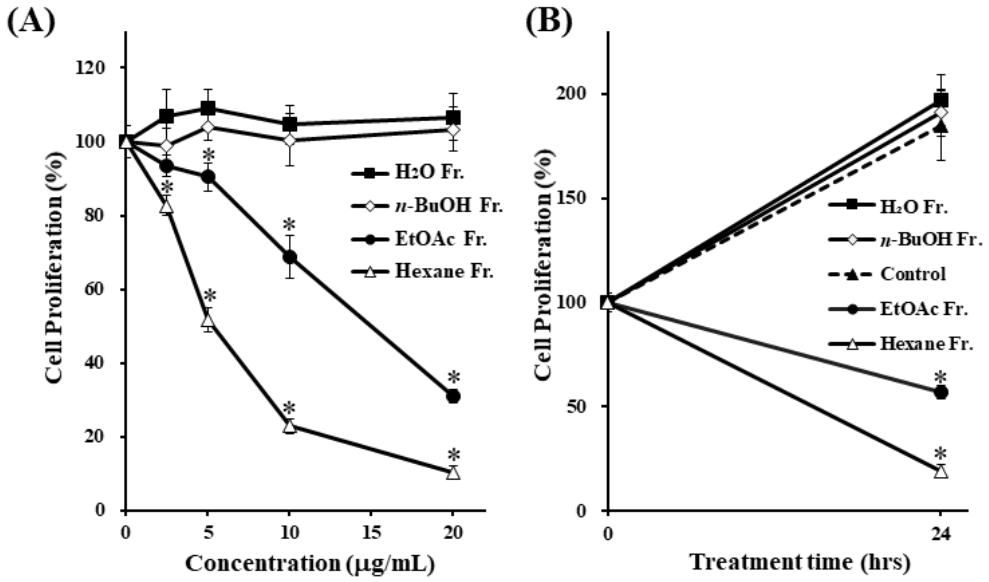

Figure 5.3. Effects of fractions prepared from Mokko extract on cell proliferation. HepG2 cells were treated with each fraction prepared from the crude extract of Mokko at various concentrations for 24 h (A), and cells were treated with each fraction (B: 20 μg/mL) for the times indicated and cell proliferations were determined using MTT assay. The data are represented as the mean ± S.D. of three individual experiments. $*p < 0.05$ compared with the control group.

5.3.2. Effect of hexane fraction on autophagosome formation and autophagy flux

To confirm whether the hexane fraction inhibits autophagy, we investigated the effect of hexane fraction on the expression levels of both LC3-II and p62. The cells were treated with hexane fraction at 5 μg/mL for various time periods, and the levels of each protein were examined using western blotting. As shown in Fig. 5.4, the hexane fraction treatment clearly increased the levels of both LC3-II and p62. These results suggest that the hexane fraction deregulates the autophagic pathway by blocking autophagic flux, thereby resulting in the accumulation of p62 and LC3-II.

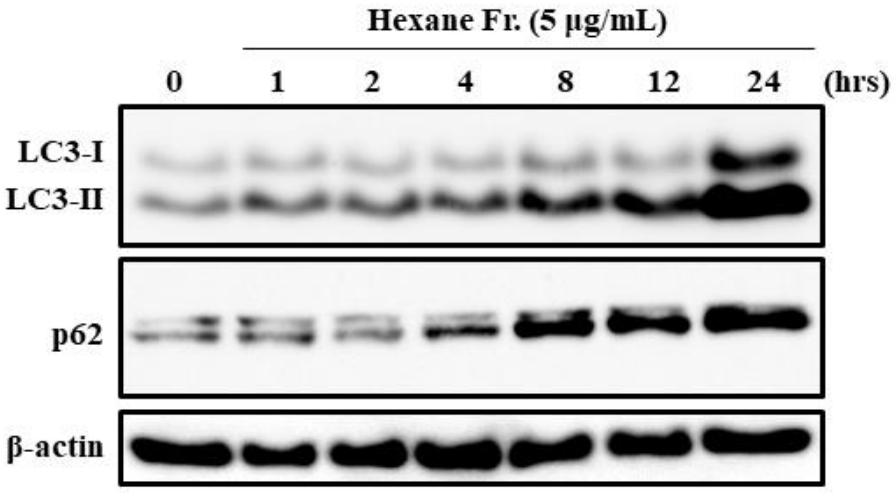

Figure 5.4. Effect of hexane fraction on LC3-II and p62 expression levels. HepG2 cells were treated with hexane fraction prepared from the crude extract of Mokko at 5 μg/mL for the times indicated. The expression levels of LC3B, p62, and β-actin were determined by western blotting. The data shown are representative of three independent treatments using the same parameters with similar results.

5.3.3. TLC and HPLC analyses of CL, DCL, MeOH extract, and fractions

Next, we confirmed the presence of major compounds in the hexane fraction. The confirmation test by TLC based on the Japanese Pharmacopoeia, and HPLC demonstrated that the hexane and EtOAc fractions mainly contained CL and DCL (Fig. 5.5 and 5.6).

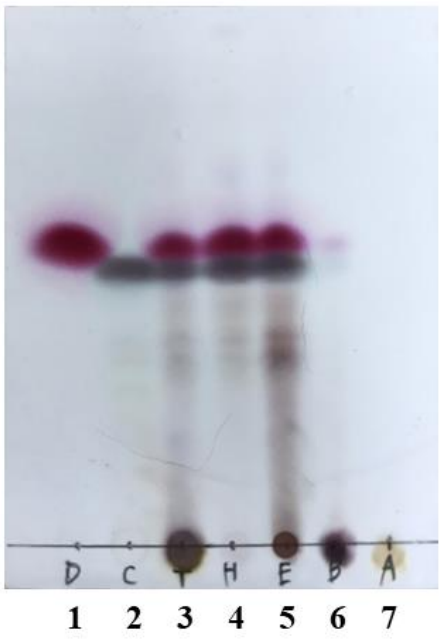

Figure 5.5. TLC analysis of CL, DCL, MeOH extract, and fractions. TLC silica gel plate was visualized by spraying with 10% aq. sulfuric acid, which was followed by heating. Solvent; Hexane:Acetone = 7:3

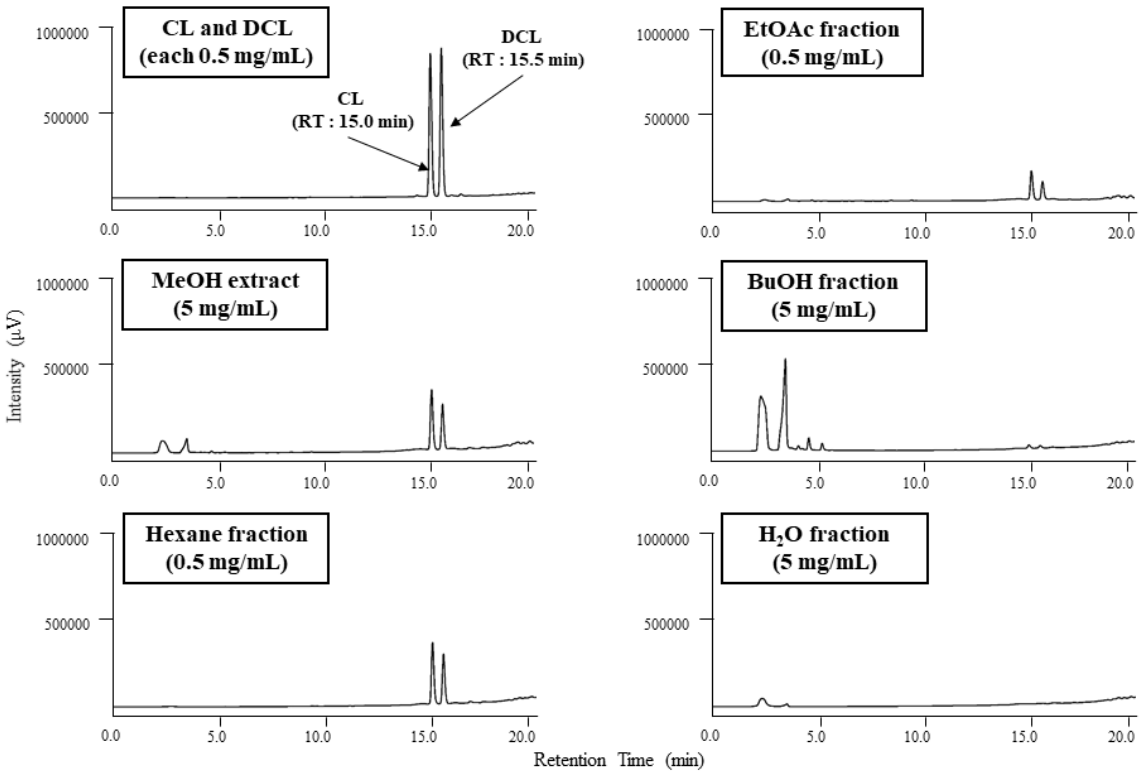

Figure 5.6. HPLC chromatograms of CL, DCL, MeOH extract, and fractions.

5.3.4. Effects of CL and DCL on cell proliferation

To investigate the effects of CL and DCL on the proliferation of the HepG2 cells, we treated the cells with 6.25, 12.5, 25, 50, and 100 μM of CL and DCL for 24 h in the MTT assay. As shown in Fig. 5.7, a significant decrease in cell proliferation was observed in the presence of CL or DCL.

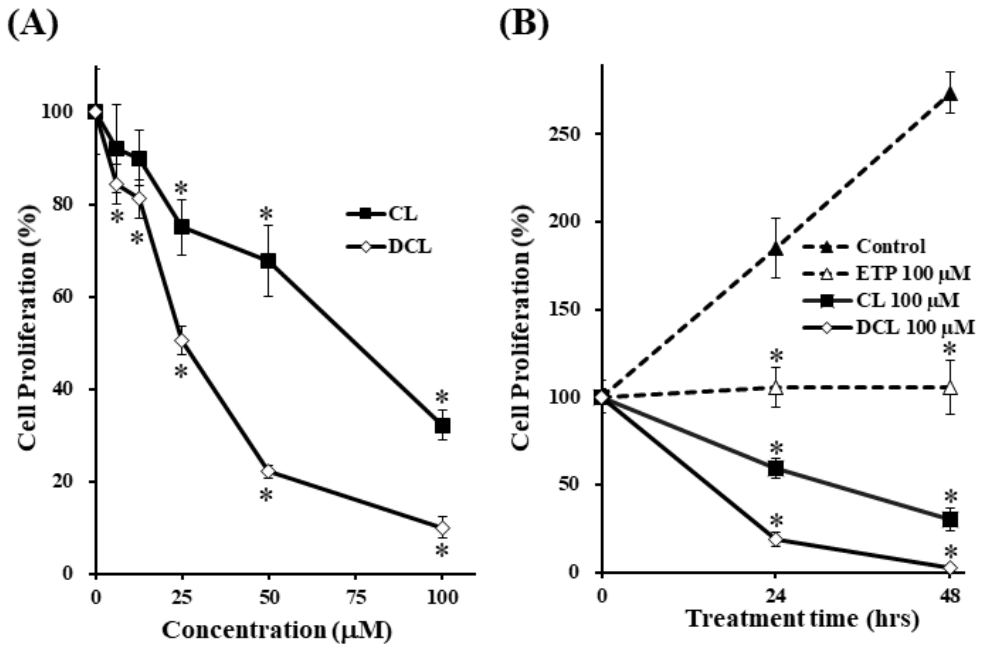

Figure 5.7. Effects of CL and DCL on cell proliferation. HepG2 cells were treated with CL and DCL at various concentrations for 24 h (A), and cells were treated with CL and DCL (100 μM) for the times indicated (B) and cell proliferations were determined using MTT assay. ETP was used as a model for inducing apoptotic cell death against HepG2 cells. The data are presented as the mean ± S.D. of three individual experiments.∗$p < 0.05$ compared with the control group.

5.3.5. Effects of CL and DCL on autophagosome formation and autophagy flux

We next examined the effects of CL and DCL on the levels of both LC3-II and p62 to confirm autophagy. The cells were treated with the CL at 10 μM and with the DCL at 20 μM for various time periods. As shown in Fig. 5.8, the CL and DCL treatment clearly increased the levels of both LC3-II and p62. These results suggest that CL and DCL trigger autophagy inhibition by blocking the autophagic flux, thereby resulting in the accumulation of p62 and LC3-II.

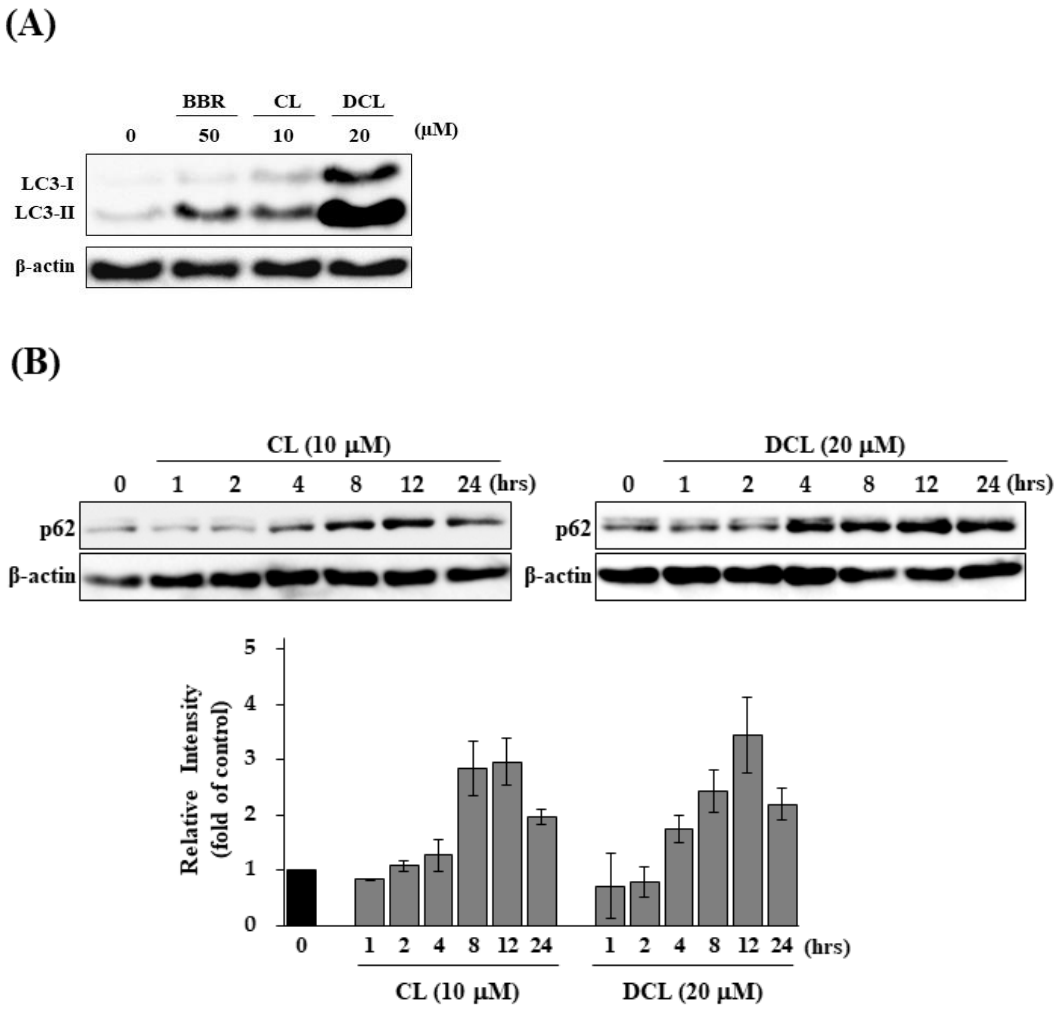

Figure 5.8. Effects of CL and DCL on LC3-II and p62 expression levels. HepG2 cells were treated with the indicated concentrations of CL and DCL for 24 h (A), or different durations (B). The expression levels of LC3B (A), p62 (B), and β-actin were determined by western blotting. BBR (50 μM) is a positive control. The data shown are representative of three independent treatments using the same parameters with similar results.

5.3.6. Effects of CL and DCL on apoptosis-related proteins

To determine whether the induction of apoptosis is associated with the antiproliferative effect of CL and DCL, we examined the effects of CL and DCL on caspase-3 and PARP. We used ETP as a positive control [20, 21]. As shown in Fig. 5.9, the CL and DCL weakly induced the activation of caspase-3 and PARP. These results suggest that the antiproliferative effect of CL and DCL might be partly caused by the induction of apoptosis.

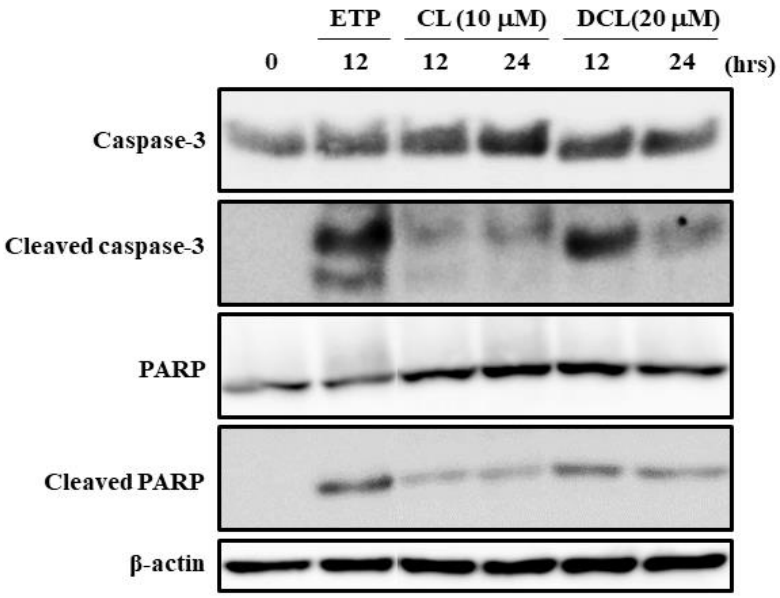

Figure 5.9. Effects of CL and DCL on the activation of caspase-3 and PARP cleavage. HepG2 cells were treated with indicated concentrations of CL and DCL for 12 or 24 h, respectively. The expression levels of caspase-3, PARP, and β-actin were determined by western blotting. ETP (100 μM, 12 h) is a positive control. The data shown are representative of three independent treatments using the same parameters with similar results.

To determine whether autophagy is involved in the apoptosis-inducing activity of ETP, we investigated the effect of ETP on autophagy-related proteins. The cells were treated with ETP at 100 μM for various time periods. As shown in Fig. 5.10, ETP treatment clearly increased the LC3-II levels. However, ETP had no effect on p62 levels during treatment. These results suggest that ETP did not block autophagic flux.

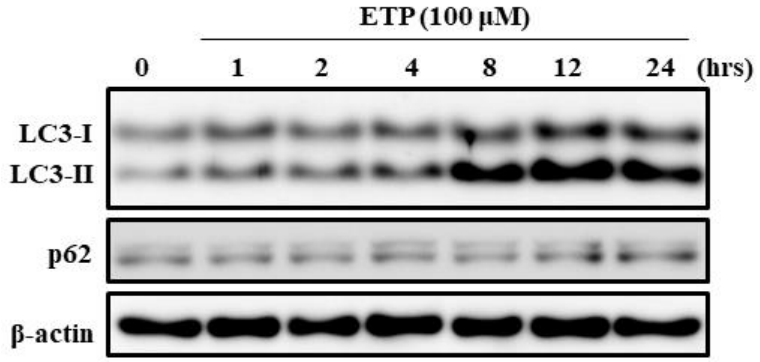

Figure 5.10. Effects of ETP on LC3-II and p62 expression levels. HepG2 cells were treated with ETP at 100 μM for the times indicated. The expression levels of LC3B, p62, and β-actin were determined by western blotting. The data shown are representative of three independent treatments using the same parameters with similar results.

5.4. Discussion

As described in this chapter, we first determined the fraction of Mokko extract by using the antiproliferative activity as an index. Among the four fractions, the non-polar (hexane) to low-polar (EtOAc) fractions exerted strong antiproliferative activity, and the hexane fraction possessed the strongest antiproliferative activity (Fig. 5.3). Moreover, the hexane fraction showed autophagy inhibition by the accumulation of p62 and LC3-II (Fig. 5.4). Next, we confirmed the main compounds contained in the hexane fraction. TLC and HPLC analyses determined that the major compounds in the hexane and EtOAc fractions were CL and DCL (Fig. 5.5 and 5.6), which are widely known to be the primary active compounds in the Mokko extract [2]. Both CL and DCL exerted the antiproliferative activity (Fig. 5.7) and deregulated the autophagic pathway by blocking the autophagic flux, thereby resulting in the accumulation of p62 (Fig. 5.8). In HepG2 cells, CL and DCL weakly induced the activation of caspase-3 and the cleavage of PARP (Fig. 5.9), thereby suggesting that CL and DCL might be involved in the induction of apoptosis. Taken together, both CL and DCL might exert antiproliferative activity with the inhibition of autophagy and induction of apoptosis. Although ETP induced apoptosis, ETP did not block autophagic flux because p62 levels were not changed by ETP (Fig. 5.10). These findings imply that the mechanisms of actions of CL and DCL are different from that of ETP. Further investigations may provide new knowledge into the link between apoptosis and autophagy.

5.5. Conclusion

In this chapter, we found that the non-polar (hexane) to low-polar (EtOAc) fractions of Mokko exerted exceedingly strong antiproliferative activity and inhibited autophagy on HepG2 cells. TLC analysis confirmed that CL and DCL were primary sesquiterpene lactones contained in the hexane and EtOAc fractions and suppressed the proliferation of HepG2 cells. The analysis of autophagy-related proteins by using HepG2 cells demonstrated that CL and DCL might inhibit autophagy, thereby leading to the accumulation of p62. Interestingly, CL and DCL weakly evoked the activation of caspase-3 and the cleavage of PARP, thereby suggesting that the antiproliferative activity by CL and DCL are also partly involved in an apoptotic process.

5.6. References

[1] Takeya, K.; Kiuchi, H.; Komatsu, K. "Section, Mokko", *Supplement to the Pharmacognosy third edition*, Nankodo Co., Ltd., Tokyo, **2018**, p.319–320. (In Japanese).

[2] Sun, C.M.; Syu, W.J.; Don, M.J.; Lu, J.J.; Lee, G.H. Cytotoxic sesquiterpene lactones from the root of *Saussurea lappa*. *J. Nat. Prod*. **2003**, *66*, 1175–1180.

[3] M.M. Pandey.; S. Rastogi.; A.K. Rawat. *Saussurea costus*: Botanical, chemical and pharmacological review of an ayurvedic medicinal plant. *J. Ethnopharmacol*. **2007**, *110*, 379–390.

[4] Zahara, K.; Tabassum, S.; Sabir, S.; Arshad, M.; Qureshi, R.; Amjad, M.S.; Chaudhari, S.K. A review of therapeutic potential of *Saussurea lappa*-An endangered plant from Himalaya. *Asian Pac. J. Trop. Med*. **2014**, *7S1*, S60–69.

[5] Cho, J.Y.; Baik, K.U.; Jung, J.H.; Park, M.H. In vitro anti-inflammatory effects of cynaropicrin, a sesquiterpene lactone, from *Saussurea lappa*. *Eur. J. Pharmacol*. **2000**, *398*, 399–407.

[6] Gokhale, A.B.; Damre, A.S.; Kulkami, K.R.; Saraf, M.N. Preliminary evaluation of anti-inflammatory and anti-arthritic activity of *S. lappa*, *A. speciosa* and *A. aspera*. *Phytomedicine*. **2002**, *9*, 433–437.

[7] Yoshikawa, M.; Hatakeyama, S.; Inoue, Y.; Yamahara, J. Saussureamines A, B, C, D, and E, new anti-ulcer principles from Chinese *Saussureae Radix*. *Chem. Pharm. Bull.* **1993**, *41*, 214–216.

[8] Ko, S.G.; Kim, H.P.; Jin, D.H.; et al. *Saussurea lappa* induces G2growth arrest and apoptosis in AGS gastric cancer cells. *Cancer Lett*. **2005**, *220*, 11–19.

[9] Tian, X.; Song, H.S.; Cho, Y.M.; Park, B.; Song, Y.J.; Jang, S.; Kang, S.C. Anticancer effect of *Saussurea lappa* extract via dual control of apoptosis and autophagy in prostate cancer cells. *Medicine* **2017**, *96*, e7606.

[10] Moon, S.M.; Yun, S.J.; Kook, J.K.; Kim, H.J.; Choi, M.S.; Park, B.R.; Kim, S.G.; Kim, B.O.; Lee, S.Y.; Ahn, H.; Chun, H.S.; Kim, D.K.; Kim, C.S. Anticancer activity of *Saussurea lappa* extract by apoptotic pathway in KB human oral cancer cells. *Pharm. Biol*. **2013**, *51*, 1372–1377.

[11] Kim, E.J.; Lim, S.S.; Park, S.Y.; Shin, H.K.; Kim, J.S.; Park, J.H. Apoptosis of DU145 human prostate cancer cells induced by dehydrocostus lactone isolated from the root of *Saussurea lappa*. *Food Chem. Toxicol*. **2008**, *46*, 3651–3658.

[12] Choodej, S.; Pudhom, K.; Mitsunaga, T. Inhibition of TNF-α-induced inflammation by sesquiterpene lactones from *Saussurea lappa* and semi-synthetic analogues. *Planta Med*. **2018**, *84*, 329–335.

[13] Chen, H.C.; Chou, C.K.; Lee, S.D.; Wang, J.C.; Yeh, S.F. Active compounds from

Saussurea lappa Clarks that suppress hepatitis B virus surface antigen gene expression in human hepatoma cells. *Antiviral Res*. **1995**, *27*, 99–109.

[14] J.Y. Hung.; Y.L. Hsu.; W.C. Ni.; Y.M. Tsai.; C.J. Yang.; P.L. Kuo.; et al. Oxidative and endoplasmic reticulum stress signaling are involved in dehydrocostuslactone-mediated apoptosis in human non-small cell lung cancer cells. *Lung Cancer* **2010**, *68*, 355–365.

[15] Peng, Z.; Wang, Y.; Fan, J.; Lin, X.; Liu, C.; Xu, Y.; Ji, W.; Yan, C.; Su, C. Costunolide and dehydrocostuslactone combination treatment inhibit breast cancer by inducing cell cycle arrest and apoptosis through c-Myc/p53 and AKT/14-3-3 pathway. *Sci. Rep*. **2017**, *7*, 41254.

[16] Y.L. Hsu.; L.Y. Wu.; P.L. Kuo. Dehydrocostuslactone, a medicinal plant-derived sesquiterpene lactone, induces apoptosis coupled to endoplasmic reticulum stress in liver cancer cells. *J. Pharmacol. Exp. Ther*. **2009**, *329*, 808–819.

[17] Dong, G.Z.; Shim, A.R.; Hyeon, J.S.; Lee, H.J.; Ryu, J.H. Inhibition of Wnt/β-catenin pathway by dehydrocostus lactone and costunolide in colon cancer cells. *Phytother. Res.* **2015**, *29*, 680–686.

[18] Tabata, K.; Nishimura, Y.; Takeda, T.; Kurita, M.; Uchiyama, T.; Suzuki, T. Sesquiterpene lactones derived from *Saussurea lappa* induce apoptosis and inhibit invasion and migration in neuroblastoma cells. *J. Pharmacol. Sci*. **2015,** *127*, 397–403.

[19] G.S. Oh.; H.O. Pae.; H.T. Chung.; J.W. Kwon.; J.H. Lee.; T.O. Kwon.; et al. Dehydrocostus lactone enhances tumor necrosis factor-α-induced apoptosis of human leukemia HL-60 cells. *Immunopharmacol. Immunotoxicol*. **2004**, *26*, 163–175.

[20] Sermeus, A.; Cosse, J.P.; Crespin, M.; Mainfroid, V.; de Longueville, F.; Ninane, N.; Raes, M.; Remacle, J.; Michiels, C. Hypoxia induces protection against etoposide-induced apoptosis: Molecular profiling of changes in gene expression and transcription factor activity. *Mol. Cancer* **2008**, *7*, 27.

[21] Xie, B.S.; Zhao, H.C.; Yao, S.K.; Zhuo, D.X.; Jin, B.; Lv, D.C.; Wu, C.L.; Ma, D.L.; Gao, C.; Shu, X.M.; Ai, Z.L. Autophagy inhibition enhances etoposide-induced cell death in human hepatoma G2 cells. *Int. J. Mol. Med*. **2011**, *27*, 599–606.

Chapter 6

Conclusions

Autophagy is involved in cancer development [1–4]. This thesis focuses on the identification of natural products that suppress cancer cell proliferation and autophagy modulation. Autophagy is important for supporting tumor growth (see page 5, Chapter 1, Fig. 1.2) [1–4]. The role of autophagy in cancer is complex because it depends on the organ, stage, and genetic context of the tumor. To develop future cancer therapy strategies, additional research is required to elucidate the role of autophagy in cancer. However, there are currently a few reports on compounds that modulate autophagy. For potential clinical applications, the identification of compounds that induce or inhibit autophagy is valuable [1, 2, 5–12]. Autophagy inducers may provide beneficial therapeutic effects in certain neurodegeneration, infection, and cytoprotection [5, 6, 11], whereas autophagy inhibitors have been suggested to be beneficial agents for cancer therapy [1, 2, 4–12]. Autophagy inhibitors can be classified according to whether their inhibitory step occurs before or after autophagosome formation. Many current clinical trials have shown that inhibitors of late-stage autophagy can be used in combination with existing anticancer drugs to overcome resistance and that this combination is very beneficial (see page 8, Chapter 1, Table 1.1) [4, 11, 12]. Moreover, both late- and early-stage interventions are required to achieve a more efficient inhibition of autophagy in order to establish a broader and more flexible cancer therapy strategy. Recent studies have shown that natural products have beneficial effects on cancer therapy by inhibiting autophagy [13-17]. These results suggest that identification of autophagy modulators from natural products that both induce and inhibit autophagy is important for cancer therapy.

The primary goal of this thesis was to discover crude extracts that suppress both cancer

proliferation and autophagy. In Chapter 2, we screened 130 kinds of crude drugs by western blotting to monitor LC3-II levels. Some research used ELISA to observe LC3 because the method of ELISA is simple and rapid. However, it is difficult to distinguish between LC3-I and –II by ELISA. On the other hand, western blotting can determine the precise effects of compounds on LC3-II. Thus, we employed the western blotting. We found that 24 crude extracts increased the levels of LC3-II. Crude extracts prepared from Goboshi (burdock fruit), Soboku (sappan wood), Mokko (saussurea root), Rengyo (forsythia fruit), and Hikai (dioscorea) significantly suppressed the proliferation of HepG2 cells and increased the levels of p62, suggesting that these crude extracts inhibited autophagy. In contrast, crude extracts prepared from Hishinomi (water chestnut), Biwayo (loquat leaf), and Binroji (areca) induced cell growth and decreased or did not affect the levels of p62. These results suggested that these crude extracts induced autophagy contributing to cell growth (Fig. 6.1). These results further indicate that the compounds contained in these crude extracts may modulate cell proliferation and autophagy in HepG2 cells. Simultaneously, these active compounds may lead to the development of new anticancer drugs as autophagy modulators and to provide new reagents for autophagy research.

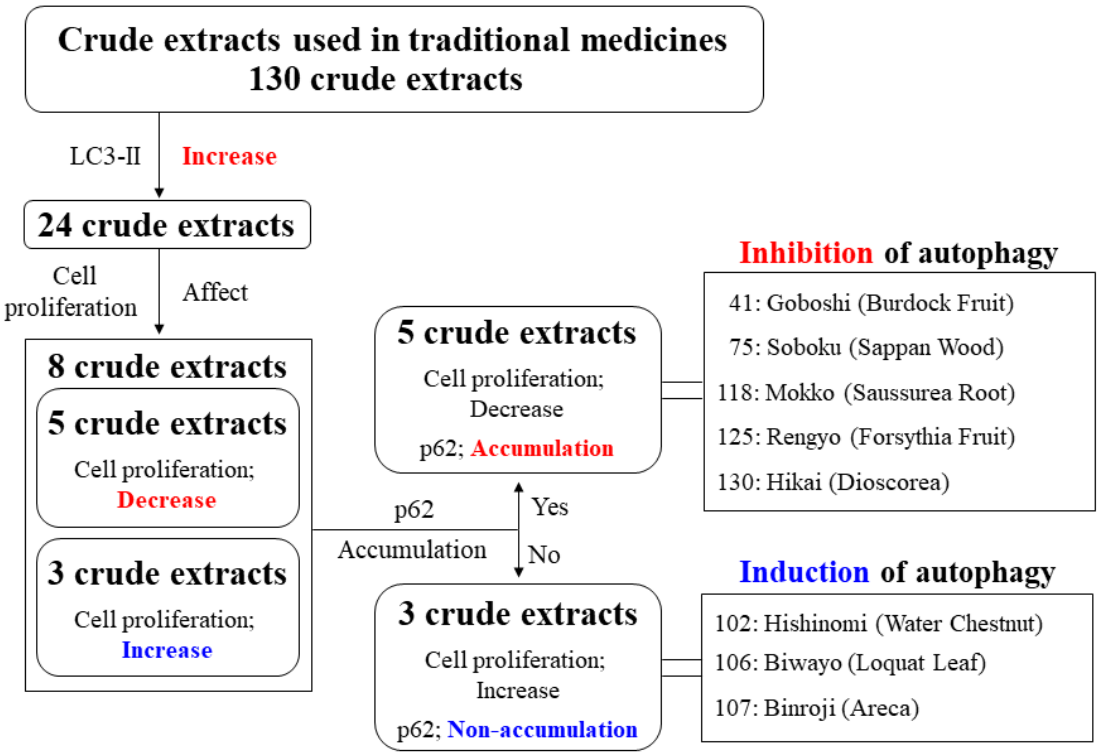

Figure 6.1. Schematic illustrating the results of screening using crude extract library.

The second goal of this thesis was to identify the major active compounds that suppress autophagy and cell proliferation from the crude extracts and to elucidate their molecular mechanisms of autophagy inhibition. 3-MA and CQ have been reported to suppress autophagy and cell proliferation in HepG2 cells [18, 19]. In addition, HCQ, an analog of CQ, is used for clinical trials to develop anticancer drug (see page 7, chapter 1) [4, 11, 12] . Therefore, this thesis focused on identifying compounds suppress autophagy and cell proliferation, like 3-MA and CQ.

In Chapter 3, we demonstrated the effects of ARG, a bioactive lignan contained in both Goboshi and Rengyo extracts, on cell proliferation and autophagy-related proteins. ARG suppressed the proliferation of HepG2 cells. Analysis of autophagy-related proteins in HepG2 and MCF-7 cells demonstrated that ARG suppressed autophagy leading to the accumulation of

p62. The stages of autophagy suppressed by ARG differed from those by 3-MA or CQ. Further, ARG suppressed starvation-induced autophagy. In contrast, ARG did not affect caspase-3 activation and PARP cleavage, suggesting that the antiproliferative activity of ARG was independent of caspase-3-mediated apoptosis. Taken together, we conclude that ARG suppressed cell proliferation and autophagy.

In Chapter 4, we demonstrated that the medium-polar (*n*-BuOH) to high-polar (H_2O) fractions of Hikai exerted strong antiproliferative activity and inhibition of autophagy on HepG2 cells. Phytochemical investigations of the most active *n*-BuOH fraction achieved the isolation of two spirostan-type steroidal saponins, dioscin (DC, **1**), yamogenin 3-*O*-α-L-rhamnopyranosyl (1→4)-*O*-α-L-rhamnopyranosyl(1→2)-β-D-glucopyranoside (YG, **2**), and a frostane-type steroidal saponins, protodioscin (PDC, **3**). Further, acid hydrolysis of **1** and **2** produced the aglycones diosgenin (**4**) and yamogenin (**5**), respectively. Compounds **1**–**5** all suppressed the proliferation of HepG2 cells. The analysis of structure-activity relationships indicated that the 25(*R*)-conformation, structures with a sugar moiety, and the spirostan-type aglycone moiety contributed to antiproliferative activity. Analysis of autophagy-related proteins demonstrated that **1**–**3** inhibited autophagy. In contrast, **1**–**3** did not significantly affect caspase-3 activation and PARP cleavage, suggesting that the antiproliferative activity of **1**–**3** occurred independently of caspase-3-mediated apoptosis. We conclude therefore that **1**–**3**, the active compounds from Hikai extracts, suppressed cell proliferation and autophagy.

In Chapter 5, we demonstrated that the non-polar (hexane) to low-polar (EtOAc) fractions of Mokko exerted strong antiproliferative activity and inhibition of autophagy in HepG2 cells. TLC and HPLC analyses showed CL and DCL were major sesquiterpene lactones contained in the hexane and EtOAc fractions. CL and DCL suppressed the proliferation of HepG2 cells. Analysis of autophagy-related proteins demonstrated that CL and DCL inhibited autophagy. Moreover, CL and DCL weakly activated caspase-3 and cleaved PARP, suggesting that the

antiproliferative activity of CL and DCL were involved in apoptosis. We conclude that CL and DCL suppress cell proliferation and autophagy, and also induce apoptosis.

In summary, this thesis reports the discovery of six autophagy-inhibiting compounds (Table 6.1) that suppressed cell proliferation of HepG2 cells. However, each compound had different characteristics in terms of the stages of autophagy inhibition and the involvement of apoptosis (Fig. 6.2).

Table 6.1. List of autophagy-inhibiting compounds identified in this thesis.

Compound name		**Content crude drug**	**IC_{50}* (μM)**	**Chapter**
ARG	Arctigenin	Goboshi Rengyo	> 100	3
DC	Dioscin	Hikai	4.09	4
YG	Yamogenin 3-*O*-α-L-rhamnopyranosyl (1→4)-*O*-α-L-rhamnopyranosyl (1→2) -β-D-glucopyranoside	Hikai	15.63	4
PDC	Protodioscin	Hikai	34.51	4
CL	Costunolide	Mokko	70.68	5
DCL	Dehydrocostuslactone	Mokko	25.36	5

* The IC_{50} value of each compound at 24 h treatments on cell proliferation.

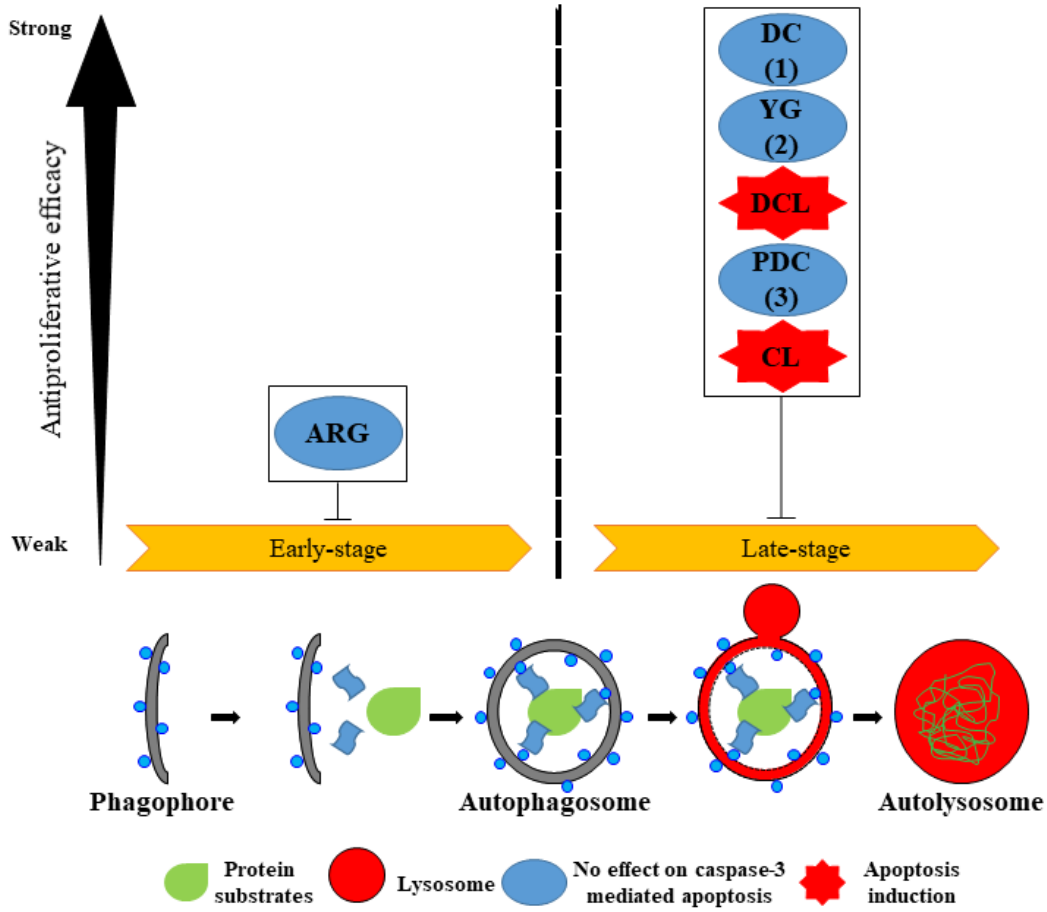

Figure 6.2. Summary of autophagy-inhibiting compounds identified in this thesis. The antiproliferative efficacy of each compound was compared based on IC_{50} values at 24 h treatments.

ARG in both Goboshi and Rengyo extracts inhibited the early-stage of autophagy. In contrast, the other five compounds inhibited the late-stage of autophagy. DC (**1**) and YG (**2**) in Hikai extract strongly suppressed cell proliferation. DC (**1**) and YG (**2**) were not involved in apoptosis-related proteins, suggesting that antiproliferative activity of DC (**1**) and YG (**2**) occurred independently of caspase-3-mediated apoptosis. In addition, although PDC (**3**) also inhibited the late-stage of autophagy, its antiproliferative activity was weaker than that of DC

(**1**) and YG (**2**). Moreover, CL and DCL in Mokko extract triggered the activation of apoptosis-related proteins suggested that CL and DCL have dual functions of autophagy inhibition and apoptosis induction.

The screening protocol used in this thesis is not suitable for identifying crude extracts that inhibit the early-stage of autophagy. In fact, five crude extracts selected for screening increased the levels of both LC3-II and p62, which are characteristics of late-stage inhibition of autophagy. Nevertheless, based on the results presented in Chapter 3, we concluded that ARG inhibits the early-stage of autophagy. Thus, this screening method may have some flexibility. This flexibility is particularly useful in research fields with many unclear points such as the study of autophagic activity.

In Chapter 3, we demonstrated that ARG suppressed cell proliferation and autophagy in HepG2 cells. Suresh *et al*. screened 500 medicinal plant extracts used in Kampo medicines. They found that a CH_2Cl_2-soluble extract of Goboshi preferentially suppresses the survival rate of cancer cells under nutritional deficiency. In addition, they reported that ARG isolated from the Goboshi extract strongly suppresses the growth of several pancreatic cancer cell lines [20]. In Japan, ARG has already been developed as investigational drug GBS-01, which is an ARG-rich Goboshi extract containing ≥ 3% ARG. A phase I/II study of GBS-01 has been performed in patients with gemcitabine-refractory advanced pancreatic cancer. The clinical safety and potential benefits of GBS-01 monotherapy were confirmed in patients with advanced pancreatic cancer refractory to gemcitabine therapy [21, 22]. The detailed method for the preparation of GBS-01 is reported in patent document JP-4963738-B2. These data strongly support our results showing that ARG has potential applications in the development of anticancer agents.

Ongoing clinical trials for cancer therapy are assessing the safety and efficacy of CQ and HCQ, which inhibit the late-stage autophagy [11]. In this thesis, DC (**1**), YG (**2**), PDC (**3**), CL, and DCL inhibit the late-stage of autophagy. The chemical structures of these compounds differ

from existing those of drugs used as inhibitors of autophagy, which may lead to the development of new autophagy inhibitor. Although HepG2 cells have been reported to be resistant to apoptosis [23], CL and DCL inhibited autophagy and induced apoptosis in HepG2 cells. There are few reports on such compounds having both activities. Thus, further research is required to determine the functions of CL and DCL using different cancer cell lines.

In this thesis, we focused on the effects of each compound on autophagy, cell proliferation, and apoptosis. Although it is known that autophagy is related with cell cycle, we could not determine the effects of each compound on cell cycle [24, 25]. Future studies are needed to elucidate the cell cycle.

In conclusion, autophagy-inhibiting compounds found in this thesis may contribute to the development of new anticancer drugs and serve as new analytical tools for autophagy research. We hope that the research approach described in this thesis, which screened for potential drugs focusing on crude drugs, will contribute to the discovery of new and improved therapies for diverse diseases.

References

[1] Degenhardt, K.; Mathew, R.; Beaudoin, B.; Bray, K.; Anderson, D.; Chen, G.; Mukherjee, C.; Shi, Y.; Gélinas, C.; Fan, Y.; et al. Autophagy promotes tumor cell survival and restricts necrosis, inflammation, and tumorigenesis. *Cancer Cell* **2006**, *10*, 51–64.

[2] Turcotte, S.; Chan, D.A.; Sutphin, P.D.; Hay, M.P.; Denny, W.A.; Giaccia, A.J. A molecule targeting VHL-deficient renal cell carcinoma that induces autophagy. *Cancer Cell* **2008**, *14*, 90–102.

[3] Yang, Z.J.; Chee, C.E.; Huang, S.; Sinicrope, F.A. The role of autophagy in cancer: Therapeutic implications. *Mol. Cancer Ther*. **2011**, *10*, 1533–1541.

[4] Marinković, M.; Šprung, M.; Buljubašić, M.; Novak, I. Autophagy modulation in cancer: Current knowledge on action and therapy. *Oxid. Med. Cell. Longev*. **2018**, *2018*, 8023821.

[5] Rabinowitz, J.D.; White, E. Autophagy and metabolism. *Science* **2010**, *330*, 1344–1348.

[6] Maiuri, M.C.; Kroemer, G. Autophagy in stress and disease. *Cell Death Differ.* **2015**, *22*, 365–366.

[7] Takamura, A.; Komatsu, M.; Hara, T.; Sakamoto, A.; Kishi, C.; Waguri, S.; Eishi, Y.; Hino, O.; Tanaka, K.; Mizushima, N. Autophagy-deficient mice develop multiple liver tumors. *Genes. Dev.* **2011**, *25*, 795–800.

[8] Komatsu, M.; Waguri, S.; Ueno, T.; Iwata, J.; Murata, S.; Tanida, I.; Ezaki, J.; Mizushima, N.; Ohsumi, Y.; Uchiyama, Y.; et al. Impairment of starvation-induced and constitutive autophagy in Atg7-deficient mice. *J. Cell Biol.* **2005**, *169*, 425–434.

[9] Wu, D.H.; Jia, C.C.; Chen, J.; Lin, Z.X.; Ruan, D.Y.; Li, X.; Lin, Q.; Min-Dong; Ma, X.K.; Wan, X.B.; Cheng, N.; et al. Autophagic LC3B overexpression correlates with malignant progression and predicts a poor prognosis in hepatocellular carcinoma. *Tumour Biol.* **2014**, 12225–12233.

[10] Kimmelman, A.C. The dynamic nature of autophagy in cancer. *Genes Dev.* **2011**, *25*, 1999–2010.

[11] Bishop, E.; Bradshaw, T.D. Autophagy modulation: A prudent approach in cancer treatment? *Cancer Chemother. Pharmacol.* **2018**, *82*, 913–922.

[12] Cynthia, I. C.; Ravi, K. A. Targeting autophagy in cancer: Update on clinical trials and novel inhibitors. *Int. J. Mol. Sci.* **2017**, *18*, 1279.

[13] Yu, R.; Zhang, Z.Q.; Wang, B.; Jiang, H.X.; Cheng, L.; Shen, L.M. Berberine-induced apoptotic and autophagic death of HepG2 cells requires AMPK activation. *Cancer Cell Int.* **2014**, *14*, 49.

[14] La, X.; Zhang, L.; Li, Z.; Yang, P.; Wang, Y. Berberine-induced autophagic cell death by elevating GRP78 levels in cancer cells. *Oncotarget* **2017**, *8*, 20909–20924.

[15] Nozaki, R.; Kono, T.; Bochimoto, H.; Watanabe, T.; Oketani, K.; Sakamaki, Y.; Okubo, N.; Nakagawa, K.; Takeda, H. Zanthoxylum fruit extract from Japanese pepper promotes autophagic cell death in cancer cells. *Oncotarget* **2016**, *7*, 70437–70446.

[16] Song, L.; Wang, Z.; Wang, Y.; Guo, D.; Yang, J.; Chen, L.; Tan, N. Natural cyclopeptide RA-XII, a new autophagy inhibitor, suppresses protective autophagy for enhancing apoptosis through AMPK/mTOR/P70S6K pathways in HepG2 cells. *Molecules* **2017**, *22*, 1934.

[17] Young, A.N.; Herrera, D.; Huntsman, A.C.; Korkmaz, M.A.; Lantvit, D.D.; Mazumder, S.; Kolli, S.; Coss, C.C.; King, S.; Wang, H.; et al. Phyllanthusmin derivatives induce apoptosis and reduce tumor burden in high-grade serous ovarian cancer by late-stage autophagy inhibition. *Mol. Cancer Ther.* **2018**, *17*, 2123–2135.

[18] Ma, T.; Li, Y.Y.; Zhu, J. Fan, L.L.; Du, W.D.; Wu, C.H.; Sun, G.P.; Li, J.B. Enhanced autophagic flux by endoplasmic reticulum stress in human hepatocellular carcinoma cells contributes to the maintenance of cell viability. *Oncol. Rep.* **2013**, *30*, 433–440.

[19] Hu, T.; Li, P.; Luo, Z.; Chen, X.; Zhang, J.; Wang, C.; Chen, P.; Dong, Z. Chloroquine inhibits hepatocellular carcinoma cell growth in vitro and in vivo. *Oncol. Rep.* **2016**, *35*, 43–49.

[20] Suresh, A.; Jie, L.; Surya, K. K.; Kurashima, Y.; Tezuka, Y.; Kadota, S.; Esumi, H. Identification of arctigenin as an antitumor agent having the ability to eliminate the tolerance of cancer cells to nutrient starvation. *Cancer Res.* **2006**, *66*, 1751–1757.

[21] Ikeda, M.; Sato, A.; Mochizuki, N.; Toyosaki, K.; Miyoshi, C.; Fujioka, R.; Mitsunaga, S.; Ohno, I.; Hashimoto, Y.; Takahashi, H.; Hasegawa, H.; Nomura, S.; Takahashi, R.; Yomoda, S.; Tsuchihara, K.; Kishino, S.; Esumi, H. Phase I trial of GBS-01 for advanced pancreatic cancer refractory to gemcitabine. *Cancer Sci.* **2016**, *107*, 1818–1824.

[22] Fujioka, R.; Mochizuki, N.; Ikeda, M.; Sato, A.; Nomura, S.; Owada, S.; Yomoda, S.; Tsuchihara, K.; Kishino, S.; Esumi, H. Change in plasma lactate concentration during arctigenin administration in a phase I clinical trial in patients with gemcitabine-refractory pancreatic cancer. *PLoS One* **2018**, *13*, e0198219.

[23] Takehara, T.; Liu, X.; Fujimoto, J.; Friedman, S.L.; Takahashi, H. Expression and role of Bcl-xL in human hepatocellular carcinomas. *Hepatology*. **2001**, *34*, 55–61.

[24] Mathiassen, S.G.; Zio, D.D.; Cecconi, F. Autophagy and the cell cycle: A complex landscape. *Front. Oncol.* **2017,** *7*, 51.

[25] Zheng, K.; He, Z.; Kitazato, K.; Wang, Y. Selective autophagy regulates cell cycle in cancer therapy. *Theranostics* **2019**, *9*, 104–125.

Acknowledgment

First of all, my heartfelt appreciation goes to Professor Hideaki Fujita, Department of Functional Morphology, Graduate School of Pharmaceutical Sciences, Nagasaki International University, for his kind support and accepting the examination of doctoral dissertation pleasantly.

I would particularly like to express my gratitude to Professor Taku Yamaguchi, Department of Pharmacotherapeutics and Neuropsychopharmacology, Graduate School of Pharmaceutical Sciences, Nagasaki International University, for his guidance, kindness, and support my research.

I would also like to acknowledgment to Associate Professor Kazuhisa Ota, Department of Molecular Pathology, Graduate School of Pharmaceutical Sciences, Nagasaki International University, whose comments made enormous contribution to my work.

I am also grateful thanks to Associate Professor Takuhiro Uto, Department of Pharmacognosy, Graduate School of Pharmaceutical Sciences, Nagasaki International University, whose kindly comments, suggestions, and appropriate guidance were of inestimable value for my study and graduate school life.

I would like to offer my special thanks to Professor Emeritus Yukihiro Shoyama, Kyusyu University and Nagasaki International University, for giving me the helpful and valuable advice to my research.

I wish to thanks to Assistant Professor Tomoe Ohta, Lecturer Shunsuke Fujii, Ms. Hisa Komori, and Ms. Asuka Kuwahara in supporting my study.

Last, I would like to express my sincere gratitude to my wife, children and family for always sending warm encouragement.

March, 2020

Shinya Okubo